CHARACTERIZING ICE COVER BEHAVIOUR

ALONG THE SLAVE RIVER

A Thesis Submitted to the College of

Graduate Studies and Research in Partial Fulfillments of the Requirements

for the Degree of Master of Environment and Sustainability

in the School of Environment and Sustainability

University of Saskatchewan

Saskatoon

Canada

By

Apurba Das

Permission to use statement

In presenting this thesis in partial fulfillment of the requirements for a Postgraduate degree from the University of Saskatchewan, I agree that the Libraries of this University may make it freely available for inspection. I further agree that permission for copying of this thesis/dissertation in any manner, in whole or in part, for scholarly purposes may be granted by the professor or professors who supervised my thesis/dissertation work or, in their absence, by the Head of the Department or the Dean of the College in which my thesis work was done. It is understood that any copying or publication or use of this thesis/dissertation or parts thereof for financial gain shall not be allowed without my written permission. It is also understood that due recognition shall be given to me and to the University of Saskatchewan in any scholarly use which may be made of any material in my thesis.

Abstract

River ice is an important component of the traditional way of life for the communities along the Slave River both culturally and economically. During the winter, a stable ice cover provides local residents with safe access to their traditional hunting, trapping, and fishing grounds along the river. Periodic spring ice breakup flooding is required to maintain the ecological balance along the Slave River Delta. Recently, however, local observations have indicated changes in ice cover characteristics (e.g. air pocket formation, double layer ice, ice cover flooding) during the winter, which increase the risks of travelling on the ice. Also prolongs dry periods during the spring are leading to rapid growth of invasive vegetation that reduces the lake and channel areas of the Delta. Although some attempts have been made to understand the patterns of spring flood frequency in the Delta, very little is known about the Slave River's ice cover characteristics and behaviour. Remote sensing techniques and field surveys were used in this study to understand the ice cover progression and to examine ice cover characteristics along the river during the winters of 2013-2014 and 2014-2015. RADARSAT-2 satellite imagery captured the changes in the ice cover and identified different types of ice during the winter seasons at two primary study sites – downstream of Fort Smith and the Slave River Delta. The mechanism of ice cover growth, with the formation of air pockets and layers underneath the ice cover was investigated. Steeper channels and several open water sections appear to be contributing to significant amounts of air entrainment into the water in winter. Changes in the hydraulic characteristics due to flow regulation and ice cover progression can also change the quantity and distribution of air pockets along the river ice cover. Additionally, the impact of flow fluctuations on the ice cover (e.g. ice cover flooding) was also observed. Increases in discharge cause the ice cover to crack or dislodge from the river banks, leading to water seeping onto the ice and flooding it, which has implications for the muskrat and beaver populations.

A geospatial model was developed to determine the spatial patterns of ice cover breakup along the river from Fort Fitzgerald to the delta. This model successfully identified the areas of breakup initiation and persistence of ice until the end of the breakup. MODIS satellite imagery was used to describe the temporal patterns and evolution of breakup events between the years 2008 and 2011. In addition to geomorphological influences, air temperature and flow conditions also have strong impacts on the spatial and temporal patterns of the ice cover breakup.

Acknowledgements

I sincerely thank my supervisor, Dr. Karl-Erich Lindenschmidt, for his guidance and support during my entire master's program and members of my advisory committee, Dr. Paul Jones, Dr. James A. Kells and Dr. Lalita Bharadwaj, for their continued support, mentorship and advice. Thank you Dr. Dirk H. de Boer, my external examiner, for insightful revisions of my thesis.

Thanks to the people who helped with data collection along the Slave River between the years 2013 and 2015, including Earl Evans and Henry McKay. Thank you too Jay Sagin and Thuan Chu for helping me to learn GIS technology and process satellite data. A cordial thank you to Meghan Carr for helping me and sharing your code to develop a geospatial model of my study site.

I would like to acknowledge the financial support received from the Canadian Water Network (CWN), University of Saskatchewan and Global Institute for Water Security. I acknowledge the use of Rapid Response imagery from the Land Atmosphere Near-real time Capability for EOS (LANCE) system operated by the NASA/GSFC/Earth Science Data and Information System (ESDIS) with funding provided by NASA/HQ. I also thank to the Canadian Space Agency's Science and Operational Applications Research (SOAR) program for providing the RADARSAT-2 images used in this study.

Table of Content

List of Table

List of Figures

List of Abbreviations

PAD	Peace-Athabasca Delta
PCA	Principal Component Analysis
SRD	Slave River Delta
SAR	Synthetic Aperture Radar
NWT	Northwest Territories
AFDD	Accumulated Freezing Degree Day
WSC	Water Survey Canada
EC	Environment Canada
MODIS	Moderate Resolution Imaging Spectroradiometer
GRU	Geomorphic Response unit

Chapter 1 Introduction

1.1 Background of Slave River ice regime

Ice is a key component of the hydraulic regime of northern rivers. River ice can have an important influence on aquatic habitats and the biological productivity of northern rivers. Ice can be a cause of flooding, particularly during the spring breakup. Such spring ice jam flooding is important for replenishing lakes and wetlands in river deltas and supplying the necessary sediment-nutrients for supporting the delta's riparian vegetation (Beltaos 2007). River ice provides a means for transportation in the winter, which is particularly important for aboriginal peoples as a means to access their traditional hunting, trapping and fishing areas.

Since the construction of the W.A.C. Bennett hydroelectric dam on the upper Peace River, the Slave River flow has become modulated, with increased flow in the winter and lower flows in spring and summer (AANDC and NWT 2012; Dubé and Wilson 2013; Prowse et al. 2002). The Peace River is the major inflow to the Slave River, contributing 60% of the Slave River's total volume flow (AANDC and NWT 2012). The other 40% stems from the Lake Athabasca and other tributaries. Therefore, the hydrological regime of the Peace River basin has a strong influence on the Slave River's hydraulic regime.

Communities along the Slave River have indicated that the changes in the flow regime are altering the ice regime of the river. Air pocket formation along the ice cover and thinner river ice pose a great risk to persons crossing the river, thus impeding traditional and subsistence winter activities. Community members began to notice the formation of air pockets along the river's ice cover in the early 1980s, about 7 years after dam operations commenced. The number of air pockets formed appear to vary from year to year, depending on the flow magnitude (pers. comm. Earl Evans, Metis Council elder, Fort Smith). A few studies have assessed the impacts of flow regulation on Slave River ice conditions during the winter (AANDC and NWT 2012; Prowse et al. 2002). Most of them have provided very limited information about the ice regime. High water levels in the winter can produce a double layer of ice along the Slave River (AANDC and NWT 2012). Additionally, high winter flows keep the ice cover thin, resulting in open water sections forming along the river. High flows can also produce a significant amount of frazil ice in the Slave River, which can be deposited downstream to increase thickness of the ice cover. Documentation on different types of

ice during freeze-up, ice cover development and progression, and patterns of spring ice cover breakup along the river, is sparse. Such information is, however, essential for the communities along the river. It is used to make decisions about to safe access to the river in the winter and also to understand the river's ecological structure and functioning. The forestry industry has also expressed interest in such knowledge to help them decide which locations along the river are the safest and most economical, for the creation of ice bridges to access and harvest remote forest stands. Additionally, detailed reporting about the different types of ice and their formation mechanisms is required, in order to improve predictability of the behaviour of the ice cover impacted by flow regulation. This research attempts to fill some of the knowledge gaps on the Slave River's ice regime.

1.2 Similarities to Peace River ice regime

Little information exists on the ice regime of the Slave River. However, a lot of the research related to the Peace River ice regime may be transferable to the downstream Slave River and provide useful insights into the Slave River's ice cover behaviours. Research has been conducted to understand the mechanisms of ice cover formation, assess the impacts of flow regulation, and document on the different types of ice along the Peace River (Jasek et al. 2013, 2011, 2003; Marko and Jasek 2009; Hicks et al. 2009; Andres et al. 2003). The Peace River lends itself well to comparison, because both rivers are part of the same river network and have similar fluvial geomorphologies. The width of both rivers exceeds 1500 m in some locations and narrows to 350 m in others. Both channels' flows are diverted into multiple channels due to many islands and sand bar complexes, and the channels are occasionally sinuous in various locations. A set of rapids along the Peace River at Vermilion Chute drops a 2.7 km-long river stretch by approximately 10 m (average slope 0.37%), while a set of four rapids from Fort Fitzgerald to Fort Smith along the Slave River drops the riverbed approximately 35 m for a distance of 23 km along the river (average slope 0.15%). The Peace River eventually reaches the Peace-Athabasca Delta (PAD) near Peace Point, and the Slave River forms the Slave River Delta (SRD) before draining into Great Slave Lake.

At the beginning of freeze-up, the Peace River's initial ice formation is usually dominated by frazil and border ice (Jasek et al. 2013; Gauthier 2006). During freeze-up, the steeper sections of the river usually generate frazil ice crystals, while relatively flatter areas are conducive to border and

skim ice cover formation. The rapids along the Peace River at Vermilion Chute are particularly conducive to the production of frazil ice (Jasek et al. 2013). The steep river slope and rapid flow velocity of this section creates high turbulence, generating much frazil ice. The frazil ice can be submerged and deposited under the downstream ice cover to form a hanging dam. Subsequent thickening of the hanging dam increases the upstream water level to shift the ice cover front upstream. Some less steep sections of the river may also produce skim and border ice covers during the freeze-up. Jasek et al. (2013) also show that the reach upstream on Vermilion Chute has a high potential for ice lodgement, as many islands and sand bar complexes make this stretch conducive to border ice formation that restrict ice floes, creating ice bridging along the river. The flow of fragmented skim ice pieces and frazil ice from upstream can be arrested at these ice bridging sections to form a juxtaposed ice cover. However, rapid river flow and high shear force underneath the ice cover may erode and thrust the juxtaposed ice cover downstream (telescoping), resulting in a consolidated ice cover. In the same way, frazil ice can also be transported far downstream and deposited under the ice cover, resulting in further ice cover thickening. Due to a similar geomorphological structure some of these ice phenomena may also be observed in the Slave River such as frazil ice generation along the set of four rapids and border ice growth along the edge of islands.

Flow regulation along the Peace River can alter the nature of the ice regime during winter. The temporal and spatial patterns of the ice cover formation have changed along the upper Peace River since the construction of W.A.C Bennett Dam. High winter discharge and relatively warmer water released from the reservoir result in almost no ice cover formation in the area nearest the dam and delay in the freeze-up processes further downstream (Prowse et al. 2002). Regulation also results in the tendency of a consolidated ice cover forming instead of a juxtaposed ice cover. The juxtaposed ice cover may form when incoming ice floes or ice pans arrest in an ice bridging or existing ice cover. This ice cover may collapse due to strong shear forces imposed on the cover and forms a consolidated ice cover. The consolidated ice cover is comparatively thicker and rougher than the juxtaposed ice cover. Particularly during the initial formation of an ice cover, high winter flows from the dam operation increase flow velocities, collapsing the ice cover and forcing the ice cover front further downstream. This leads to hydraulic thickening of the ice cover, which has resulted in ice jam flooding in the past. This ice cover is rough, thereby increasing overall channel resistance, which increases the water level upstream (Prowse et al. 2002).

Secondary consolidation often follows (collapse and thickening of a consolidated ice cover), which can lead to extreme flooding events along a river (Hicks et al. 2009; Andres et al. 2003). Mid-winter water level increases have also caused ice cover flooding and aufeis formation along the river. Rapid flows may increase under ice water pressure and push the water up, causing cracks to develop in the ice cover (Beltaos 2013). These cracks then allow the pressurized water to seep through and flood the ice cover. The subsequent freezing of successive seepage of flood water from underneath the ice cover produces aufeis on the ice cover, which increases the thickness of the ice. The aufeis is often linked to the formation of bulges at the top of the ice cover.

1.3 Spring flood regime of the Peace and Slave rivers

Ice is an important factor in the flood regime of the Peace and Slave rivers. In particular, breakup ice-jam flooding is necessary to maintain a sustainable ecosystem in the Peace-Athabasca Delta (PAD) as well as the Slave River Delta (SRD). Ice jam flooding during the spring break-up replenishes the lakes and their distributary channels, supplying the necessary sediment-nutrients to the lakes and wetlands (Beltaos 2008; Brock et al. 2007, 2008). The delta's ecosystem also supports riparian vegetation, fish, waterfowl, and animals along the delta. These resources are also crucial in enabling the local residents to maintain their cultural and ecological integrity in their relationship with the delta.

Flow regulation, due to the W.A.C Bennett Dam on the upper Peace River, is affecting flood frequency downstream. The communities along both rivers report that magnitude and frequency of spring flooding along the PAD and SRD have decreased (Brock et al. 2007, 2008, 2010). As a result of these changes in the river, the channels in the delta are drying up, active delta areas are becoming smaller and the aquatic abundance of the delta is diminishing. Many factors may give rise to reduced flood frequency in the delta, including river discharge, ice breakup patterns, and climate change (Beltaos and Carter 2009; Prowse et al. 2006). A higher peak flow along the river is required to inundate the Slave River Delta during the spring breakup. One study has shown that most of the active delta areas were flooded when spring discharge of the Slave River at Fort Fitzgerald gauge station exceeded 5370 m^3/s (Brock et al. 2008). High snow accumulation and rapid spring melt into the river also contribute to flooding in the delta. The high magnitude of snow accumulation in winter increases water levels, while rapid spring melt can contribute to the creation of ice jams and high water levels along the river.

1.4 Research purpose

This research examines the mechanisms of freeze-up and ice cover progression and documents the different types of ice along the Slave River. Particular foci are air pocket and air layer formation along the river ice cover, and the patterns of spring ice cover breakup.

The specific objectives of the work are to:

- determine the freeze-up patterns and impacts of regulated flow changes on the ice cover along the Slave River,

- investigate air pocket and air layer formation along the river ice cover, and

- characterize the patterns of the spring ice cover breakup along the Slave River.

1.5 Thesis Structure

This thesis is written in manuscript style, following the guidelines set by the College of Graduate Studies and Research, University of Saskatchewan. The thesis combines three manuscripts, each of which constitutes a single thesis chapter. Each chapter contains an introduction with a concise background summary of the problems, the data and methods used in the research, a description of the study site and a discussion of the results and conclusion. The first manuscript (Chapter 2), "Monitoring the freeze-up and ice cover progression of the Slave River", describes the mechanisms of ice cover formation along the Slave River and documents the different ice types and examines impacts of flow changes on the river ice cover in winter.

The second manuscript (Chapter 3), "Air pocket formation along the Slave River ice cover", investigates air pocket and air layer formation along the river ice cover. The third manuscript (Chapter 4), "A geospatial model to determine patterns of ice cover breakup along the Slave River", examines spring ice cover breakup patterns and describes the geospatial model developed to identify the most significant areas of ice cover breakup initiation and persistence of ice during the spring breakup.

A brief summary of the research findings and the ice regimes along the river for the winters 2013-2014 and 2014-2015 are discussed in Chapter 5. The conclusion (Chapter 6) highlights the overall

findings of the research and discusses the contributions, significance, and limitations of the current work and recommendations for future research on the ice regime of the Slave River.

1.6 Copyright and Author Permissions

The manuscripts in Chapter 2 and 4 of this thesis have been accepted for publication, and the manuscript in Chapter 3 has been submitted and is under review. To comply with copyright issues and authors' permission, the citations for all the manuscripts in preparation are given below. In accordance with the guidelines of the College of Graduate Studies and Research for the manuscript style thesis, the student is the main author or makes the major contribution to each of the manuscripts.

Chapter 2: Das, A., Sagin, J., Van der Sanden, J., Evans, E., McKay, H., and Lindenschmidt, K. E. (in press). Monitoring the freeze-up and ice cover progression of the Slave River. *Canadian Journal of Civil Engineering.* http://www.nrcresearchpress.com/doi/abs/10.1139/cjce-2014-0286?src=recsys#.VP4WMfnF98E.

Chapter 3: Das, A., SRDP, and Lindenschmidt, K. E. (submitted). Air pocket formation along the Slave River ice cover. *Cold Regions Science and Technology.*

Chapter 4: Lindenschmidt, K. E., and Das, A. (accepted). A geospatial model to determine patterns of ice cover breakup along the Slave River. *Canadian Journal of Civil Engineering.* http://www.nrcresearchpress.com/doi/abs/10.1139/cjce-2014-0377#.VP4WB_nF98E.

Preface to Chapter 2: Monitoring freeze-up and ice cover progression of the Slave River

The first objective of this research was to determine freeze-up patterns and impacts of regulated flow changes on the ice cover along the Slave River. Chapter 2 mainly focuses on the monitoring of the freeze-up mechanism and documents different types of ice cover formation during the 2013-2014 winter. The impact of regulated flows on the river ice cover is also discussed in this chapter. RADARSAT-2 satellite and time-lapse camera imagery captured different types of ice and the mechanisms of ice cover formation progression along the river during the course of winter. Ice cover flooding, due to mid-winter water staging, was also determined through satellite imagery. Field observations, with measurements of ice thicknesses, were used to understand the ice cover growth in various sections along the river.

The manuscript from this chapter has been accepted for publication in the Canadian Journal of Civil Engineering.

Das, A., Sagin, J., Van der Sanden, J., Evans, E., McKay, H., and Lindenschmidt, K. E. (in press). Monitoring the freeze-up and ice cover progression of the Slave River. *Canadian Journal of Civil Engineering*.http://www.nrcresearchpress.com/doi/abs/10.1139/cjce-2014-0286?src=recsys#.VP4WMfnF98E

Contributions of Authors: Apurba Das (70%) carried out the bulk of the research analyses and the writing of the manuscript. Jay Sagin (5%) processed the RADARSAT satellite images and helped to write the method of processing satellite imagery. Joost Van der Sanden (5%) provided the RADARSAT-2 satellite images and proof-read the manuscript in the final stages before submission. Earl Evans (5%) and Henry McKay (5%) carried out the field surveys as guides and measured the ice cover thicknesses for this research. Karl-Erich Lindenschmidt (10%), supervisor of this research, developed the theoretical framework of this study and made necessary revisions to the manuscript.

Chapter 2 : Monitoring freeze-up and ice cover progression of the Slave River

2.1 Introduction

Ice constitutes an important control on the flow regime of a river in winter. Ice along northern rivers can be an important component to the traditional and cultural lifestyles of indigenous peoples as the ice provides transportation links to hunting, trapping, and fishing areas. Changes in the ice regime can impact and even alter these traditional lifestyles.

The construction of the W.A.C. Bennet Dam on the upper Peace River, AB, Canada has significantly altered the flow regime of the Slave River, NWT, Canada by modulating the flow hydrograph over the course of the year (lower flood peaks in summer and higher discharges in winter). These changes in the flow regime have also resulted changes on the ice cover characteristics during winter. For example, air pockets underneath the ice cover and double ice layers, with air and water sandwiched between the top and bottom ice layers, can create a major hindrance to travel and fishing for Slave River communities (AANDC and ENR 2012). Community members along the river have observed periodic winter kills of muskrat and beaver populations along the Slave River are also attributable to ice cover flooding since the additional ice layer on top of the ice cover can trap and drown the animals in their over-wintering shelters. Open water sections on the river ice have also been observed which were not common in the past (AANDC and ENR 2012). Little has been documented in the literature about the Slave River's more recent ice cover characteristics and behaviour. To understand and perhaps mitigate the impacts of ice cover changes on the livelihoods of residents along the river, it is important to monitor and understand the freeze-up processes along the Slave River. The manner in which the river freezes over often sets the stage for the ice cover conditions during the course of winter, right into breakup.

Hydraulic, geomorphologic and meteorological conditions and flow regulation affect the ice regime along the river. Flow regulation due to dam operations can change the thermal and flow conditions of a river and change the characteristics and behaviour of the river's ice cover, e.g. types of ice and timing of freeze-up (Beltaos 2013). Higher water discharges during the winter can maintain open water sections along the river (Vuyovich et al. 2009; Ghobrial et al. 2013). Also, fluctuating winter discharges may cause cracking or dislodgement of the ice cover causing

pressurized water to seep onto and flood over the cover (Lindenschmidt and Davies 2014). The physical characteristics of the river can also be an important influential factor controlling the behaviour of ice during freeze-up. For example, width constrictions in less steep river sections are potential areas for ice bridging that can accelerate the freeze over of a river (Lindenschmidt and Chun 2013). Steeper river sections with rapids may lead to a greater rate of frazil generation and entrainment of air into the flows (Gherboudj et al. 2007) which can lead to rapid freeze over and air bubble entrapment in the ice. The amount of snow on the ice cover immediately after freeze-up may also affect the rate of ice thickening in certain sections. Deeper snow may decrease the rate of ice thickening resulting in thinner ice covers (Woo et al. 2007). On the other hand, deeper snow may also increase the rate of ice thickening through the formation of snow ice.

RADARSAT-2 satellite images are extensively used for tracking the processes of river ice freeze-up and changes in winter ice cover characteristics along rivers (e.g. van der Sanden et al. 2009; Lindenschmidt et al. 2011). RADARSAT-2 operates with a synthetic aperture radar (SAR) sensor that transmits and receives C-band microwaves to produce an image of the earth's surface (CCRS 2009). Differences in the strength of the received signal, also known as the radar backscatter, enable the detection of the location of the river ice cover front, the classification of ice types and estimation of ice cover thicknesses (e.g. Lindenschmidt et al. 2010; van der Sanden and Drouin 2011). There are two general scattering mechanisms involved in the interaction between river ice and the radar signal – surface scattering and volume scattering. In surface scattering, a large proportion of the transmitted radar signal is scattered at the air-ice and ice-water interfaces, particularly if the interfaces have rough ice surfaces. In volume scattering radar signals transmitted throughout the thickness of the ice layer are scattered due to impurities in the ice volume, such as cracks, inclusions and voids in the ice. (Unterschultz et al. 2009; Lindenschmidt et al. 2010). These scattering mechanisms of the river ice mainly depend on the physical properties of the ice, such as its structure and degree of wetness, the former being influenced by ice-cover formation processes at freeze-up and the latter by air temperature. During freezing conditions, that is when the ice is free of liquid water, microwaves will penetrate the ice-air interface and scatter at the ice-water interface and/or at dielectric discontinuities (cracks, air inclusions, bubbles, and impurities) within the ice volume. Microwaves that impinge on a smooth thermal ice-water interface will mostly reflect in the forward direction, i.e. away from the radar sensor. As a result thermal ice covers generate little backscatter and will appear dim in a satellite SAR image. Similar to thermal ice,

open water typically appears dark in SAR images because it scatters the majority of incident microwaves in the forward direction. On the other hand, "white" ice covers with a relatively rough ice-water interface will scatter a significant portion of the incident signal back towards the sensor and will therefore show as bright areas in a SAR image (Unterschultz et al. 2009). The radar return signal of ice covers that include large amounts of dielectric discontinuities results primarily as a result of so-called volume scattering. This type of scattering is known to generate relatively high backscatter signals that show as bright areas in radar images. For example, a consolidated ice cover produces relatively brighter images because this type of ice cover consists of the accumulation of frazil ice and ice pieces that increase the roughness and dielectric discontinuities within the ice cover. Therefore, increasing the roughness of the surface ice cover will increase the backscattered return signal. More dielectric discontinuities will also produce stronger volume scattering which returns a high proportion of signal to the satellite (Lindenschmidt et al. 2011). Increasing the concentration of more frazil ice or juxtaposing two or more different types of ice along the river can also lead to further increases in backscattering signal to generate corresponding brighter areas in the images (Gauthier et al. 2006). Frazil ice can be transported long distances under the ice and deposited far downstream of the river (Jasek et al. 2013, 2015).

Real-time imagery collected through time-lapse photography is also an effective way of tracking the changes in a river ice cover during freeze-up (Fjeldstad et al. 2002; Vuyovich et al. 2009). Time-lapse cameras can be used for continuous monitoring of the river ice during the entire course of winter, especially for remote areas or where access to the river during winter is difficult (Vuyovich et al. 2009). Observations of the ice formation through time-lapse imagery can be used to validate the results obtained by other tools such as sonar measurements (Ghobrial et al. 2013) and RADARSAT satellite imagery.

The main purpose of this research is to investigate the mechanism of ice cover formation along the Slave River, and document the different ice types using RADARSAT-2 satellite and time-lapse imagery. The impacts of flow changes on the ice cover are also investigated.

2.2 Methods

2.2.1 Study area

The Slave River (Figure 2.1) is a large transboundary river flowing from Alberta to the Northwest Territories (NWT). The 440 km long river conveys flows in a northerly direction from the Peace River, Athabasca River, and Lake Athabasca to Great Slave Lake, with more than half of its total volume stemming from the Peace River. Its bed drops approximately 35 m between Fort Fitzgerald and Fort Smith, over a series of four rapids: Cassette Rapids, Pelican Rapids, Mountain Rapids, and Rapids of the Drowned. The river eventually drains into Great Slave Lake near Fort Resolution at the Slave River Delta (AANDC and ENR 2012).

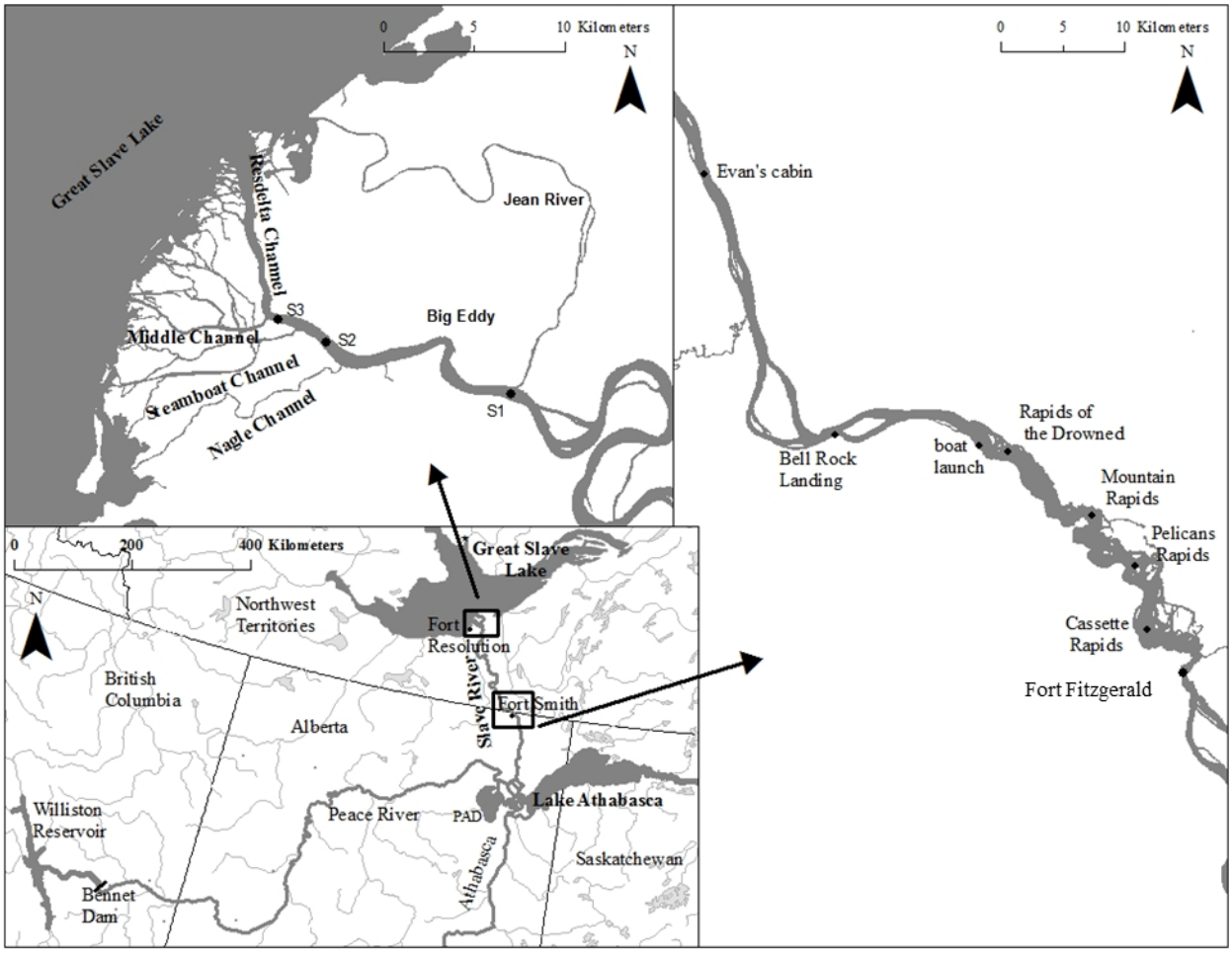

Fig. 2.1 Slave River and Slave River Delta.

The Slave River Delta, located on the southeastern side of Great Slave Lake, is a source of food and subsistence income for the Fort Resolution communities. The delta encompasses an area of approximately 640 km^2 and is interwoven with several active channels, the main ones being: Steamboat Channel, Resolution delta Channel, Middle Channel, Eastern Channel and Nagle

Channel (Figure 2.1). Additional water is diverted from the Slave River via the Jean River to empty into Great Slave Lake.

Since the commencement of the W.A.C Bennet Dam operations on the upper Peace River winter flows have significantly increased along the Slave River. The mean daily discharge curve of the 1960s present pre-dam flow conditions along the river; the remaining curves present the historical trend of flows of the river from 1970 to 2000 (Figure 2.2). The 1960s discharge curve present the pre-dam scenario of flows along the river. A significant decreasing trend was observed in the fall and summer discharge between the 1960s and 2000s. The annual total volume of water flowing in the Slave River has remained unchanged, despite the seasonal variation in the flows. This flow regulation by the Bennet Dam operations may be altering the quality of the ice cover of the Slave River.

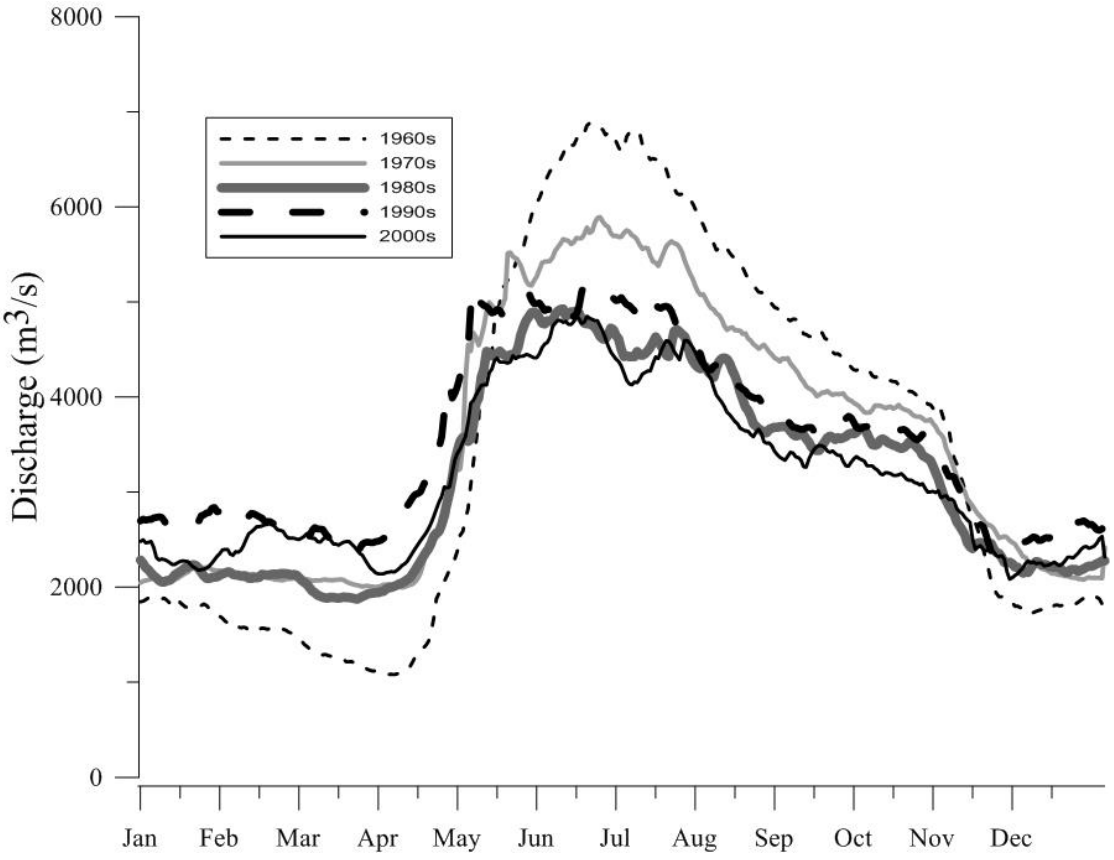

Fig. 2.2 Mean daily discharge at Fort Fitzgerald averaged over 10 years for each day of the year. (Data source: Water Survey of Canada, Gauge # 07NB001).

2.2.2 Field Data

Two study areas were selected along the Slave River for the field sampling program: Evans' cabin and the Slave River Delta. Evans' cabin (Figure 2.1) is situated approximately 40 km downstream from the Rapids of the Drowned. The study sites in the Slave River Delta extend for approximately 16 km from the Jean River to the Steamboat Channel. In total, three areas were selected in the delta for surveying: at the bifurcation of Jean River (S1), between the Nagle and Steamboat channels (S2), and between the Steamboat and Middle channels (S3) (Figure 2.1). The study sites were selected depending on accessibility to the river from the banks and also considering the local knowledge about the safest ice cover along the river. Potential locations of the air pocket formation observed by the local people in past years also considered to select the study sites along the river.

Ice surveys were carried out during the entire course of winter, from December 2013 to March 2014, and included transects of measurements of total ice thickness, snow or white ice thickness, and the depth of snow overlying the ice cover. An auger was used to drill holes into the ice and a measuring staff was implemented to measure ice thicknesses and snow depths. A total of 24 holes were drilled along the transect at Evans' cabin to measure the depth of snow ice and total ice thicknesses. Using the staff, snow depths were measured from the top surface of the snow to the snow-ice interface. Snow ice thicknesses of the cover were determine in partially drilled holes, which were dry to detect the transition from white ice to black ice in the cover. The measuring staff had an L-bracket at the end which, when lowered through a hole completely augured through the ice, could be hooked on the underside of the ice cover to determine the cover's thickness. This direct field measurement of the ice thicknesses and snow depths is reliable, accurate and provides a systematic measurement. Due to the remoteness of the studied sites and time constraints (≈ 6 hours of sunlight per day) only three holes were drilled along each transect of the delta**,** however this amount was deemed sufficient for understanding the development of the ice cover along the river.

For a more detailed analysis near Fort Smith the transect at Evans' cabin was qualitatively divided into three sections according to the amount of flow and assuming that the flow velocity is usually lower near the shoreline and higher in the main channel. The "slow flow" section extended from the east shoreline to the middle portion of the channel (augered holes 1 to 8), the "fast flow" section was in the middle of the channel (augered holes 9 to 18) and the "medium flow" section was near

the west shoreline (augered holes 19 to 24). These categories may help us to determine if ice thicknesses along the river are impacted by different flow velocities. Qualitative observations were also made during the field sampling program such as the different types of ice, frequency of air pockets underneath the ice, and double layers of ice. Several air pocket holes were punctured and venting of air from the ice cover was observed during the surveys. The observation of this venting of air through the punctured hole, also captured in a video, which helped us to further analyze this phenomenon.

Table 2.1 A chart of field data collection along the river at Evans' cabin on 14 January, 2014.

	Hole No.	Snow depth (cm)	Snow ice thickness (cm)	Total ice thickness (cm)	Comment	Average of the total ice thickness (cm)
1 (slow)	1	32	3	52		60.25
	2	18	4	66		
	3	17	0	58.5		
	4	14	5	58.5		
	5	16	6	58.5		
	6	9	14	68		
	7	20	10	0	Sand Bar	
	8	13	0	0	Sand Bar	
2 (fast)	9	15	3	62		57
	10	20	0	51	Some dirt in ice	
	11	20	0	61		
	12	20	0	59		
	13	21	0	51		
	14	18	0	38	Double layer ice	
	15	15	0	58.5		
	16	12	0	58.5		
	17	15	0	56		
	18	18	0	56		
3 (medium)	19	16	0	56		53.8
	20	16	0		Double layer ice	
	21	18	0	49		
	22	14	2.5	52		
	23	15	51	51	All snow ice	
	24	15	61	61	All snow ice	

2.2.3 RADARSAT-2 Imagery

Canada's RADARSAT-2 synthetic aperture radar (SAR) satellite was tasked to track ice cover changes along the Slave River from November 2013 to March 2014. As shown in Table 2.1, a combination of wide fine mode (F0W3) and wide standard quad-polarization (SQ21W) was acquired. The F0W3 images were not available for the study area of Fort Smith and only two SQ21W images were available to study the freezeup near the Fort Smith area. The F0W3 images comprise two channels each, that is, one corresponding to the HH-polarization and the other to the HV-polarization. On the other hand, the SQ21W images comprise four channels corresponding to the HH-, HV-, VH-, and VV-polarization. These are the different combinations of microwave transmit-receive polarization configurations for the RADARSAT-2 sensor: HH – horizontal transmit/horizontal receive (co-polarized), HV – horizontal transmit/vertical receive (cross-polarized), VH – vertical transmit/horizontal receive (cross-polarized), and VV – vertical transmit/vertical receive (co-polarized). These polarizations can be used to extract different information about river ice characteristics (Lindenschmidt et al. 2011), e.g. co-polarization configurations of the radar signals can easily detect rough ice surfaces (Lindenschmidt et al., 2010), whereas cross-polarization can be useful to pinpoint finer features in the ice cover (Sandven and Johannesen, 2006) and produce better contrast between level ice and ice ridges (Mäkynen, 2007).

The F0W3 images were converted to TIFF format for subsequent processing using ArcGIS 10.2 Arctool (http://www.arcgis.com) modules and ET GeoWizard from ET Spatial Techniques (http://www.ian-ko.com). A centerline was constructed for the Slave River along which points were added every 100 m. Circular buffers of 100 m in diameter were applied to the centerline points to which the Arctool "Zonal Statistics" was applied to extract the mean backscatter intensity values. A visual analysis and backscattering values of the RADARSAT-2 imagery were used to determine the different types of ice along the river. Significantly lower backscattering values ranging from -18 to -22 dB, produced darker sections in the satellite imagery and were considered to be open water sections along the river. Dark sections with relatively higher backscattering values between -15 and -18 dB counted as predominantly thermal ice. Comparatively brighter sections with return signals ranging from -12 to -15 dB were considered to be juxtaposed ice covers. Return

values greater than -12 dB were considered to stem from thick consolidated ice covers along the Slave River Delta.

In the case of the SQ21W RADARSAT-2 imagery at Fort Smith, orthorectifying images were not available, therefore visual analysis of ice conditions and qualitative analysis of backscattering values were used to determine different types of ices along the river. Open water sections appear black with very low backscattering value; low backscattering values of reddish color were considered to be thermal or skim ice along the river. Comparatively higher backscattering signals from juxtaposed or consolidated ice cover produced brighter images along those river sections in the images.

Table 2.2 RADARSAT-2 images attained during the freeze-up over the Slave River, near Fort Smith and the Slave River Delta.

RADARSAT-2 image (Slave River Delta)		RADARSAT-2 image (Fort Smith)	
Date	Beam (incidence angles)	Date	Beam (incidence angles)
21 November 2013	F0W3 (38.7º - 45.3°)	04 November 2013	SQ21 (40.2º - 41.6°)
15 December 2013	F0W3 (38.7º - 45.3°)	28 November 2013	SQ21 (40.2º - 41.6°)
08 January 2014	F0W3 (38.7º - 45.3°)	22 December 2013	SQ21 (40.2º - 41.6°)
01 February 2014	F0W3 (38.7º - 45.3°)		
25 February 2014	F0W3 (38.7º - 45.3°)		

2.2.4 Time-lapse camera imagery

Several time-lapse cameras were installed to monitor the ice conditions along the Slave River during the winter 2013 – 2014. Three time-lapse cameras near Fort Smith, at Bell Rock Landing, the boat launch and immediately below the Rapids of the Drowned helped track freeze-up in this area. One time-lapse camera in the Slave River Delta tracked the freeze-up at the start of the Resolution Delta Channel. This study used Moultrie D-333 7 megapixel waterproof outdoor

cameras with different photo capture modes such as time lapse, hybrid, and motion detection. These cameras are capable of capturing photos and video, day and night and able to take 30,000 images on 6 alkaline C-cell batteries (Figure 2.3). The cameras are also suitable for extreme weather conditions and are able to stamp the moon phase, air temperature, time, date and camera ID onto the imagery. All cameras were mounted on trees (Figure 2.3) and were programmed to take three pictures per day. The captured images were stored on 16 GB internal SD memory card inserted in the cameras. More than 300 pictures were qualitatively analyzed to determine the changes of ice conditions during freeze-up.

Fig. 2.3 Time lapse camera and battery (left) and camera mounted on a tree (right).

2.2.5 Meteorological and hydrometric data

Mean daily air temperature data was retrieved from Environment Canada's weather station at Fort Smith, from which accumulated freezing degree days (AFDD) were calculated. The Stefan equation was used to express the ice thicknesses as a function of the accumulation degree days of freezing AFDD:

$$h = a\sqrt{AFDD} \qquad [1.1]$$

Where, h is the ice thickness and a is an empirical coefficient depending on the conditions of snow cover, winds, and solar radiation etc.

Water flows were obtained from the real-time gauging station on the Slave River at Fort Fitzgerald, (No. 07NB001) operated by Water Survey of Canada (WSC). Although this is the only active gauge station along the river, it still give us a good overview of the river's flow regime.

2.3. Results

2.3.1 Ice regimes along the Slave River

Frazil ice generation along the Slave River typically begins during the second week of November (Figure 2.4) when air temperatures are consistently below 0° C and the discharges along the Slave River have gradually reduced. A steep stretch of the river between Fort Fitzgerald and Fort Smith is open all winter and significant turbulence in the super-cooled water is a source of frazil ice throughout the winter. Frazil ice coalesces to form ice floes that are transported downstream until their flow is arrested at an ice bridge or a constriction of a river. Frazil ice is also deposited under existing ice cover along the river. A juxtaposed ice cover begins at the Slave River Delta and extends upstream along the Slave River. Ice bridging in many sections along the river create additional juxtaposing ice covers to create backwater staging and areas of thermal "black" ice. The ice regime along the Slave River depends greatly on the local climate conditions and the hydraulics and geomorphology of the river reaches.

Fig 2.4 Frazil ice transportation along the river downstream of the Rapids of the Drowned near Fort Smith.

2.3.2 Winter 2013 – 2014

2.3.2.1 Ice regime along the Slave River near Fort Smith

Time series of average daily air temperature, discharge and water level conditions along the Slave River during the winter 2013 – 2014 are shown in Figures 2.5 and 2.6. Air temperatures began to decrease to freezing during the third week of October 2013 and consistently remained below freezing from 28 October 2013 onwards (Figure 2.5). During this time, flow along the Slave River progressively decreased and the water level increased gradually as the ice cover formed (Figure 2.6). Freezing air temperatures and low flow conditions initiated frazil pans along the Slave River and the first frazil pans were detected by the time-lapse cameras near Fort Smith on 7 November 2013. During the second week of November, air temperatures dropped below -10 °C and fluctuated between -10 °C and -26 °C until 23 November 2013. During this time the number of ice floes along the river increased significantly and border ice progressed from both shorelines of the river toward the middle of the channel (Figure 2.7). Also, ice bridging occurred at different locations along the river arresting ice floes to form a stable ice cover that progressed in the upstream direction. The backwater effects (Figure 2.7) due to stable ice cover formation was recorded at the Fort Fitzgerald gauge station. This occurs when a stable ice cover forms downstream of the gauge station to create storage effects resulting in increased flows upstream of the edge of the stable ice cover. A solid ice cover was observed immediately downstream of the Rapids of the Drowned on 20 November 2013, although there were still many open water sections along the river. For example, an open water section was captured by time-lapse imagery from the camera at Bell Rock Landing near Fort Smith until 1 December 2013 (Figure 2.7), which was finally frozen over by 4 December 2013

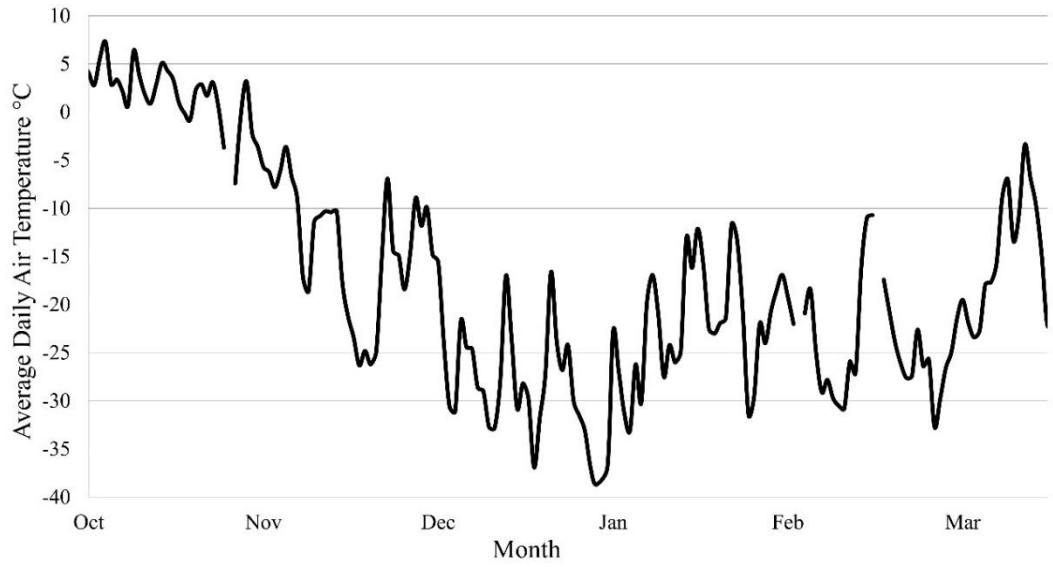

Fig. 2.5 Mean daily air temperatures during the winter 2013-2014 recorded at Fort Smith (data source: Environment Canada, 2014).

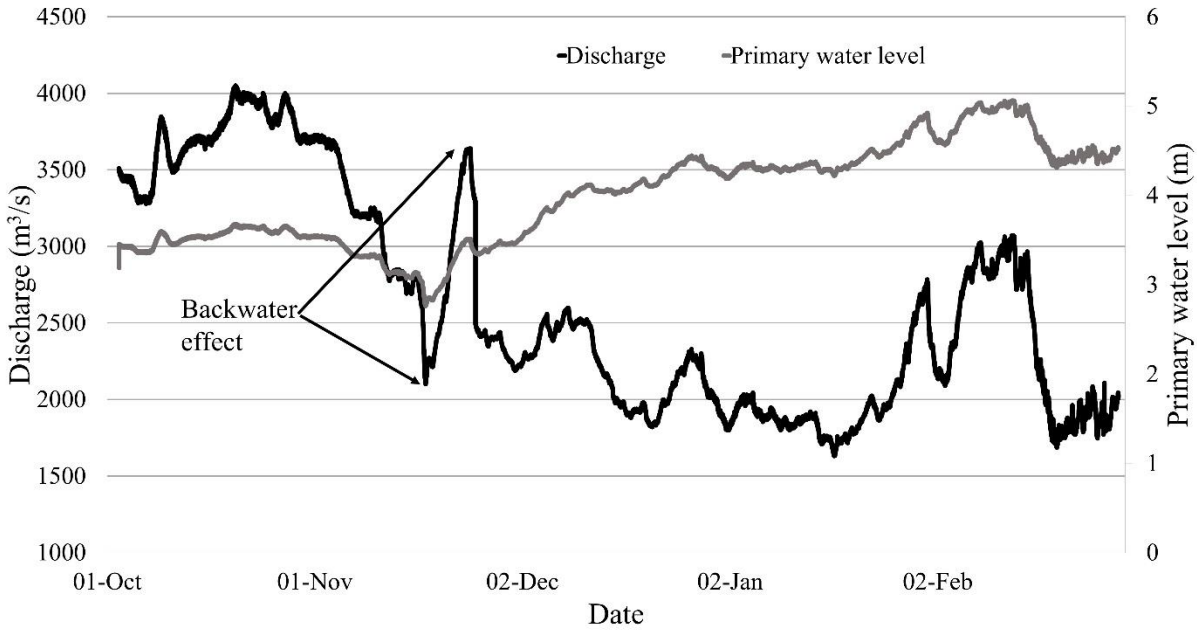

Fig. 2.6 Mean daily discharge and water level condition during the winter 2013-2014 at the gauge station at Fort Fitzgerald (data source: Water Survey of Canada, Gauge # 07NB001).

Fig. 2.7 River ice conditions along the Slave River during freeze-up at the Fort Smith study sites, left panel: border ice progressing toward the middle of the channel at the Rapids of the Drowned on 17 November 2013; right panel: open water section observed at Bell Rock Landing on 1 December 2013.

The changes in the ice conditions along the Slave River near Fort Smith areas could also be tracked by RADARSAT-2 images acquired 28 November and 22 December 2013 (Figure 2.8). The color-composites shown in Figure 2.8 represent a combination of the HH-, HV-, and VV-polarization shown in red, green, and blue, respectively. In the first satellite image several open water and ice bridging sections along the Slave River can be detected. An ice bridging section formed approximately 8 km downstream from the Rapids of the Drowned to develop a juxtaposed ice cover as the flow of ice pans was arrested at this bridging location (Figure 2.8). Another ice bridging section was also observed just downstream of Bell Rock Landing where ice pans formed a consolidated ice cover. Numerous thermal (skim) ice sections along the river are also depicted in the satellite imagery created by the backup of water upstream of ice bridging sections. The ice bridging section may reduce the water velocity and then a thin layer of skim ice forms in super-cooled water along the river.

By 22 December the river was mostly dominated by a consolidated ice cover and several thermal ice sections can be observed in the RADARSAT-2 image along the river. Low backscattering signals (reddish color) reveals the thin layers of thermal ice with air layers between the ice cover along the Slave River. Several air layers underneath of the ice cover were observed at approximately 20 km downstream of Fort Smith during the field ice surveys. This spatial pattern

of intermittent consolidated “white” ice and thermal “black” ice sections extends approximately 80 km along the river reach downstream of the Rapids of the Drowned.

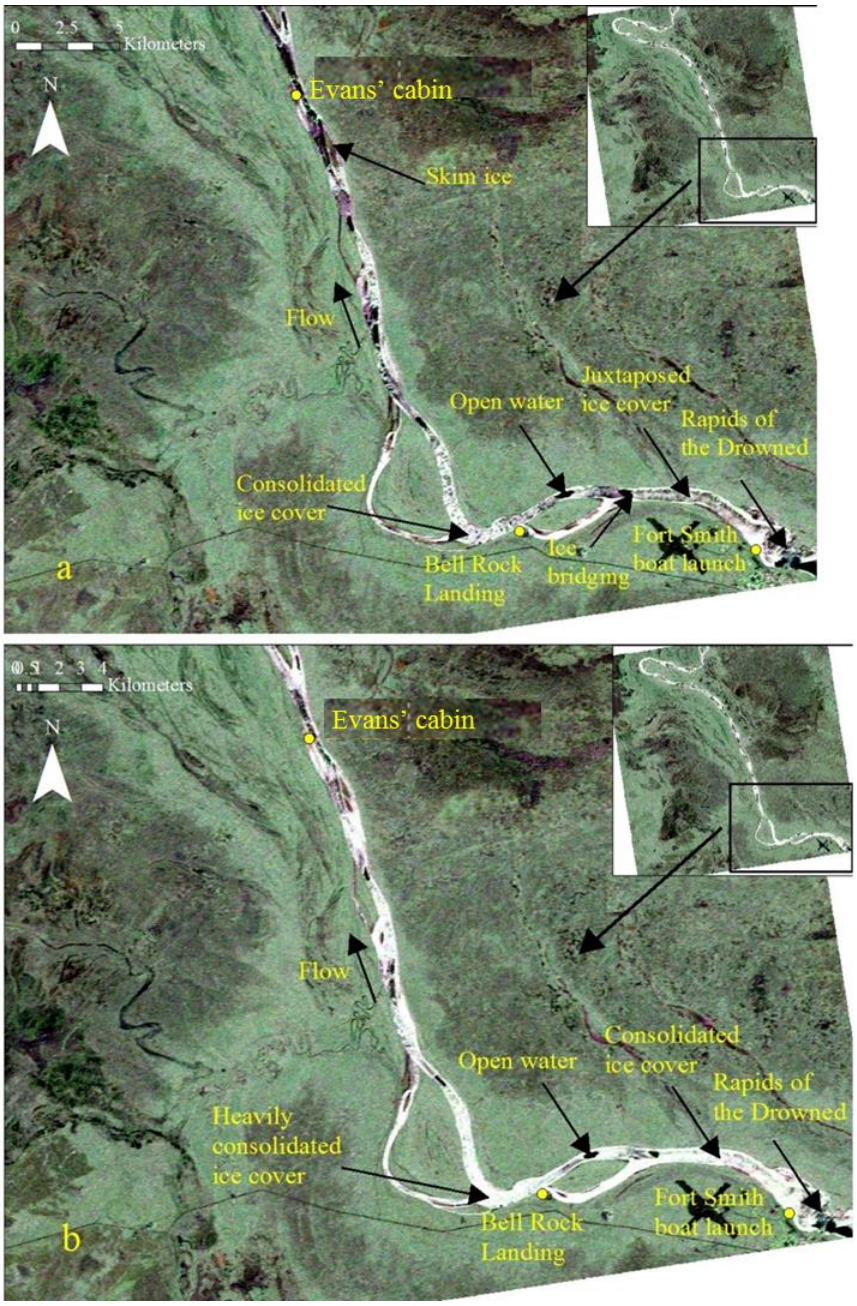

Fig. 2.8 Color-composites of RADARSAT-2 SQ21W images along the Slave River, extending from Rapids of the Drowned to approximately 80 Km downstream of the river. Image acquired on 28 November 2013 (a) and 22 December 2013 (b). Red = HH, Green=HV, and Blue=VV (RADARSAT-2 Data and Products © MacDonald, Dettwiler and Associates Ltd. (2013) –All Rights Reserved. RADARSAT is an official trademark of the Canadian Space Agency).

A stationary ice cover has formed along the Slave River during the first week of December 2013 and the first field surveys at Evans' cabin were carried out on 16 December 2013. The average ice thickness along the river transect was approximately 0.36 m and the average snow depth was about 0.12 m. Several air pockets underneath of the ice cover were observed near the banks of the river. Compressed air and water were released through holes punctured in the ice cover along the river transect, videos of which can be found at http://youtu.be/lTy5OVRe5cA and http://youtu.be/uc2QEntaeG0, respectively.

A second survey was carried out at Evans' cabin on 14 January 2014 with a total number of 24 holes augured (approximately 25 m distance between two drilling holes) along the river transect. The average ice thickness was 0.57 m and snow depth varied from 0.2 m to 0.9 m. Air bubbles and pockets underneath the ice cover were observed along the middle section of the channel at holes 16 and 18 and a double layer of ice was identified at holes 14 and 19 (Table 1).

Two surveys were undertaken during the first and third weeks of February 2014. By 2 February 2014, the ice cover along the Slave River near Fort Smith had significantly thickened. The average ice thickness at Evans' cabin was measured to be 0.96 m and the snow depths ranged from 0.29 m to 0.54 m. On 17 February 2014 the average ice thickness had increased by 27% to 1.22 m and the snow depths varied between 0.31 m and 0.70 m. Also a 0.20 m thick air pocket was augured through in the ice cover. A final ice field survey was carried out at Evans' cabin on 18 March 2014. Warmer air temperatures during this month led to decreasing ice cover thicknesses, measured to be 0.78 m, approximately 36% less than the previous survey in February. A summary of average ice thicknesses and profile of ice cover progression along the transect is shown in Figure 2.9. Although, there are no significant differences between the ice-cover thicknesses in terms of flow categories along the river, other factors such as changes of water temperature or accumulated freezing degree days (AFDD) can play a major role to ice cover thickening along the river, which is discussed in the final results section.

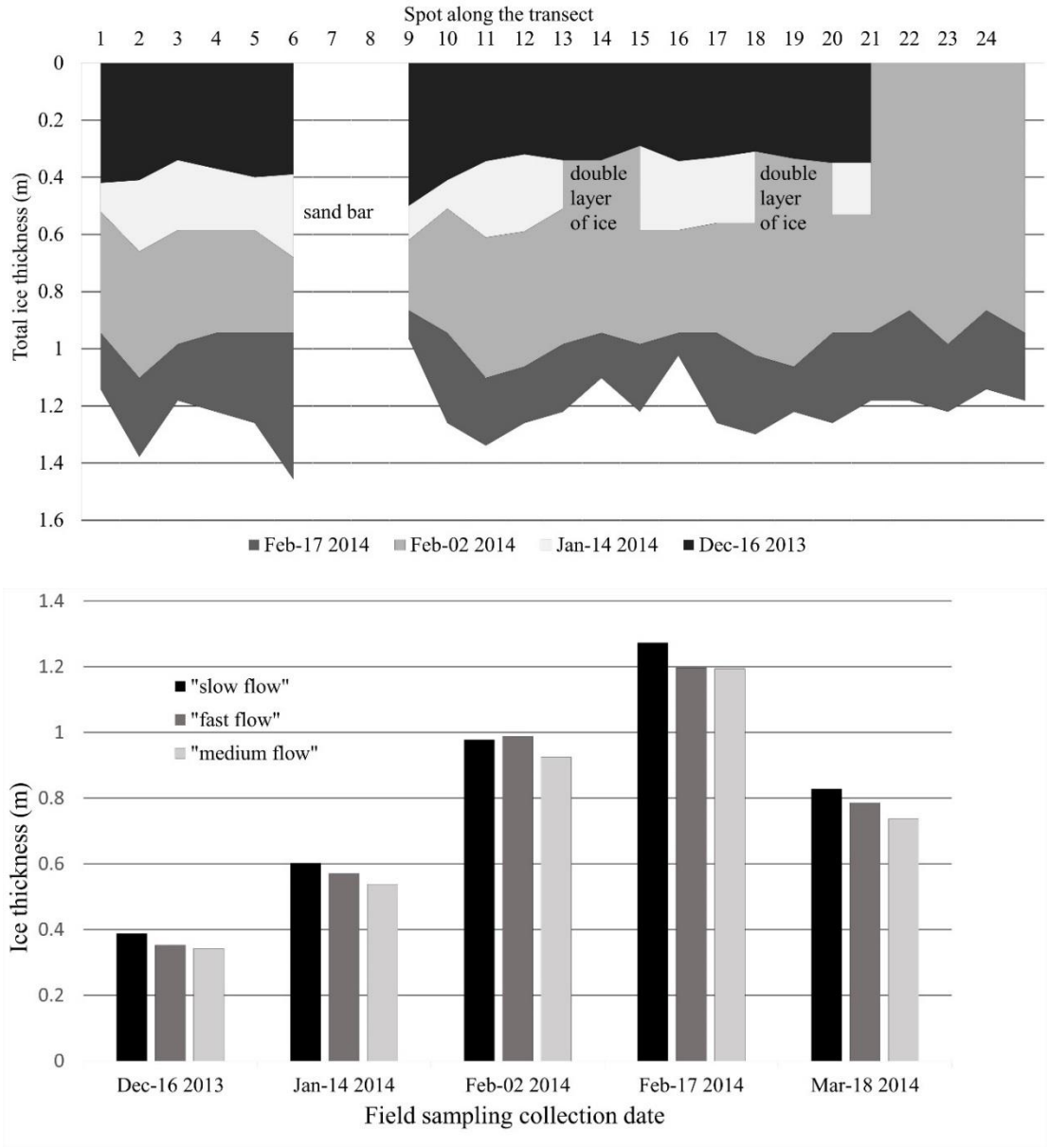

Fig. 2.9 Profile of ice cover progression (top) and summary of average ice thickness (bottom) along the Slave River at the Fort Smith study site (Evans' cabin) during the winter 2013-2014.

2.3.2.2 Ice Regime at the Slave River Delta

The freeze-up along the Slave River at the Slave River Delta is different compared to that near Fort Smith. A comparatively milder sloping river bed and low turbulence along this river reach led to the formation of a thicker layer of columnar ice after freeze-up. During the freeze-up ice floes from upstream of the river continuously juxtaposed to develop an initial ice cover at the delta, unless they are arrested at an ice bridging section or any river constriction (Figure 2.10). Frazil

ice from as far upstream as the rapids was also continuously deposited under the ice cover throughout the winter. Air pockets and layers were also formed particularly at the upstream end of the delta, just downstream of the Jean River, which was evident in the "brightening" of ice cover areas in the satellite imagery acquired during the winter.

Fig. 2.10 River ice condition along the Slave River Delta at the Resolution Delta Channel on 06 November 2013.

Longitudinal profiles of backscatter return signal (HH polarization) were extracted from five RADARSAT-2 satellite images acquired between November 2013 and February 2014 to understand patterns of the ice cover progression along the main Slave River Delta channel (Figure 2.11). On 21 November 2013 most of the river sections at the Slave River Delta were ice covered. An ice bridging occurred at Big Eddy located approximately 5 km downstream of the Jean River from which a consistent consolidated ice cover extended in the upstream direction (Figure 2.12a). An ice cover had already formed at the river's mouth at Great Slave Lake which extended 2 km upstream from the lake along the Resolution Delta Channel. Lower backscatter values ranging from -12 to -22 dB were recorded in the lower portion of Slave River Delta channel indicative of ice layers ranged from juxtaposed, thermal ice and open water along the channel.

Ice thickening and deposition of frazil ice underneath of the ice cover resulted in a large increase in the backscattering values extracted from the image acquired on 15 December 2013. However, low backscattering (approximately -18 dB) between Big Eddy and Nagle Channel (approximately 23 km upstream from Great Slave Lake) reveal the persistence of open water or a thin thermal ice cover on the water surface. During this time the river between Nagle Channel and Steamboat Channel was dominated mostly by thermal "black" ice (Figure 2.12b). By 08 January 2014 thickening ice increased backscattering slightly along all ice covers in the delta. Low backscattering signals (reddish and black color) between the Nagle and Middle Channels indicate the predominance of thermal ice along the Slave River (Figure 2.12c). Several areas of relatively thin ice with underlying air pockets and layers were observed along this area during the ice field surveys.

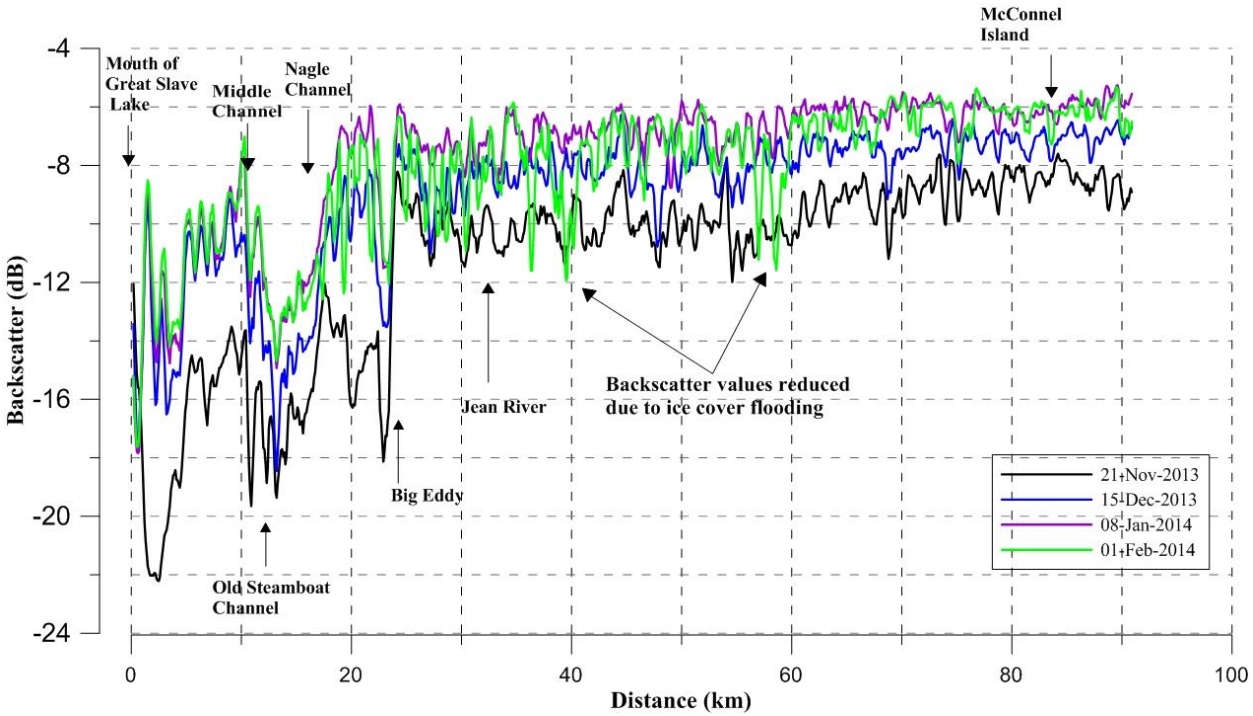

Fig. 2.11 RADARSAT-2 backscattering profile along the Slave River at the Slave River Delta (about 91 km long sections along the Slave River Delta, from McConnell Island to Great Slave Lake).

At the end of January and throughout February 2014, there was a fluctuation in the Slave River flows, between 1600 m^3/s and 3100 m^3/s. This fluctuation is due to the changing discharge from upstream flow regulation and also increases ice thicknesses or collapses ice cover along the river. Discharge of the river at the end of January 2014 increased from below 2000 m^3/s to about 2780 m^3/s and by the second week of February 2014 flows increased to 3000 m^3/s and remained so until the following week (Figure 2.6). These flow fluctuations led to ice cover changes along the Slave River Delta between February and March 2014. Increasing discharges along the river increased the water pressure underneath of the ice cover resulting in cracking of the ice and dislodgement of the ice cover from the banks allowing water to seep onto and flood over the cover.

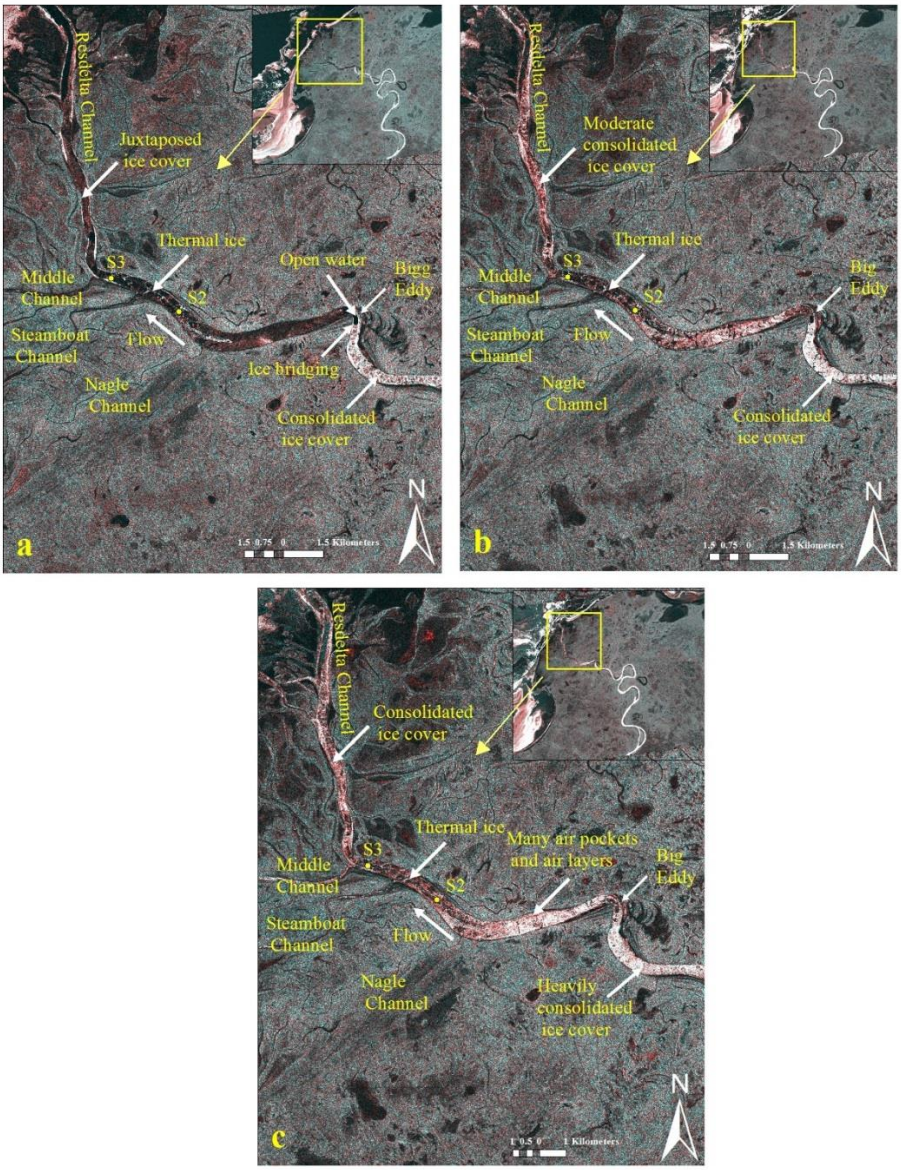

Fig. 2.12 RADARSAT-2 F0W3 (HH + HV composite) imagery covering the area from Great Slave Lake to approximately 20 km upstream of the Slave River Delta, images acquired on 21 November 2013 (a), 15 December 2013 (b) and 08 January 2014 (c). (RADARSAT-2 Data and Products © MacDonald, Dettwiler and Associates Ltd. (2013) –All Rights Reserved. RADARSAT is an official trademark of the Canadian Space Agency).

On 1 February 2014 the level of backscatter recorded by the satellite imagery was reduced significantly due to the scattering of microwaves incident on flooded areas in the forward direction, i.e. away from the sensor. Numerous dark areas indicative of flood water were also depicted in the satellite image (Figure 2.13). For example, many flooded areas (dark) approximately 36, 39 and 57 km upstream from Great Slave Lake (Figure 2.13) reduced the backscatter values to less than -11 dB by 1 February 2014 (Figure 2.10). By 25 February 2014 more flooded areas (black color) were observed in the imagery along the river at the Slave River Delta (Figure 2.13). A high water discharge during mid-February exacerbated water seepage to flood more areas along the river banks.

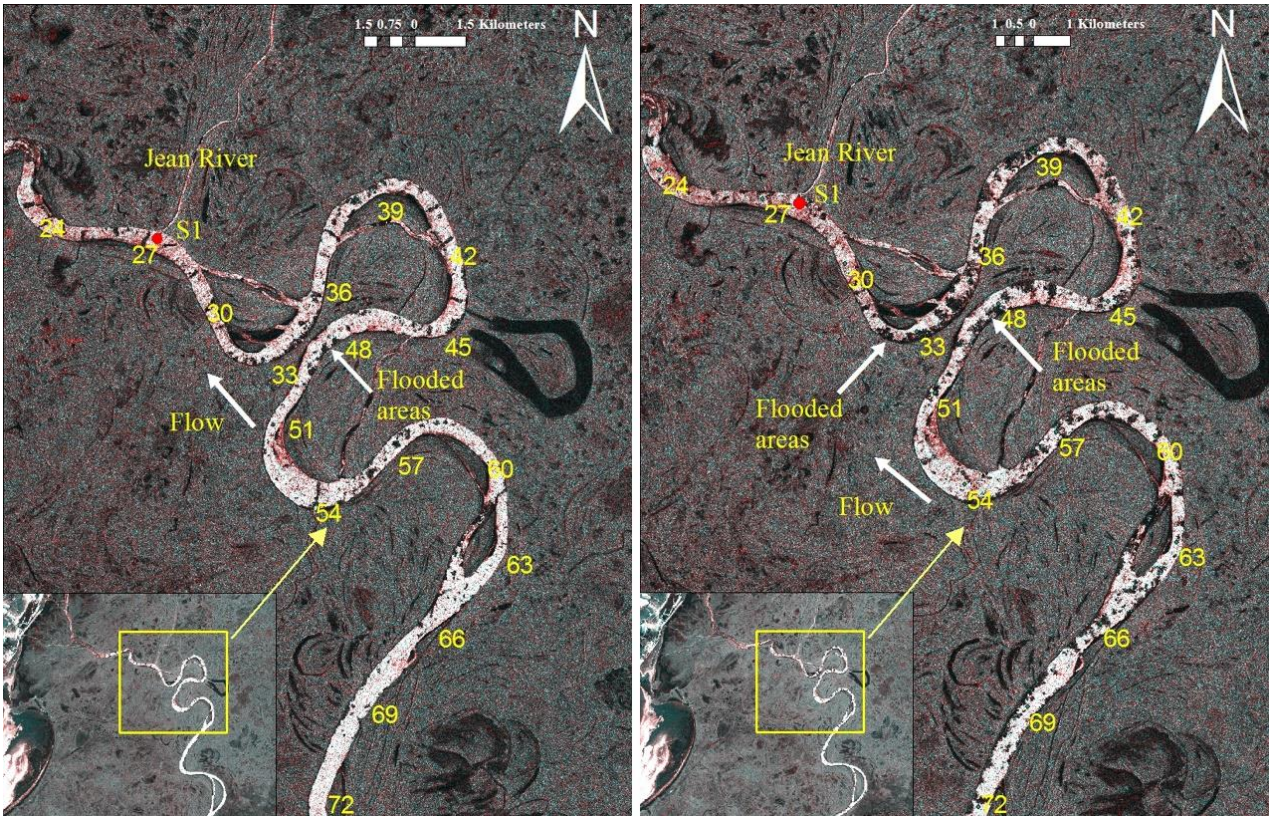

Fig. 2.13 RADARSAT-2 satellite images indicating ice cover flooding (black color on the ice cover) in the lower reach of the Slave River on 1 February 2014 (left panel) and 25 February 2014 (right panel), numbers indicating the km distance of the specific reaches along the river from Great Slave Lake . (RADARSAT-2 Data and Products © MacDonald, Dettwiler and Associates Ltd. (2013) – All Rights Reserved. RADARSAT is an official trademark of the Canadian Space Agency).

Ice surveys along the Slave River Delta were carried out between February and April 2014. The first ice surveys were taken at the entrance to the Jean River and between the Nagle and Steamboat channels on 01 February 2014. At this time the ice cover along the delta's main channel was not uniform and total ice thicknesses varied between 0.44 m and 0.75 m. The average ice thickness near the Jean River was measured to be about 0.50 m and approximately 0.71 m near the Nagle Channel. Average snow depths at the Jean River site were higher (about 0.38 m) than those near the Nagle Channel sites (about 0.19 m). Deeper snow may have insulated the ice cover to slow the ice thickening rate along the river. Thin ice, layers of air bubbles and pockets underneath the ice were also observed between the Nagle Channel and Old Steamboat Channels.

On 3 March 2014 an additional site near Middle Channel was added to the ice surveying program. The total ice thickness at the Jean River increased, albeit the ice thicknesses were less than the other two sites. The average ice thickness at the Jean River was approximately 0.61 m and near the Nagle and Middle channels were about 0.87 m and 0.77 m, respectively. Also average snow depths at the Jean River site were higher, averaging 0.32 m compared to 0.25 and 0.30 m at the Nagle and Middle Channels sites, respectively.

The final ice surveys in the Slave River Delta were undertaken on 2 April 2014. Though ice cover thicknesses decreased at the confluence of the Jean River, ice thicknesses increased near the Nagle and Middle channels of the river. The average ice thickness at the confluence of Jean River was 0.48 m while average ice thicknesses near the Nagle and Middle channels were approximately 1 m and 0.81 m, respectively. The average snow depth at the start of the Jean River was 0.39 m, significantly higher than at Nagle and Middle channels, respectively 0.18 m and 0.23 m. Deeper snow may have decreased the rate of ice thickening at the Jean River along the river. Air bubbles and slush underneath of the ice cover were also observed along several sections of the channel. A summary of field surveys data is provided in Figure 2.14.

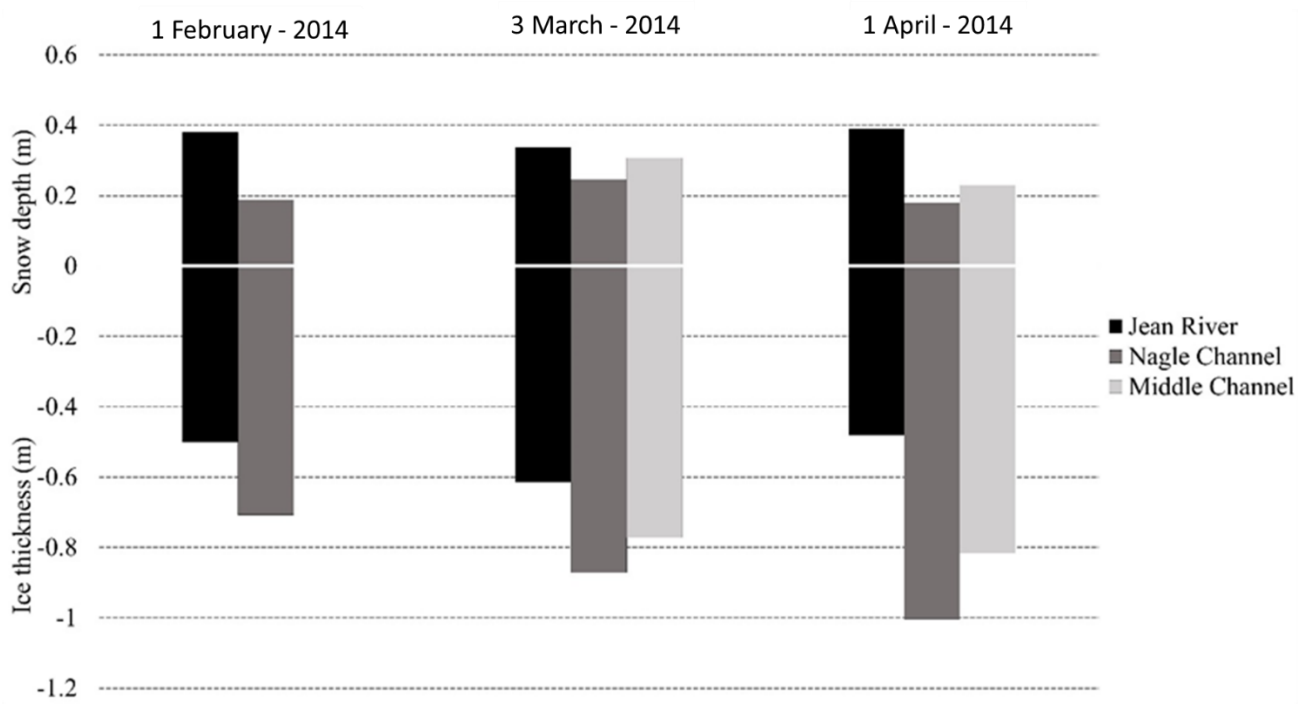

Fig. 2.14 Ice thickness and Snow depth at the Slave River Delta between February and April 2014.

Ice thickness data acquired at Evans' cabin and the delta are plotted against the square root of AFDD in Figure 2.15. Ice thickening at Evans' cabin significantly increased between January and February 2014. During the field surveys between December 2013 and January 2014 air was bled out from under the ice cover allowing the ice cover to come in contact with the underlying water and increase the ice thickening rate. In contrast, ice thicknesses in the Slave River Delta were thinner than at Evans' cabin. Ice covers in the delta area, such as at Nagle Channel and Middle Channel were comparatively thicker than those at the Jean River site. In the delta, lower density of air pockets allowed for thicker ice than areas with higher air pocket density (Jean River). During April 2014 ice thicknesses at Jean River had already decreased but an increasing trend of ice cover thicknesses was still observed between the Nagle and Middle channels. Therefore, the insulating effect of the air pockets can inhibit the rate of ice thickening along the river.

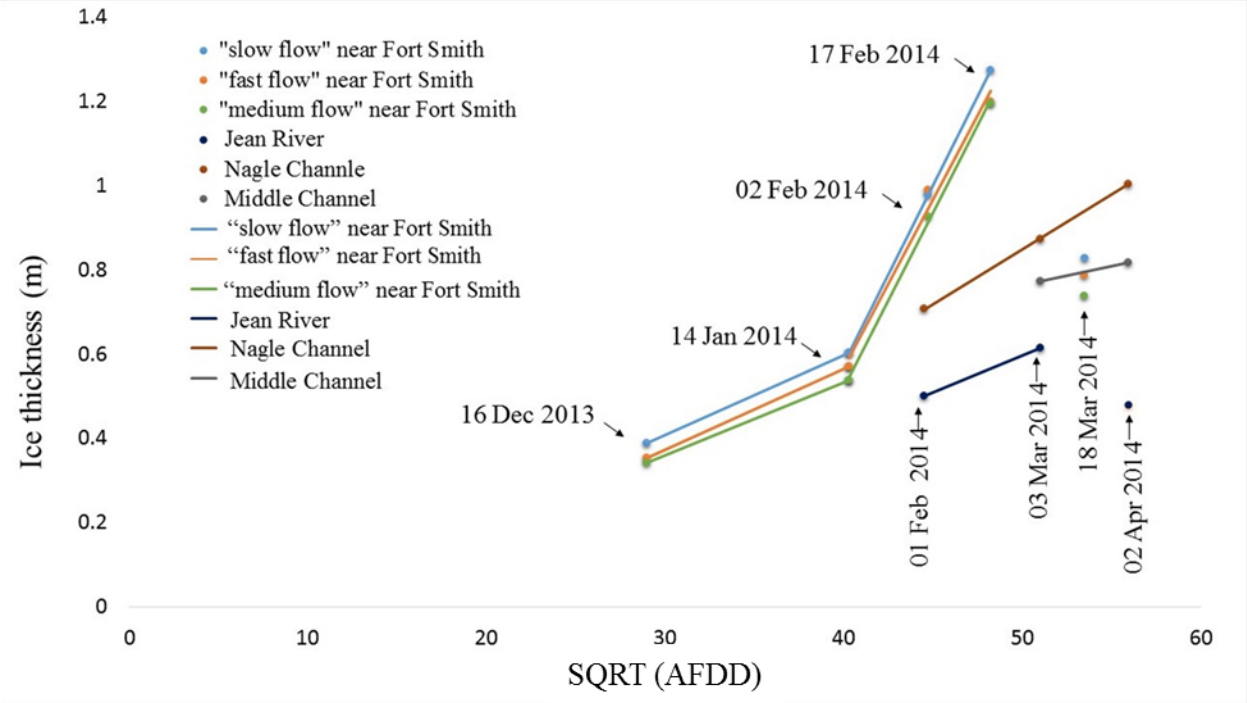

Fig. 2.15 Ice thickness versus the square root of the accumulated freezing degree days (AFDD) with linear regressions according to the Stefan equation.

2.4 Discussion and conclusion

There are various patterns of ice formation along different sections of the Slave River. The most upstream portion of our study site, extending from the Rapids of the Drowned to at least 80 km downstream, has a pattern of intermittent sections of consolidated and thermal ice covers, since this section is narrower than the downstream reach. Also several open water areas formed immediately downstream of those ice bridging sections. Therefore, ice cover formation processes are a reflection of the different geomorphological characteristics along the river. Studies have found that various geomorphologic parameters can influence the formation of different types of ice covers along rivers (Lindenschmidt and Chun 2013; Chao et al. 2014). Narrower and sinuous sections are potential areas for ice bridging along the river. Once an ice bridging is formed, ice floes can be arrested at that section leading to a juxtaposed ice cover to finally form a consolidated ice cover upstream of the bridging (Beltaos 2013). The ice covers in the Slave River Delta are thicker and consist of more thermal ice than the upstream Slave River due to the influence of Great Slave Lake. An ice bridging approximately 5 km downstream along the river led to the formations

of a juxtaposing and consolidated ice cover during the course of winter 2013-2014. There are indications from observations and satellite imagery that frazil ice generated at the rapids can be transported for long distances along the river before it is deposited under the ice cover. This was also inferred from studies carried out at Vermillion Chute along the Peace River (Jasek et al. 2013 2015).

An increase in the mid-winter discharge caused the ice cover to form cracks or to dislodge from the river banks to allow water to spill onto the ice surface and flood large sections of the ice cover. Water level fluctuations in winter can cause the ice cover to crack and cause flooding of the top surface of ice covers (Lindenschmidt and Davies 2014). The subsequent freezing of this flood water can trap and drown muskrats and beavers as was witnessed along the Jean River in the previous winter (personal communication with communities along the river).

A number of studies have used satellite imagery to understand river freeze up and to document different types of ice along the river (e.g. Jasek 2013; Lindenschmidt and Chun 2013; Lindenschmidt et al. 2011; van der Sanden and Drouin 2011; Unterschultz et al. 2009). In this study we analyzed a series of RADARSAT-2 images to identify dominant ice types along the river near Fort Smith and in the Slave River Delta. Ice cover progression and their changes along the delta are also described using backscattering values of RADARSAT-2 satellite imagery acquired in this study. Backscattering profiles of RADARSAT images were also used elsewhere to map the ice cover formation (Gauthier et al. 2006) and in determining the ice cover thicknesses along a river (Lindenschmidt et al. 2010; Jasek et al. 2003). Remote sensing is a useful technique to map the ice cover progression and to classify different types of ice along the river, particularly in remote areas such as the Slave River. It is very difficult to observe the ice cover conditions during the winter because of limited access to most places along the Slave River from the shorelines. Also, the ice cover is not always safe to travel on due to numerous open water sections and many air pockets concealed under the snow cover. Pockets of compressed air along the underside of the ice cover keep the ice thin and unstable. Therefore, taking in-situ ice measurement or sample collections by individuals is not always possible. However, puncturing the pockets to release the air and allowing water to fill the void increases the ice thickening rates. Air pockets and layers were found along the entire course of the studied river stretch.

Since the ice regime of the Slave River can change due to variability of flows and different meteorological conditions from year to year, it is difficult to attain a complete understanding of the ice regime from one year of observations and measurements. Hence, further research with additional sampling techniques (e.g. under ice camera) is necessary to extend our knowledge of the river's ice cover behaviour and characteristics. For example, extracting ice core samples using a core barrel will help to further our understanding of the complexity of the air pocket formation phenomenon. Also, ice maps of the river's ice cover extracted from satellite imagery during the course of winter may be a good means to communicate changes in ice cover characteristics to the local communities. Hazards to winter travel along the river, e.g. locations of high air pocket densities and areas of flooding, could be revealed. The findings of this study can help local residents to identify safe routes to trap lines and fishing areas. Finally this study will provide future guidelines for researchers to increase their predictability of river ice cover formation and progression along the Slave River.

Preface to Chapter 3: Air pocket formation along the Slave River ice cover

Chapter 3 focuses on the formation of air pockets along the river ice cover and fulfills the second objective of this research. Field observations of the ice and hydraulic parameters together with the geomorphological structure of the river provide insight into the understanding of this phenomenon. Steeper channels and several open water sections appear to be contributing to significant amounts of air entrainment into the water during winter. Changes in the hydraulic characteristics of the river during ice cover formation and progression also change the quantity and distribution of air pockets along the river's ice cover. This research also developed a conceptual model to discuss the characteristics and formation of the air pockets.

The manuscript from this chapter has been submitted to the Journal of Cold Region Science and technology.

Das, A., SRDP, and Lindenschmidt, K. E. (submitted). Air pocket formation along the Slave River ice cover. *Cold Regions Science and Technology*.

Contributions of Authors: Apurba Das (75%) contributed a major part of the research analyses and all the writing of the manuscript. The Slave River and Delta Partnership (SRDP) (10%), the people from the local communities, contributed their traditional knowledge in this research. Karl-Erich Lindenschmidt (15%) helped to develop the conceptual model and mesh together traditional and western knowledge to aid in understanding air pocket formation along the river ice cover. Additionally, he revised the manuscript during the writing.

Chapter 3 : Air pocket formation along the Slave River ice cover

3.1 Introduction

Changes in the behaviour and characteristics of the Slave River ice cover due to flow regulation are a key concern for the communities along this river in the Northwest Territories (NWT). In particular air pockets or air layers in the ice cover significantly impact traditional ways of living and subsistence activities during winter. These formations pose a major obstacle to winter travel to hunting, trapping and fishing areas. There is a great risk to travel on the river ice because large, trapped air pockets within the ice cover make the ice at these locations thin and unstable, and impede thermal thickening of the ice cover. The bulges that these pockets form are difficult to detect especially on cloudy, hazy days when there is little light contrast to highlight contours along the snow covering the ice. The air pockets can become quite large and snowmobiles have broken through the pocket areas, making winter travel on the ice at times a very treacherous ordeal (AANDC and ENR 2012). The main purpose of this research is to investigate plausible reasons for air pocket formation along the Slave River ice cover.

3.2 Ice formation with air entrainment

The mechanisms of ice cover formation and progression depend on meteorological factors as well as various hydrodynamic characteristics of the river, such as flow conditions, water temperature and the geomorphology of the river (Beltaos 2013).In the channels of the river, where the flow velocity and turbulence intensity is sufficient and strong enough, frazil ice crystals are nucleated and grow in super-cooled water. In this stage, many frazil ice crystals are generated at an intense rate and the process is called secondary nucleation (Beltaos 2013; Hicks 2008). It is a process that produce of new crystals due to presence of ice crystals. This process creates very small crystal nuclei which can further increase the rate of ice crystallization, either by collisions between the ice crystals or fluid shear forces throughout the water column. Due to their adhesive nature, frazil ice particles attach to each other or other material (e.g. sediment particles) to form frazil slush or flocs (Beltaos 2013; Hicks 2008). At some point, this frazil slush becomes large and buoyant enough to float to the water surface and create frazil pans. These flow downstream until their flow is arrested at a stationary ice cover or an ice bridging section of the river.

In areas (near the river banks, and edge of the islands), where the water velocity is low and turbulence intensity is not sufficient, the super-cooled water generates a smooth ice cover from crystals at the water surface which continue to grow in the horizontal and vertical directions to form a skim ice layer (Beltaos 2013). The thermally grown skim ice often leads to formation of border ice if it is attached to the banks of the river or islands. This type of ice can have a major impact on the ice regime of the river. As border ice grows thermally downwards and horizontally towards the middle of the channel from the banks, the wetted perimeter and overall flow resistance increase. As a result, upstream water levels rise, which reduces the flow velocity and sediment transport capacity (Beltaos 2013). At some point, this border ice can impede the continued downstream progress of ice pans or create an ice bridging along a constriction or narrow channel of the river. The ice pans continue to form and become denser until their movement is arrested at an ice bridging section. The surface ice will continue to accumulate and progress upstream along the river to form a stationary ice cover called a juxtaposed ice cover. This ice cover then thickens thermally downwards or by additional deposition of frazil ice particles underneath the ice cover to form a consolidated ice cover. An ice cover can also be thickened at the upper surface through snow ice development. The snow ice, often called white ice, looks white due to the high concentration of air inclusions between the ice crystals and the anisotropic orientation of the crystals. Very turbulent sections along the river or reaches downstream of rapids or waterfalls can introduce air into the water column, which accumulates as large bubbles under the ice cover and can be imbedded as air pockets in the ice cover as it thermally thickens. An example of large air bubbles forming and flowing under ice covers can be seen at https://www.youtube.com/watch?v=1SJZyeA2gvs and https://www.youtube.com/watch?v=a7yqPb8gIW4.

At hydraulic structures dissolved oxygen saturation depends on a variety of factors, such as water temperature, water depth, content of dissolved oxygen upstream of the structure and water pressure. The concentration of oxygen becomes relatively high in super-cooled water (Scheiber and Gutmann, 1993). However, the amount of dissolved oxygen may decrease with increasing water temperatures. As water flows under the ice cover, it warms slightly from its super-cooled state allowing air to be released from the water and become trapped under and within the ice cover as the ice thermally thickens. Deeper water columns in the river downstream of structures may also increase the dissolved oxygen saturation in the downstream reach because less air can escape

(Li et al. 2010). Deeper flows reduce the rate of oxygen transfer (slower degassing) transporting more dissolved oxygen downstream (Li et al. 2010). Therefore, the increased water staging due to river ice cover formation may increase the dissolved oxygen saturation downstream of structures and rapids.

Water pressure can also retain air-supersaturation in the water (FEI 2014). Increased rates of water flow underneath the ice channel mimics piped flow to increase the water pressure and hence cause more dissolved oxygen to be retained in the river water. The amount of dissolved oxygen saturation downstream of a hydraulic structure is found to be linearly related to dissolve oxygen content in the upstream reach (Li et al. 2010). Therefore, initial high dissolved oxygen in the upstream portion lead to higher levels of dissolved oxygen saturation along the reach downstream from the hydraulic structure.

Literature directly addressing the subject of air pocket formations under river ice covers is sparse. A few studies have been carried out to examine the characteristics of air inclusions in river ice and air bubble formation in ice (Carte 1961; Gherboudj et al. 2007; Yoshimura et al. 2008). The main source of air bubbles or air pockets in ice is the dissolved oxygen in water (Carte 1961). During the formation of ice, water at the ice-water interface becomes supersaturated, allowing the air to be released from the water. This oxygen then becomes trapped under and within the ice cover as the ice thermally thickens. The physical characteristics (e.g. size, shape, and density) of air bubbles in ice mainly depend on the amount of dissolved oxygen in the water, the rate of freezing and type of ice. Increasing the dissolved air in water can increase the growth of bubble formations in ice. Steeper and more rapid flowing sections of a river contribute to rapid freezing and super-cooling of the water which facilitates the higher entrainment of air into water. As a result, more air inclusions and bubbles form in the ice. Rapid freezing can lead to higher concentrations of relatively smaller bubbles in the ice; however, slower freezing produces fewer and larger sized bubbles in the ice (Carte 1961).

The characteristics of air bubbles in different types of ice have also been studied by Gherboudj et al. (2007), who suggest that columnar or black ice, which is clear and transparent, may contain some air bubbles. However, thin layers of frazil ice within the thermal or black ice layers can contain significant amounts of air bubbles (Gherboudj et al. 2007).

3.3 Study area

The Slave River is one of the largest transboundary rivers in Canada (Figure 3.1). It is essentially a continuation of the Peace River at the Peace Athabasca Delta (PAD), where additional flows from the Athabasca River/Lake Athabasca system contribute to the Slave River's discharge. The Slave River flows 440 km northward before flowing into Great Slave Lake, draining a total catchment area of 616,400 km^2. Many small and large islands braid the river along its flow path, with the flow width ranging between 300 and 2000 m. About halfway along the river, there is a series of four rapids (Cassette Rapids, Pelican Rapids, Mountain Rapids, and Rapids of the Drowned) where the river bed drops 34 m from Fort Fitzgerald to Fort Smith. The mouth of the river, near Fort Resolution, forms the Slave River Delta which consists of several active channels: Nagle, Steamboat, Middle, and Resolution Delta Channels. In addition, the Jean River diverts water from the Slave River around the delta to Great Slave Lake.

Two study sites (Figure 3.1) along the Slave River were selected for ice cover surveys: Evans' Cabin and the Slave River Delta. The field guides suggested these sites due to their past observations of air pocket formation at these locations. Also accessibility and familiarity of the locations were also considered to select these sites. As the river is very remote and far from the locality the study locations were also selected, considering the day length during the winter seasons. The first study area is situated near Fort Smith, 42 km downstream from the Rapids of the Drowned. The width of the river in this area is approximately 700 m. The second study site begins about 10 km upstream from Great Slave Lake and extends 12 km upstream to include the entrance to the Jean River. The average channel width at this site varies from about 400 to 700 m.

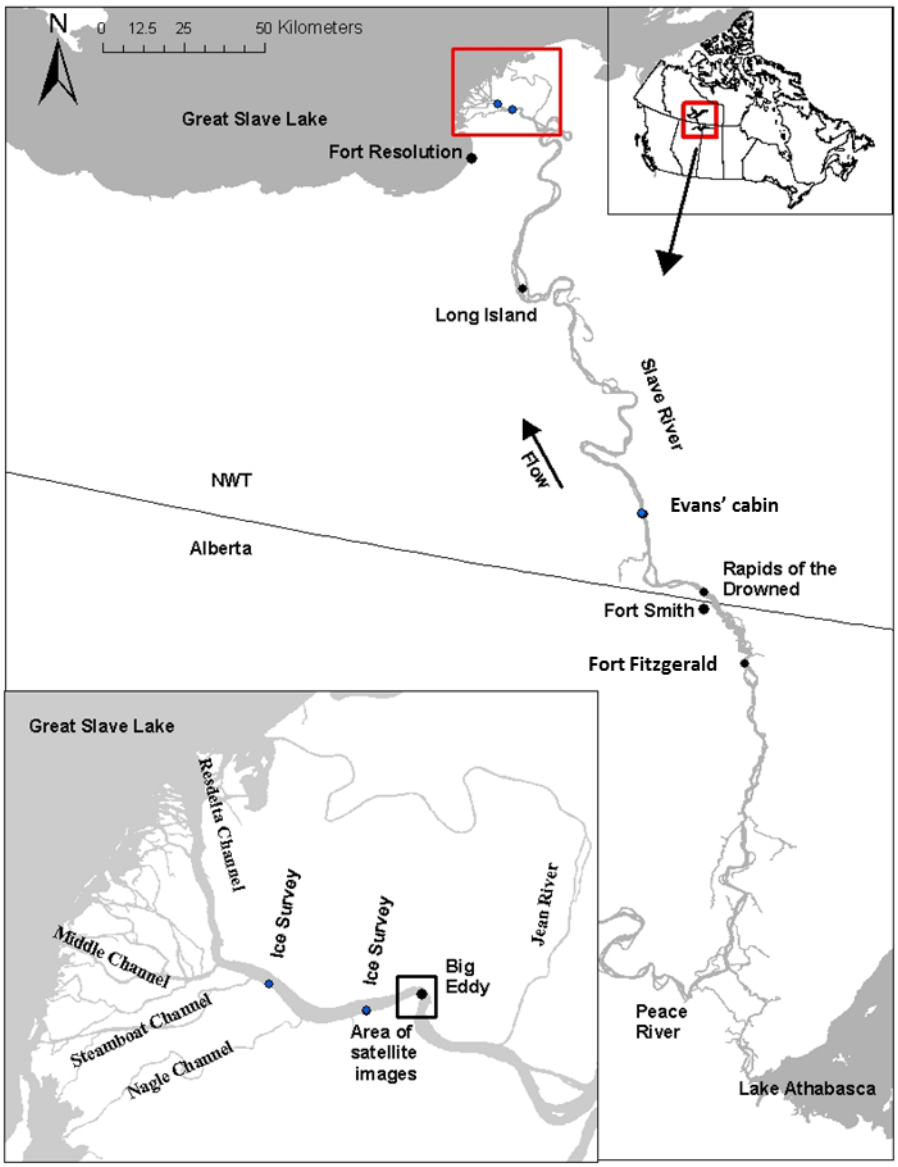

Fig. 3.1 Slave River and Slave River Delta.

3.4 Data

3.4.1 Field sampling

The first field sampling campaigns along the Slave River were undertaken during the 2013– 2014 winter. The sites at Evans' Cabin and in the Slave River Delta were selected to measure ice thicknesses and observe changing ice conditions during the course of the winter season. The locations of the air pockets were determined during an aerial survey at the beginning of May 2014,

when all the snow along the river had melted but the ice cover had not yet broken up. The aerial survey extended from Fort Smith to the Slave River Delta.

Ice sampling continued during the 2014-2015 winter at the same sites. These surveys included measurements of ice cover thickness, observations of river ice cover conditions and extraction of ice cores with a core barrel. These cores were then examined to study ice layer profiles at and near air pockets.

3.4.2 Meteorological and hydrometric data

The daily air temperature data from Fort Smith was retrieved from the Environment Canada weather office website (http://wateroffice.ec.gc.ca/). Temperature is an important factor related to the start and progression of the ice cover formation along the river. Mean air temperatures were compared in the study areas between the winters of 2013-2014 and 2014-2015. The accumulated freezing degree days (AFDD) was then calculated for the winter period from October to March to compare the rate of freezing of the two different years along the Slave River. The AFDD is calculated by cumulatively adding the average daily air temperature below 0 °C on each successive day.

Water flow and level data were obtained from the real-time gauge at Fort Fitzgerald (Slave River at Fort Fitzgerald, 07NB001), operated by the Water Survey of Canada (WSC). Different flow conditions of the river can significantly alter the pattern of ice formation and the structure of the ice regime. Changes in ice cover characteristics and behaviour can be attributed to the nature of the flow in the river and its tributaries (Beltaos 2013). This study analyzed the daily average discharges of the Slave River during the winters of 2013-2014 and 2014-2015.

3.4.3 RADARSAT-2 imagery

Radarsat-2 satellite images were acquired along the river in both winter 2013-2014 and winter 2014-2015, in order to understand the ice cover conditions and to identify different types of ice cover along the river. The methodology of the derivation of ice types along the Slave River from satellite images was explained in chapter 2.

3.5 Results and discussion

During the 2013-2014 winter, several air pockets were observed along the river ice cover in both study areas. Although concealed by the snow pack, many air pocket locations were revealed as bulges protruding from the ice cover. Most of the air pockets at Evans' Cabin were observed on the main channel and near one bank where the water velocity is comparatively high. Downstream from the Rapids of the Drowned, where the river is always open, the air can entrain at the water surface and flow under the ice cover. The air degasses and accumulates on the ice underside to form pockets and layers. The link http://youtu.be/lTy5OVRe5cA provides a video of a hole punctured through the top of an air pocket with the air venting from the ice cover. Venting continued for approximately 5 minutes before water gushed out like a geyser, shown at the link http://youtu.be/uc2QEntaeG0. Thin ice covers with air layers within the ice cover were also observed in several areas along the Slave River Delta (Das et al. 2015).

The aerial survey just before breakup also revealed the air pocket density in various locations along the river. Most of the air pockets at Evans' Cabin were detected near the shoreline and main channel of the river (Figure 3.2). The Slave River Delta had a high density of air pockets with plenty of small and large sized air pockets distributed over the ice cover. The ice at many air pocket locations had melted, leaving behind circles of open water in the ice cover (Figure 3.3). Ice cover thicknesses over the air pocket areas were comparatively thinner so that, during the pre-breakup warming period, air pocket areas opened up first along the river.

Fig. 3.2 Air pockets on the main channel and right bank of the Slave River near Evans' Cabin.

Fig. 3.3 High concentration of air pockets at the Slave River Delta.

During the 2014-2015 winter field survey, much attention was dedicated to examining air pockets and observing the ice cover conditions of the Slave River. Many air pockets were observed during field sampling on 24 and 25 January 2015 near Evans' Cabin. The air pockets were observed mainly along the main channel of the river where the flow velocity was relatively high. In areas with a high flow current, an uneven underside of the ice cover may provide cavities for trapped air. The unevenness of the ice cover underside was substantiated by ice thickness measurements taken from more than thirty spots at the site, with thicknesses varying from 0.4 to 0.8 m. Air pockets were found to be irregular in shape, with several of them joined together. The dimensions of the air pockets ranged from 0.2 m to 1 m in length. Air trapped within the ice cover looked white, making the pockets visible through the transparent black ice cover (Figure 3.4).

Fig. 3.4 Air trapped within the ice cover looks white and is visible through the transparent black ice cover (photos taken on 24 January 2015 at Evans' cabin near Fort Smith).

Several layers of ice and air pockets were examined in partially drilled auger holes. Air pockets can extend vertically downward and also horizontally throughout the ice cover. Some of the pocket were filled with compressed air, so when a hole was punctured through the top of the ice into an air pocket, compressed air escaped quickly. The pocket then filled with water through cracks of the bottom layer of the ice, providing a link between the air pocket and the pressurized water column. The air pocket filled up with pressurized water and then gushed out and flooded the top surface of the ice cover. A conceptual model of the air pocket, derived from field observations, is shown in Figure 3.5. Air pockets may form underneath the ice cover when the ice cover thermally thickens downward. As the winter progresses, air detrained from the turbulent water can accumulate between the ice cover and river water. Continued downward thermal ice thickening can trap the air, enclosing the air pocket within the ice cover. Snow accumulation on the ice cover may be heavy enough to break through the top ice layer, collapse the air pocket, and flood and freeze the void at the puncture location. Subsequent thermal thickening may occur. The air in those pockets located closer to the upper ice surface, with no hydraulic connectivity to the underlying water column via cracks through the ice, will not be compressed. The air becomes pressurized if the pocket is hydraulically connected to the pressurized water column via cracks, especially those pockets that are embedded closer to the ice-water interface.

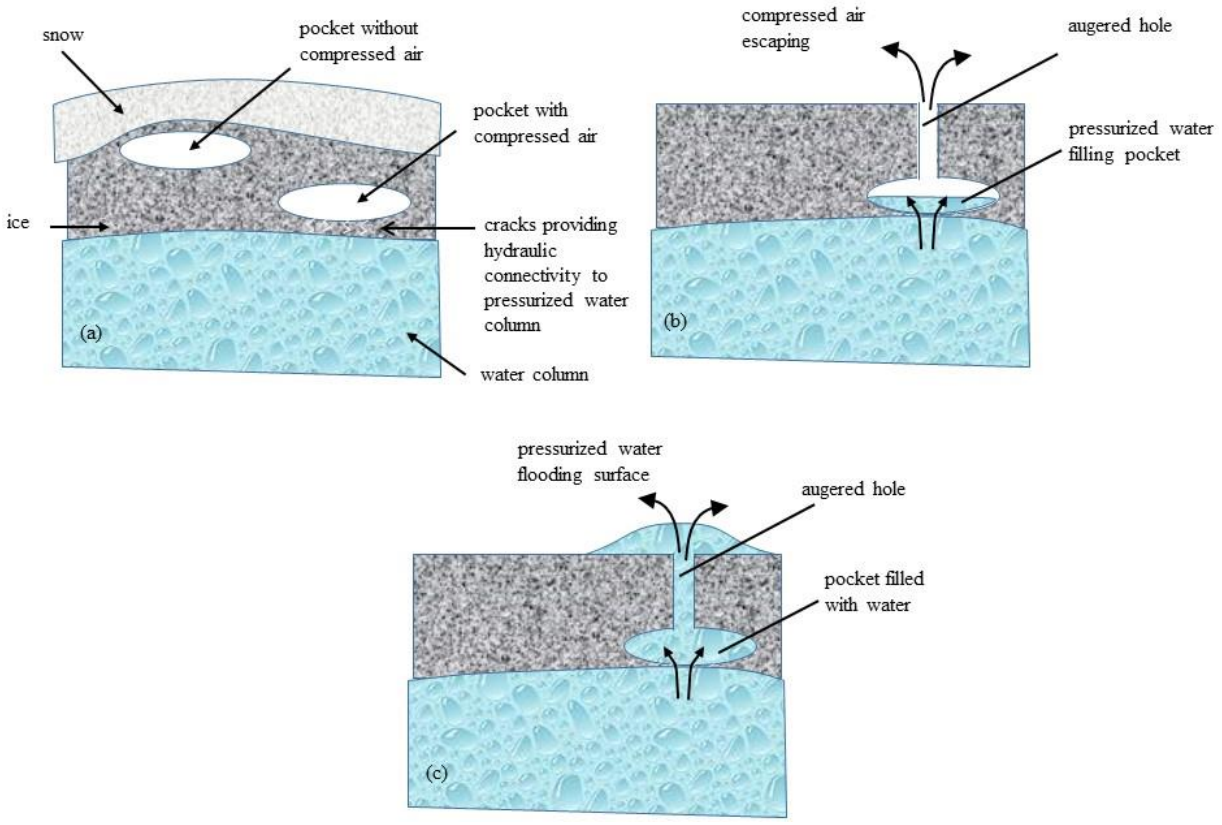

Fig. 3.5 Conceptual model of air pocket observations along the Slave River.

Several ice cores were also collected at Evans' cabin, in order to examine the vertical ice profiles and determine if slush ice accumulates on the ice cover underside. Ice cores were extracted at locations with and without air pockets. A solid and intact ice core was extracted from the locations with continuous ice without air pockets. However, another ice core was fragmented in several pieces due to air pockets or layers within the ice cover (Figure 3.6). No slush ice was observed. The average total ice thickness and average snow depth were measured to be 0.65 m and 0.23 m, respectively. Although the site was mostly dominated by black or thermal ice cover, snow ice was also present and averaged 0.2 m in thickness.

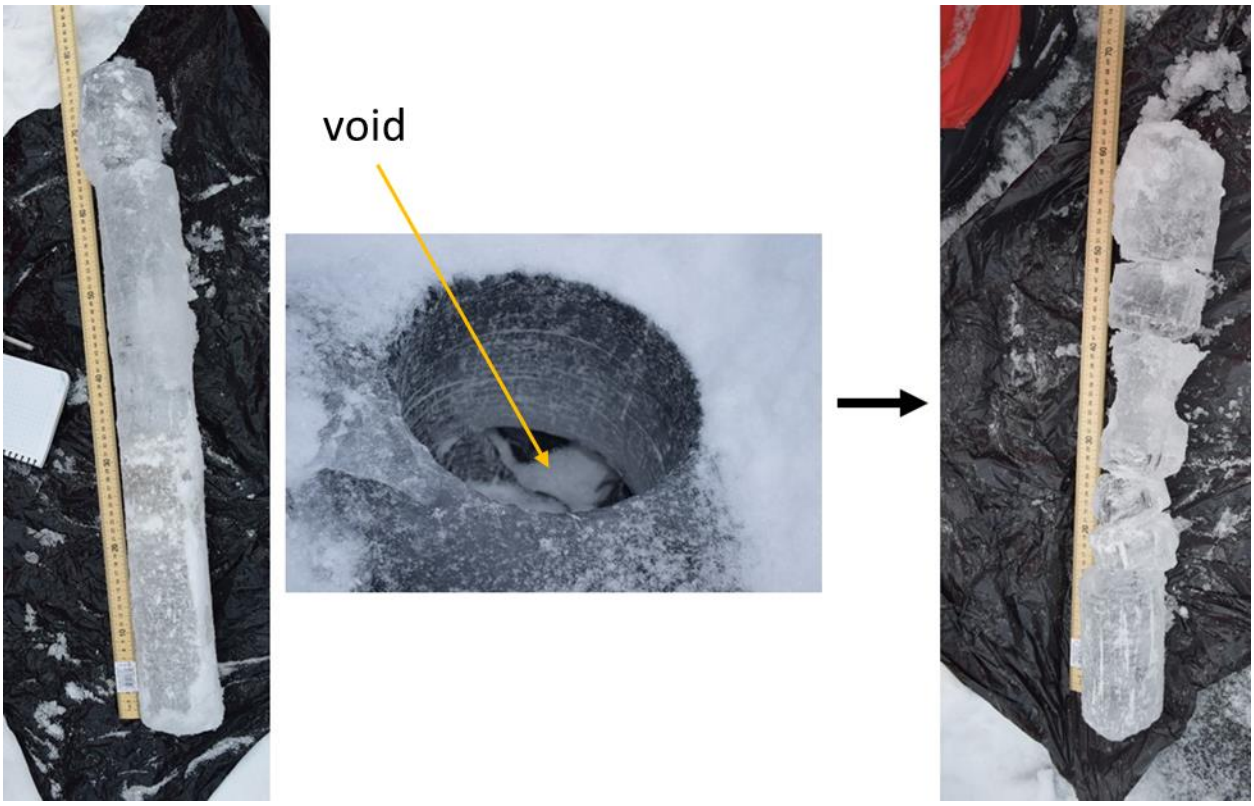

Fig. 3.6 Ice cores were collected at locations without air pockets (left panel) and with air pocket layers (right panel), extracted near Evans' cabin on 24 January, 2015. The augured hole (middle panel) shows voids at its sides.

Several ice cores were also collected on 30 January 2015 between Big Eddy and Nagle Channel in the Slave River Delta. The ice cover consisted mostly of black ice and very few air pockets were observed during the field survey. Most of the ice cores were continous and intact. The average total ice cover thickness and average snow ice depth were 0.52 m and .18 m, respectively. Snow accumulation on the ice cover was also quite thick, with an average snow depth of 0.3 m.

RADARSAT-2 satellite images were acquired during both winters, 2013-2014 and 2014-2015, to monitor the river ice cover condions. As depicted in Figure 3.7 (left panel), at the beginning of the 2013-2014 winter an ice bridging occurred at Big Eddy, upstream from which a juxtaposed, consolidated ice cover formed. The relatively narrow and sinuous channel at Big Eddy is conducive to ice bridging and arrest the flow of ice pans to form a stable ice cover. An open water section was maintained just immideately downstream of this ice bridge, further downstream

(approximately 3 km) of which a thermal ice cover formed with some slush deposited on the cover's underside. The turbulent flow and open water at Big Eddy may have supplied the air and frazil entrained in the water, that was subsequently deposited on the underside of the downstream ice cover. This supply of air and frazil ice persisted, as indicated by the brightening (increased backwater signal) of the image along that river location in the December 2013 image and more brightening (increased whitening and reddish tinge) in the January 2014 image. Field observation at the end of January 2014 detected air pockets along that area.

At the beginning of the following winter (2014-2015), the river discharge was 25% lower at freeze-up than during the freeze-up of the previous winter (Figure 3.8). In Figure 3.7 (right panel), there is no indication of ice bridging at Big Eddy and the ice cover consisted more of a continuous thermal ice cover (black ice) with some patches of consolidated ice (white/reddish patches) along the reach. No ice pockets or layers were observed during this winter's field surveys.

High turbulence of the water due to high flows may lead to more air detraining from the water, resulting in higher amounts of air inclusion in the ice cover. Relatively low flow conditions during the 2014-2015 winter may have formed smooth black or thermal ice cover along the river, resulting in less air pocket formation between the ice cover.

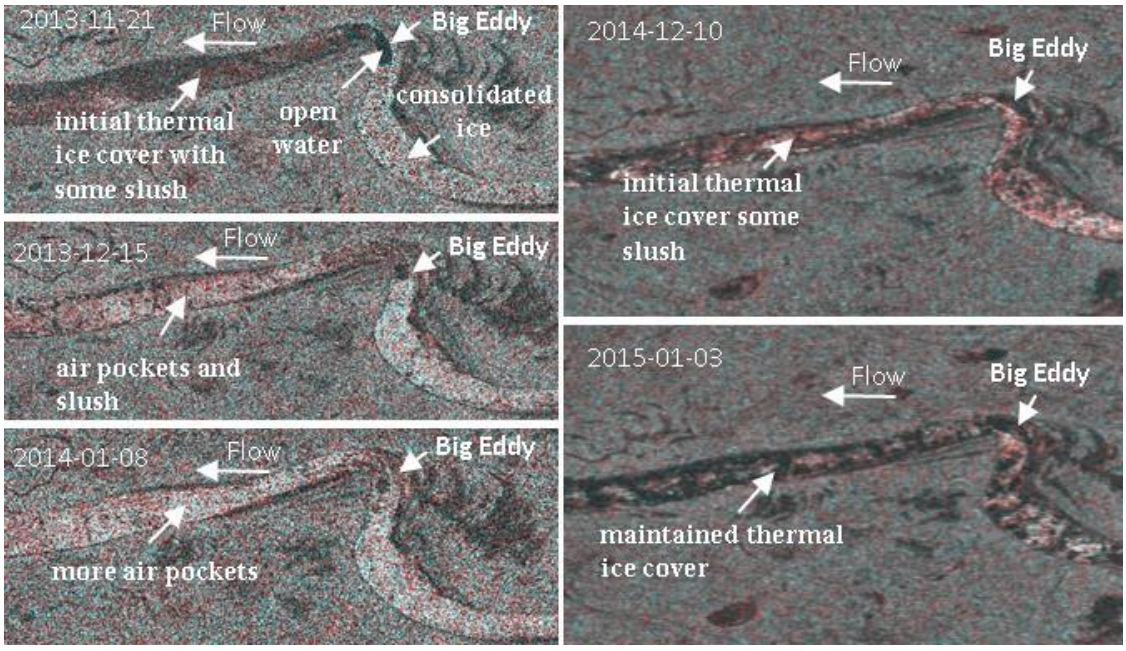

Fig. 3.7 FOW3 RADARSAT-2 satellite images along the Slave River Delta retrieved from Slave River Delta in the winters 2013-2014 (left panel) and 2014-2015 (right panel). (RADARSAT-2

Data and Products © MacDonald, Dettwiler and Associates Ltd (2013-2015) — All Rights Reserved. RADARSAT is an official trademark of the Canadian Space Agency).

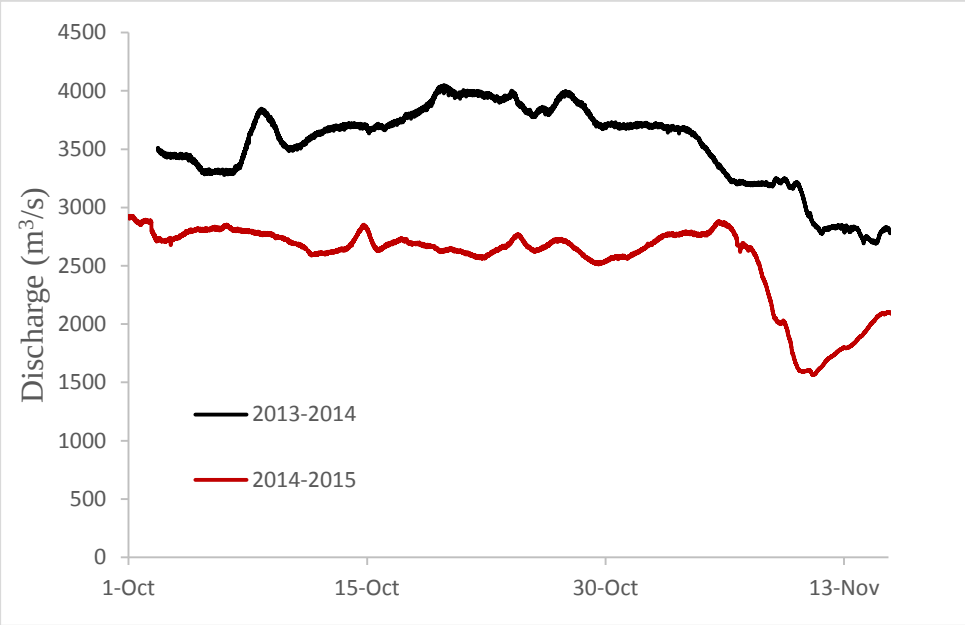

Fig. 3.8 Discharge along the Slave River at the Fort Fitzgerald gauge station (Data source: Water Survey of Canada, Gauge # 07NB001).

Two years of ice surveys and observations of the Slave River reveal that air pocket formation in the ice cover is a complex ice process, which can likely be attributed to the physical structure of the river and hydraulic characteristics of the river. There is a set of four rapids along the Slave River between Fort Fitzgerald and Fort Smith, along which a significant amount of air can entrain into the water due to the high turbulence. Several sections along the river are also continously open during the entire course of winter, especially the sections just below the Rapids of the Drowned (Figure 3.9). Once air entrains and is dissolved into the water, it can be transported long distances under the ice until it is detrained and degassed from the water and trapped in enclaves under the ice cover.

Fig. 3.9 Open water sections along the Slave River, below the Rapids of the Drowned (right panel) and Sawmill Island (left panel).

The Slave River is a braided river. There are many small and large islands creating multiple water channels along the river. Therefore, border ice forming around the islands and along the edge of the river banks could be the most dominant factor changing the flow characteristics of the river. As the ice in the side channels between an island and the mainland thickens, flow through the side channel is constricted and is diverted towards the main channel, making the flow progressively more turbulent during the course of winter. Additionally, when the border ice extends towards the middle of the channel and thickens vertically, the wetted perimeter of the channel will be increased, resulting in overall channel resistance and an increase in the water level. A rise in the hydraulic resistance of the river may force more water into the main channel and increase its flow velocity and turbulence intensity. This can result in large numbers of air bubbles and a higher density of air pockets forming in the ice cover. Field observations at Evans's Cabin revealed the main channel of the river had a higher number of air pockets compared to other portions of the channel.

Varying flow characteristics can lead to different ice cover formations along the river. The flow fluctuations of the Slave River during the course of winter change the ice cover characteristics and behaviour, such as ice cover cracking and flooding. Water level increasing can also lead to the formation of open water sections during the winter. High water velocities and turbulence can maintain open leads, which further contributes to the entrainment of air at the water surface.

Analysis of the accumulated freezing degree days (AFDD) over the entire winter season may provide a useful tool to understand the rate of freezing during each winter, as well as the variation in freezing in different years. Figure 3.10 illustrates the AFDD of the Slave River at Fort Smith

for the winters 2013-2014 and 2014-2015. As the rate of freezing during the freeze up of both study years was similar, it can be concluded that changes in ice characteristics and variations in the number of air pockets along the river ice cover can be mainly attributed to the flow characteristics of the river.

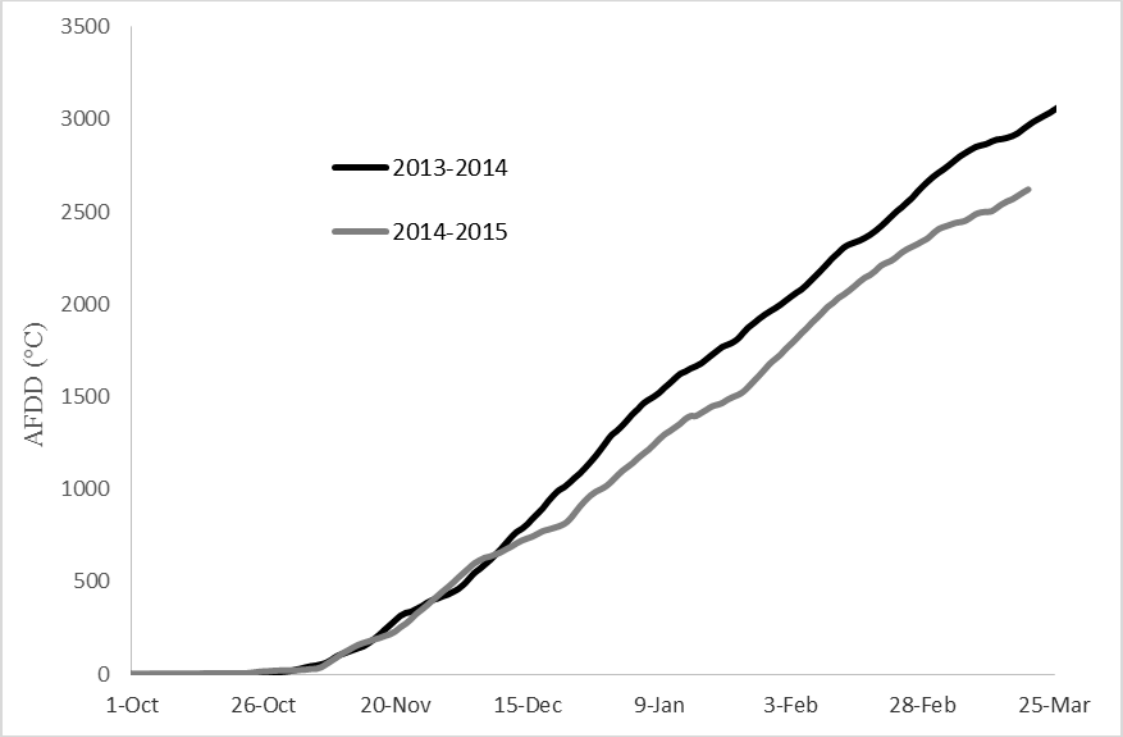

Fig. 3.10 Accumulated freezing degree days (AFDD) at Fort Smith between winters 2013-2014 and 2014-2015.

3.6 Conclusion

The results of this study suggest that air pocket formation is dependent on the physical structure and hydraulic characteristics of the river. Steep sections along the set of four rapids around Fort Smith, with several open water sections along the river, contribute a significant amount of air entrainment into the water. The entrained and dissolved air may then be transported under the ice cover. Detrained and degassed air can then be trapped in the ice cover to form air pockets. The flows along the Slave River fluctuate during the course of winter. This variability of the flows affects the underside of the ice surface and dissolved air concentrations along the river. High velocity and high turbulence of the water may create a greater quantity of air bubbles, which may become trapped between the ice cover when the ice cover thermally thickens. Air pockets usually

form in areas of faster water flows and high water turbulence, therefore the formation of air pocket can be mainly attributed to flow characteristics of the river.

Preface to Chapter 4: A geospatial model to determine patterns of ice cover breakup along the Slave River

The third objective of this research is to characterize the spring ice cover along the Slave River. Chapter 4 investigated the spring ice cover breakup patterns along the river. MODIS satellite images were used to trace ice cover breakup event between 2008 and 2011. A geospatial model was introduced to understand how the geomorphology of the river affects ice cover breakup patterns, and to locate the most likely areas of breakup initiation and ice persistence of the ice cover during the breakup period. Relatively narrow river sections are conducive to the initiation of breakup and relatively wide sections have a strong predisposition for persistent ice. The magnitude of the river flows during the breakup has a strong influence on flooding in the Slave River Delta.

The manuscript from this chapter has been accepted for the publication in the Canadian Journal of Civil Engineering.

Lindenschmidt, K. E., and Das, A. (2015). A geospatial model to determine patterns of ice cover breakup along the Slave River. *Canadian Journal of Civil Engineering.* http://www.nrcresearchpress.com/doi/abs/10.1139/cjce-2014-0377#.VP4WB_nF98E.

Contributions of Authors: Apurba Das (80%), co-author of this paper, contributed to a major portion of this research and the writing of the manuscript. Additionally, he prepared and organized the necessary data to develop the geospatial model for this study. Karl-Erich Lindenschmidt (20%), primary author of this paper, applied the geospatial model to characterize the spring ice cover breakup along the Slave River and also made necessary revisions to the manuscript.

Chapter 4 : A geospatial model to determine patterns of ice cover breakup along the Slave River

4.1 Introduction

The Slave River is a transboundary river and the Slave River Delta (SRD) is a freshwater ecosystem which is considered to be one of the most productive in the Northwest Territories (NWT) (AANDC and ENR 2012). The delta includes a wide variety of vital habitats for plant and animal species; the population of waterfowl is notably abundant. One of the key requirements needed to replenish and maintain a healthy, balanced delta ecosystem is seasonal flooding. The construction of the Bennett Dam on the upper Peace River in 1968 resulted in significant changes in the annual flow regime of the Slave River. Due to flow regulation, the annual hydrograph has been modulated with winter discharge in the Slave River having significantly increased, while spring discharge has dramatically reduced (AANDC and ENR 2012; Prowse et al. 2002). This reduction in seasonal variation in flows may impact spatial and temporal patterns of the springtime ice cover breakup along the Slave River.

In recent years, the frequency of large magnitude spring floods has reduced along the Slave River and Slave River Delta (AANDC and ENR 2012; Prowse et al. 2002). This decrease in flooding has resulted in prolonged dry periods, leading to an influx of invasive vegetation more tolerant to dry conditions (e.g. willows). This increase in dryness and encroachment of invasive flora have resulted in a shrinkage of wetlands in the Slave River Delta. In order to better comprehend the cause of these recent arid conditions, a clear understanding of the Slave River hydrology, and that of its delta, is necessary. River ice is an important element of a river's hydrology and examining the ice breakup patterns is essential to determine possible causes of reduced flood frequency and for the development of possible mitigation measures through adjustment in flow regulation in the Slave River.

A very limited number of studies exist that describe the spring breakup phenomenon along the Slave River. One such example, Brock et al. (2008), used water isotope tracers and total suspended sediment (TSS) concentrations to examine the occurrence of ice jam flooding in the Slave River Delta. They identified flood and snowmelt induced lakes in the Slave River Delta during the spring of each year from 2003 to 2005. Moderate flooding occurred in 2003, no flooding occurred in

2004, and a major flood was recorded in 2005. The results indicate that the Slave River discharge was one of the most important and dominating factors in flooding the Slave River Delta. The occurrence of ice jams may be an important prerequisite for spring flooding.

A number of different factors are involved in the phenomenon of spring ice cover breakup along a river, such as the meteorological, hydraulic, and geomorphological conditions of the river. During the pre-breakup period, warmer air temperatures may decrease the ice cover thickness and an increase in solar radiation may reduce the ice strength to trigger the initial fracture of a river ice cover. At this time precipitation and local snow melt increase the discharge, leading to continued fragmentation and movement of ice along the river (Beltaos 2008). Once an ice run begins the blocks, broken from large ice sheets, move downstream. The movement of the floes is sometimes arrested at an obstacle or pre-existing solid ice cover, and an ice jam is formed. Channel morphology can also strongly influence the occurrence and formation of ice jams along the river. Complex river structures such as the presence of islands, high sinuosity and abrupt changes in slope are also important factors leading to the formation of ice jams (De Munck et al. 2011, Kalinin 2008). Ice jams can remain intact for a few minutes or for several days and cause backwater effects and flooding along the river (Woo 2008). However, further increases in water level, flow velocity as well as shear stresses on the jam can release the jam and set the ice fragments back into motion continuing the process until the ice has cleared from the river. Therefore, identifying probable ice jamming locations during breakup is vital to understanding the entire pattern of ice breakup along a river.

Predicting the occurrence of ice jamming is very difficult. A better approach may be to determine the predisposition of certain river reaches to ice jamming (De Munck et al. 2011). Kalinin (2008) identified six potential geomorphological features of rivers which can influence ice jam formation: islands, bridges, sharp bends, loops, tributaries and narrowing river sections.

A geospatial model (Lindenschmidt and Long 2013; Lindenschmidt and Chun 2013) has been developed to determine locations along a river most susceptible to ice dislodgement and jamming. The geospatial model is based on the assumption that ice cover characteristics and behavior along the river are mainly influenced by the fluvial geomorphology, so that ice dislodgement and jamming during breakup is related to physical characteristics of the river such as its slope, width, sinuosity, and obstructions (e.g. islands). Due to interdependencies of geomorphological features,

only a subset of these features may be required to determine a reach's predisposition to certain ice cover behaviours. The geospatial model clusters certain geomorphological parameters such as sinuosity, slope, and width into unique typologies by applying multivariate statistical analysis, principal component analysis (PCA). Certain patterns or sequences of typologies can be grouped into units called Geomorphic Response Units (GRUs). Correlations are then sought between GRUs and certain ice cover behavior such as breakup, dislodgement and jamming.

This study uses a series of Moderate-resolution Imaging Spectroradiometer (MODIS) satellite images to examine river ice cover breakup patterns along the Slave River and to validate the geospatial model as an indicator of potential ice behaviour. MODIS imagery are frequent (~ 1/day) enough to track the successive changes of the ice cover during spring break up including open water sections and ice dislodgement, however they are unable to track the land surface during the night and areas covered by clouds. Some studies have used MODIS imaging to better understand ice cover behavior in fluvial systems. For example, Pavelsky and Smith (2004) used MODIS imagery to determine ice cover and jamming behaviors along large Russian rivers (The Ob, Lena, and Yenisey) and a Canadian river, the Mackenzie, all of which drain into the Arctic Ocean. They utilized a series of MODIS imagery to map ice cover breakup fronts and identify the location of open water sections on a daily basis. In another study, an automated threshold decision tree technique was applied on MODIS images to track ice along the Susquehanna River in the northeastern USA (Chaouch et al. 2014). Threshold values were calculated using near infrared reflectance; lower infrared reflectance pixel values are indicative of open water, and higher infrared reflectance pixel values pinpoint ice covered sections along a river.

MODIS satellite images have also been used to monitor lake ice. For example, MODIS imagery was applied to track patterns of lake ice seasonality in conjunction with teleconnected climate oscillations (Spencer et al. 2008), while Reed et al. (2009) used MODIS imagery in this same area to assess the seasonal variability in snow pack, lake ice, and vegetation dynamics. Although these studies suggest that MODIS imagery is a feasible tool for automatic detection and monitoring of ice covers along rivers, additional in situ observations and ice characteristics data are vital for the final interpretation of results. Also essential is the understanding of a river's flow regime, temperature variations and geomorphological change setting on ice cover behavior during spring break up.

The specific objectives of this research are (i) to track ice cover behavior and breakup patterns along the Slave River during the breakup season and (ii) to develop a geospatial model to identify the most significant areas of persistent ice cover during the spring breakup

4.2 Methodology

4.2.1 Study Site

The Slave River (Figure 4.1) flows 434 km from Alberta to the NWT and drains the Peace-Athabasca-Slave River basin, a total drainage area of 616,400 km^2. It begins at the Peace-Athabasca Delta (PAD), flowing northward to finally drain into Great Slave Lake near Fort Resolution, NWT. The Peace River is the major water source of the Slave River and contributes more than half of its total annual flow; the Athabasca River and Lake Athabasca catchments contribute the remaining water to the river.

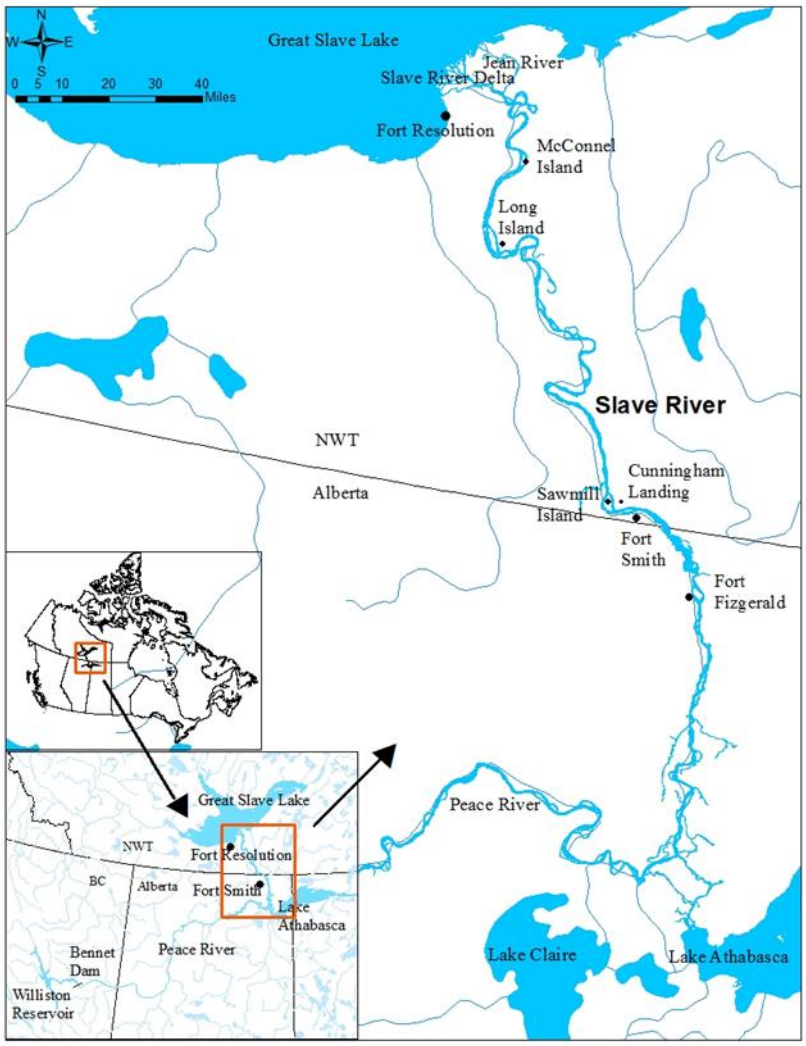

Fig. 4.1 Slave River with its important locations.

The Slave River is a braided river with split flows around a number of small and large islands all along the river. Most of the upper portion of the river is relatively straight and its average effective width ranges from approximately 550 to 1400 m. Midway along the river, a steeper flow drops at Fort Fitzgerald (Figure 4.2), along a set of four rapids: Cassette, Pelican, Mountain Portage, and Rapids of the Drowned. Further downstream the river is marked by relatively sinuous stretches and a number of islands and bars, all potential locations for the persistence of ice and ice covers during the spring breakup. At the river outlet the Slave River Delta covers an area of approximately 640 km^2 consisting of several active channels and numerous shallow lakes. The main channels are: Old Steamboat Channel, Resolution Delta Channel, Middle Channel, Eastern Channel and Nagle Channel.

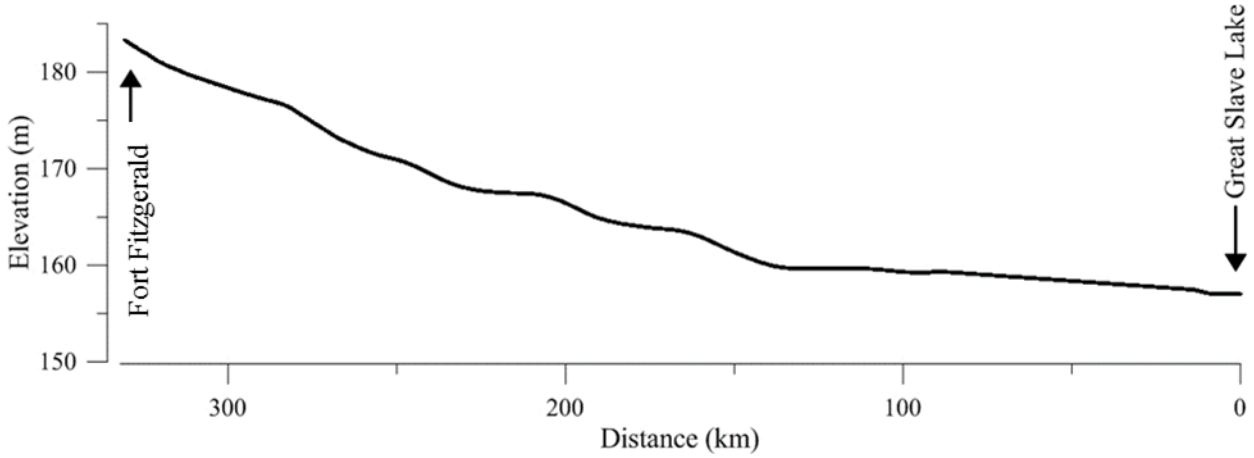

Fig. 4.2 Smoothed longitudinal profile of the Slave River from Fort Fitzgerald to Great Slave Lake.

4.2.2 Geospatial Model Development

A Geographic Information System (GIS) was used to derive the geomorphological parameters from a digital elevation model (DEM) and delineate the river network to develop the geospatial model. A centerline along the river's polygon was constructed first, then points were inserted every 50 m along this centerline. Transects were added at each centerline point to intersect both shores of the river. The length of the transect extending from the right to left shore then defined the total stream width at each centerline point. The effective width was calculated by excluding the island width from the total width (Figure 4.3). To calculate the longitudinal slope of the river, the elevations at the centerline were extracted from the DEM. The DEM data was downloaded from GeoGratis dataset (http://geogratis.cgdi.gc.ca/) at the scale of 1: 50,000. The elevation values were then extracted to centerline points using ArcGIS tools. The longitudinal profiles of the elevation points were smoothed using a running-average, from which longitudinal bank slopes at each centerline point were calculated. Sinuosity was calculated using an 8 km window. The dimension of the window along the channel centerline was determined by calculating the maximum variability in the parameters. Sinuosity was then calculated by dividing the actual flow path within the window along the stream centerline with shortest flow length of the same window.

$$Sinuosity = \frac{actual\ flow\ path}{shortest\ path\ length} \qquad [4.1]$$

Therefore, for a straight river channel sinuosity is equal to 1 and for a meandering river channel sinuosity is greater than 1.

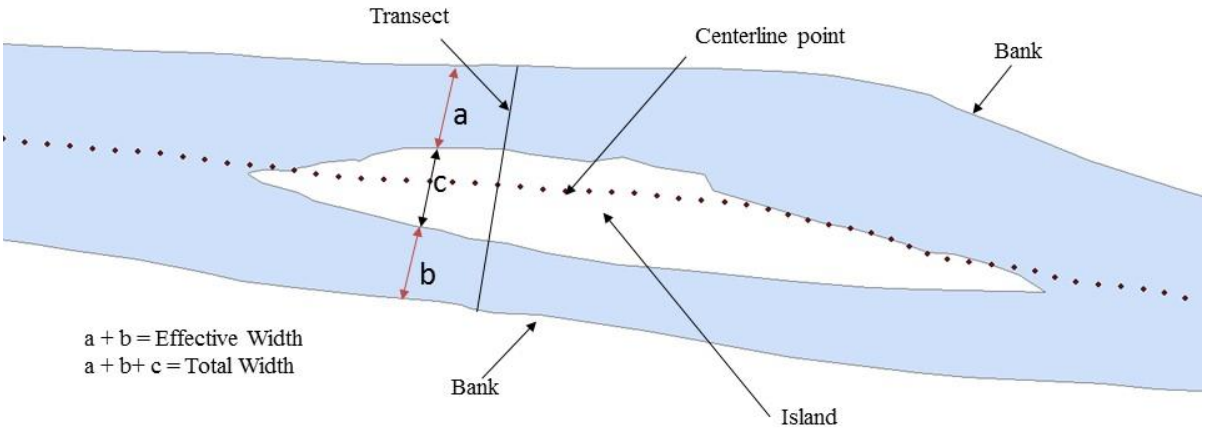

Fig. 4.3 The delineation of geomorphological variables from the river network.

The values of effective width, bank slope, and sinuosity were then grouped applying a multivariate statistical analysis called Principal Component Analysis (PCA). PCA converts potentially correlated values into a dimensionally smaller number of linear, independent values called principal components. The first principal component accounts for the largest portion of the variability in the dataset and each succeeding component accounts for the remaining variability in the dataset. The explained variances of principal components one to three were 43%, 31% and 25%, respectively. The values of the principal components were then converted into a binary number by assigning 0 for the negative scores and 1 for the positive scores and each unique combination of binary values represented different geomorphic typologies. Finally, these typologies were color coded along each centerline point and grouped to form geomorphic response units (GRUs), in which correlations to the different ice characteristics patterns are being sought.

4.2.3 MODIS satellite imagery

The MODIS is an important instrument of the National Aeronautics and Space Administration's (NASA's) earth observing system (EOS). MODIS sensors are mounted on the Terra and Aqua satellites and receive data in 36 different spectral bands. The spatial resolution - the visible, near-

infrared, and infrared bands - range from 250 to 1000 m (Chaouch et al. 2014). The Slave River is large enough that the finest resolution available from MODIS, 250 m, can be used to track river ice breakup. Time frames with relatively cloud-free acquisitions were used to characterize ice cover dislodgement and breakup patterns. A fairly complete set of daily images acquired during ice cover breakup for the year's 2008 to 2011 are provided in Figure 4.4.

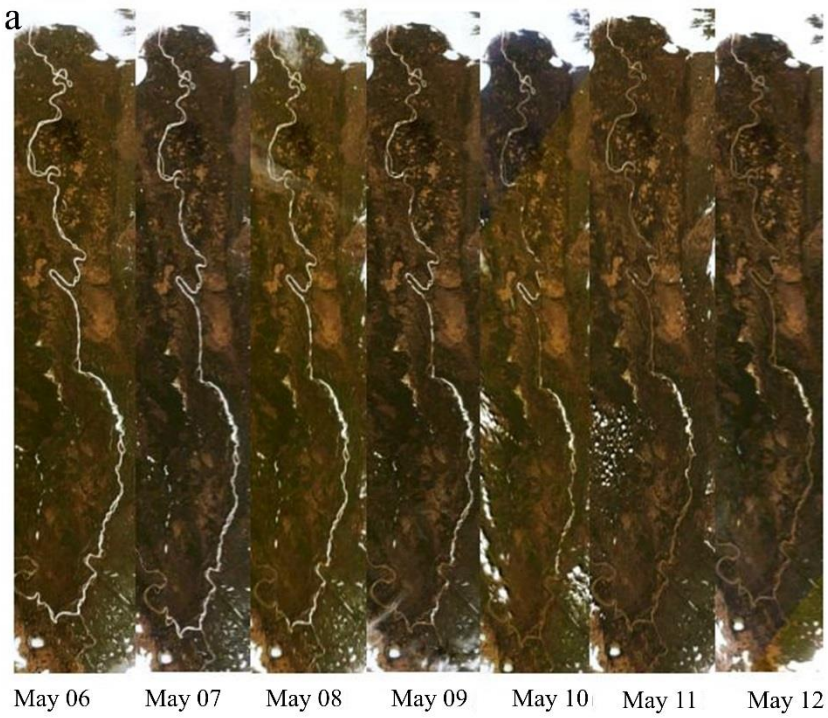

b

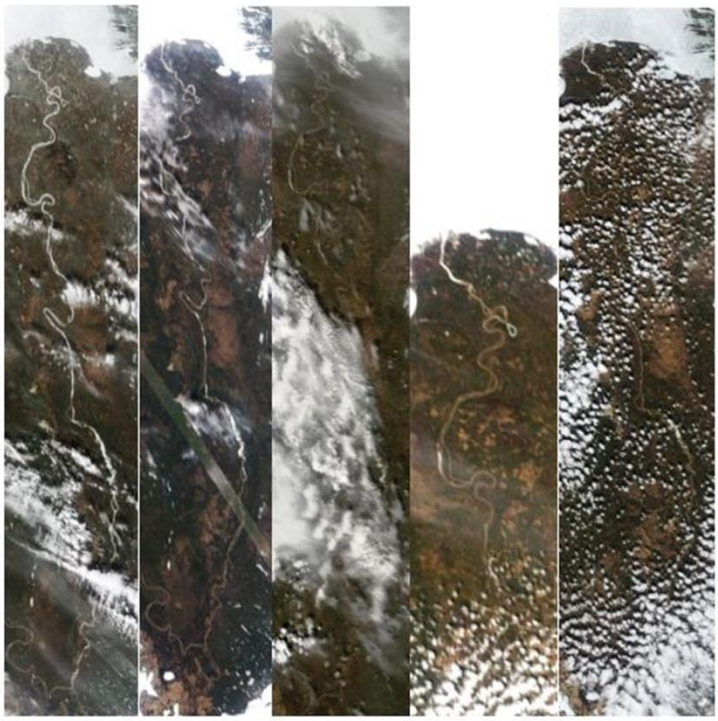

May 04 May 08 May 09 May 10 May 11

c

April 19 April 20 April 21 April 22 April 23

d

Fig. 4.4 Typical time-series of MODIS imagery acquired for the Slave River for the years (a) 2008, (b) 2009, (c) 2010, and (d) 2011. River ice appears white and open water is brown (turbid).

4.2.4 Meteorological and water level data

Daily mean air temperature data recorded at Fort Smith was retrieved from the Environment Canada weather office website. Temperature is an important factor that triggers decay of the river ice cover from the top and bottom surfaces and initiation of ice dislodgment. The study analyzed the air temperature to determine its impact on spatial and temporal patterns of the breakup event. Besides this, the accumulated freezing degree days (AFDD) was also calculated to see the total heat input into the river during the seasons. This is an empirical approach and air temperatures are the input data and the AFDD is calculated by summing the average daily air temperatures below 0°C. Temperature above 0°C can also be included in this calculation, however it reduces the AFDD value. The AFDD value can help us to determine the timing of breakup initiation along the river. Mean air temperature and an ensemble of AFDDs of all the winters between 2008 and 2011 are provided in Figures 4.5 and 4.6, respectively.

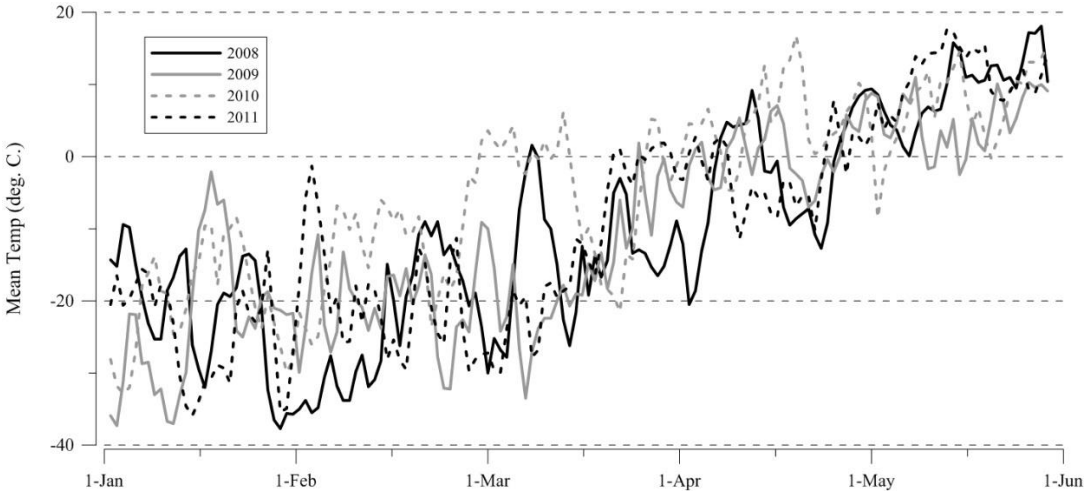

Fig. 4.5 Temperature variation at Fort Smith from winter to breakup seasons for the years 2007 to 2011.

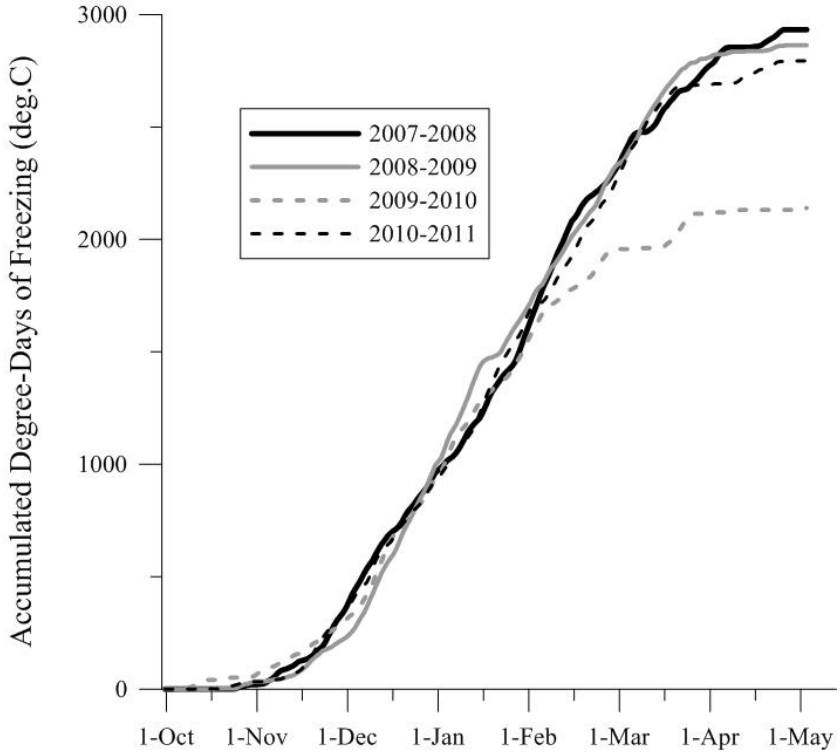

Fig. 4.6 An ensemble of accumulated freezing degree days for all winters between the years 2007-2008 and 2010-2011 at Fort Smith, NWT.

Water flows were obtained from the real-time gauge at Fort Fitzgerald, (Slave River at Fort Fitzgerald, 07NB001) operated by Water Survey of Canada (WSC). Flow conditions of the river, especially during the pre-breakup period significantly impact the temporal and spatial patterns of the breakup event. As the discharge increases, so too do water depth, velocity and surface width and the shear forces begin to increase contributing to ice cover dislodgement. A certain level of discharge is also require for ice jam flooding along the river to occur. The study analyzed the daily average discharges of the Slave River during the breakup period between 2008 and 2011 (Figure 4.7).

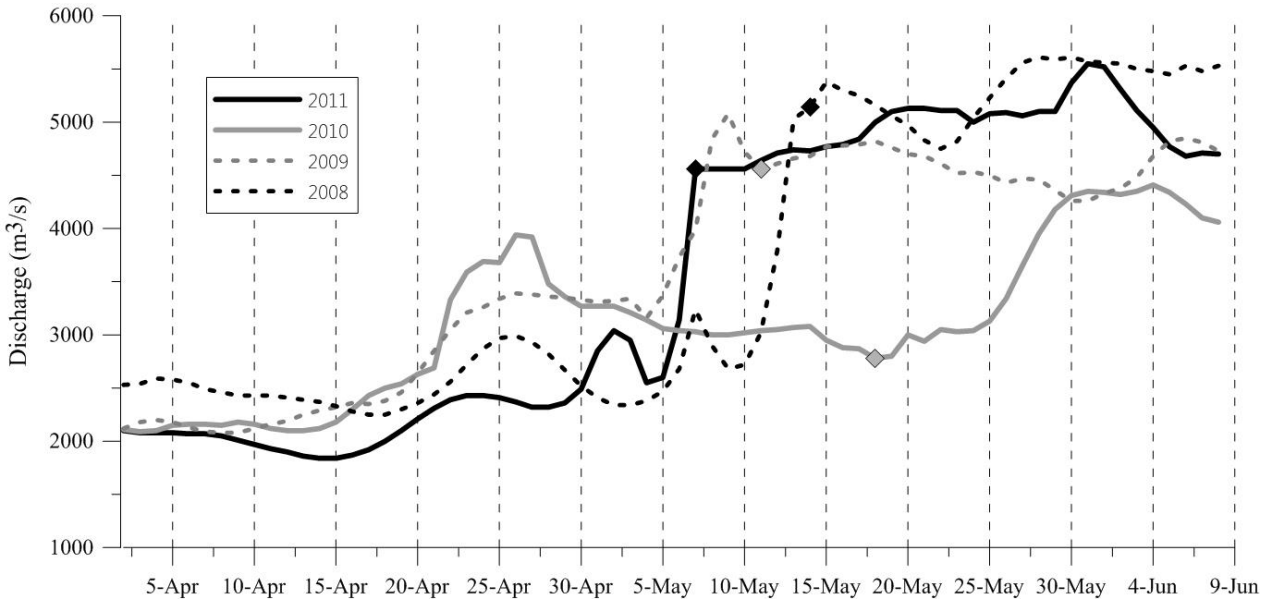

Fig. 4.7 Mean daily discharge hydrographs at Fort Fitzgerald during breakup events of the years 2008-2011. The marker points indicate the last day that ice causes backwater effects, as identified by the B values in the WSC flow data (e.g., 18 May for 2010).

4.3 Results and Discussion

4.3.1 Breakup patterns along the Slave River

Breakup of the ice cover along the Slave River usually begins near Cunningham Landing at Sawmill Island, downstream from the Rapids of the Drowned near Fort Smith. Subsequently, the breakup progresses from the upstream part of the river near the Peace-Athabasca-Delta (PAD) northward. Ice breakup patterns along the Slave River are not always consistent, as revealed by the MODIS imagery. In 2008, a series of MODIS images (Figure 4.4a) clearly illustrated the

progression of the ice cover breakup which started at Sawmill Island on 6 May and then moved slowly downstream. First, an open water section appeared in the most upstream portion of the Slave River near the PAD on 9 May. On that day, MODIS images revealed an ice clear stretch downstream of the river, slightly upstream of Long Island, in a meander of the river. There was still ice on 12 May in a 25 kilometres stretch (with a series of four rapids) between Fort Smith and Fort Fitzgerald, which is the area of highest potential for persistent ice throughout the breakup along the river. The flow hydrograph of 2008 (Figure 4.7) from the Fort Fitzgerald gauging station shows that the increase in discharge from the spring freshet occurred in the second week of May and that the average flow ranged between 2300 m^3/s and 5300 m^3/s during the breakup event, a relatively medium flow condition. Flow hydrographs also denote the last day of ice effect on water levels on 14 May.

In 2009, the ice breakup (Figure 4.4b) started on 4 May and continued into mid-May. MODIS data from 5 to 7 May was undecipherable due to cloud cover. On 8 May the MODIS image showed the river was mostly ice free from Peace Point to Fort Smith; however, there was still ice in the rapids area near Fort Smith as well as in some areas in the lower river reach. Ice was still found at Long Island on 10 May, and from Mountain Rapids to Rapids of the Drowned on 11 May. Flow hydrographs (Figure 4.7) during the breakup event illustrated relatively medium flow conditions in 2009, ranging between 2500 m^3/s and 5000 m^3/s. The last day of ice effect was on 11 May which was two days earlier than in 2008.

Patterns of ice cover breakup in 2010 (Figure 4.4c) along the Slave River were similar to 2008 and 2009 although the breakup started about three weeks earlier than in the previous year. MODIS images detected the first open water section on 19 April at Sawmill Island. Significantly low flow conditions were recorded on the river in the year 2010, ranging between 2800 m^3/s and 4400 m^3/s and a medium flow freshet occurred in the third week of April. The last day of ice effect on Fort Fitzgerald water levels (Figure 4.7) was on 18 May, a breakup event which extended one month longer than the previous year.

In 2011, ice cover breakup (Figure 4.4d) progressed in the same way as in the previous year; breakup started early in May and lasted until 7 May, with open water conditions at Fort Fitzgerald. The breakup period was shorter than the previous three years, although medium flow conditions prevailed in 2011, varying from 2000 m^3/s to 5100 m^3/s (Figure 4.7).

Flow variations can be the reflection of temporal and spatial patterns of the ice cover breakup along the river. As discharge increases, high flow shear forces applied on the ice cover trigger ice cover breakup. Eventually the forces exceed the internal resistance of the ice cover to these forces resulting in ice cover fracture and dislodgment. Although, ice cover breakup along the river usually begins in early May (only exception is 2010 when breakup started in the third week of April), the length of the breakup period may vary from year to year. In this case, besides flow patterns, other factors such as stream morphology and temperature patterns can play an important role in governing the initiation and duration of the breakup event.

4.3.2 Geospatial Model

The geospatial modelling aspect of this study focuses on the river stretch downstream of Fort Fitzgerald. PCA dimensionally reduces the values of the geomorphological parameters, producing negative and positive scores of the three geomorphological variables. Then each score is assigned the binary number 1 (for positive score) and 0 (for negative score). Each unique binary combination of the scores then constitute a specific typology. A total of eight unique typologies (numbered 0 to 7) were produced from three geomorphological parameter (sinuosity, slope, and effective width), with each typology was coded with a different color. All of the typologies were then assigned to each 50 m segments along the river. The typologies along the river from Fort Fitzgerald to Great Slave Lake are illustrated in Figure 4.8. Based on MODIS satellite imagery, the locations of initial breakup coincided with a GRU consisting mostly of Typology 0 (blue) (Figure 4.9) and the areas of persistent ice cover until the end of breakup occurred in another GRU with a large cluster of Typology 3 (green) (Figure 4.10).

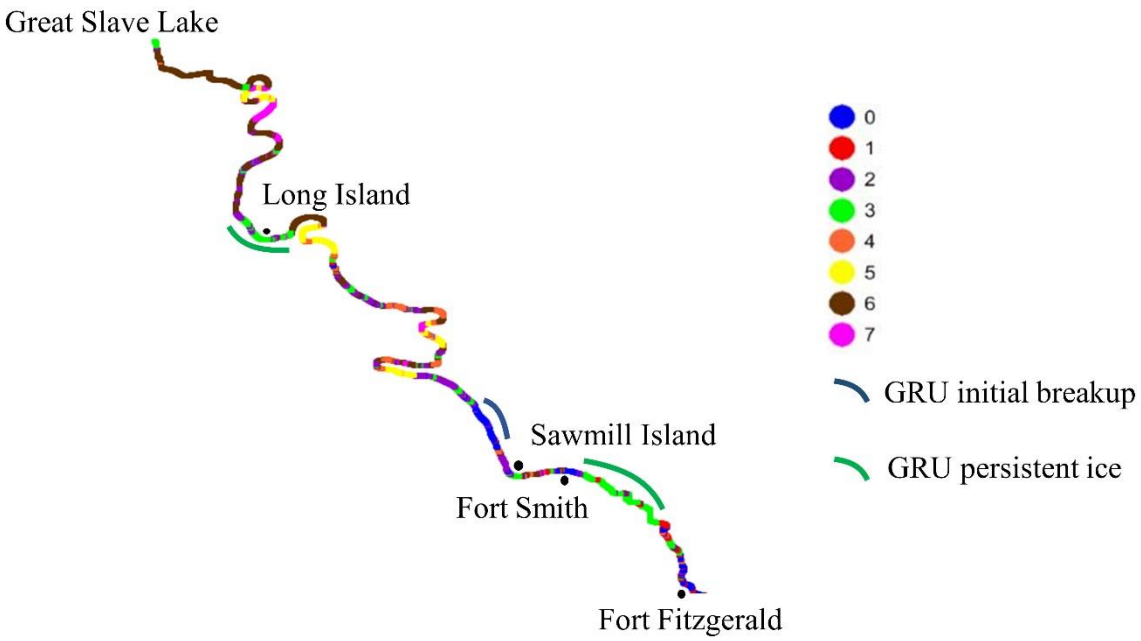

Fig. 4.8 Typologies along the Slave River from Fort Fitzgerald to Great Slave Lake.

A long stretch (approximately 20 km in length) of Typology 0 extends 12 km downstream from the Bell Rock Landing near Fort Smith (Figure 4.9). The stretch is relatively straight and narrow and opens up, first at the upstream end and further in the downstream direction. When flow discharge of the river increases, changes in water level in the narrower sections are greater than in the wider sections. The abrupt change in water level in the narrower river sections may expedite the breakup along the river. Typology 0 consists of segments that are also relatively steep along the river (Figure 4.11). Steeper sections of the river can increase the flow velocity and shear forces applied to the underside of the ice cover. These factors led to fracturing the river ice cover and initial breakup along the river. A number of small stretches of Typology 0 also occurred at various locations along the river where breakup initiated in the studied years 2008-2011 (Figure 4.9).

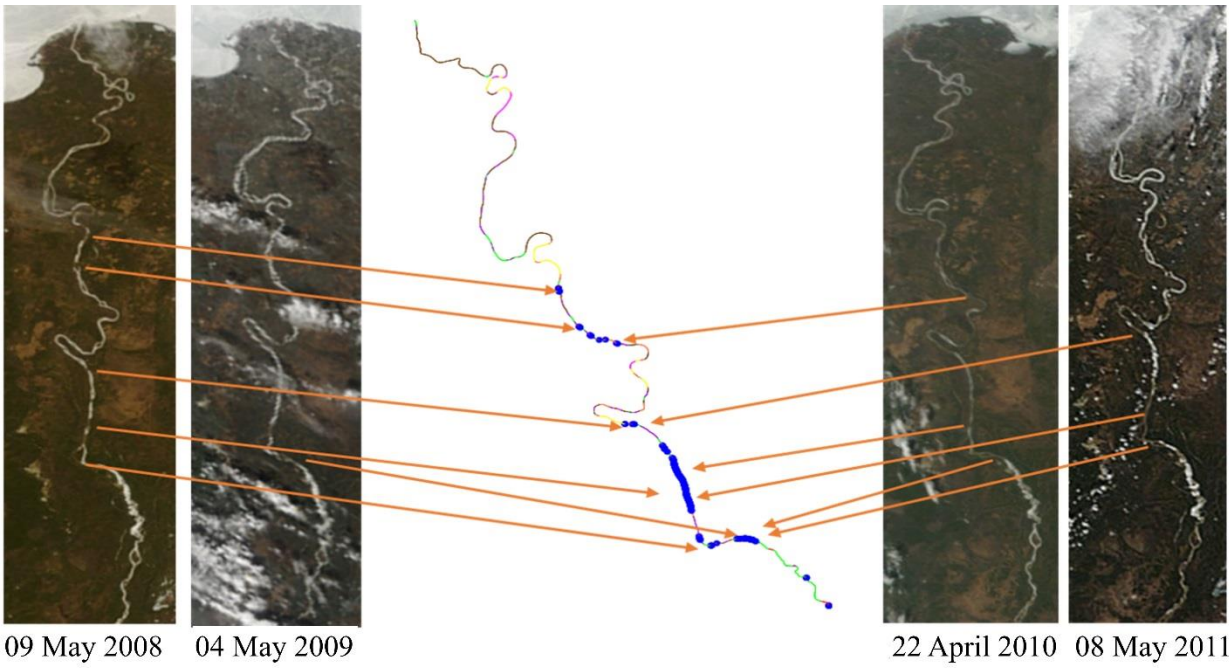

Fig. 4.9 Geomorphic Response Unit (GRU) of initial breakup along the Slave River.

Typology 3 typically had persistent ice in various locations along the river until the end of the breakup period. Two potential areas of persistent ice were identified in the MODIS imagery acquired between 2008 and 2011. The areas coincided with a GRU consisting of a cluster of Typology 3. One GRU extended from Fort Fitzgerald to Fort Smith, a stretch of ice that persisted the longest. The stretch is marked by a series of four rapids, with many small rock islands and an abrupt widening of the channel. Local observation confirm that the ice cover in this location was significantly thick (2~3 m) and persistent until the end of the breakup. The steeper river slope immediately downstream of the rapids may contribute significant amounts of frazil depositions to produce a hanging dam and relatively thicker ice cover sections along the river. Therefore, the ice cover in this locations may take relatively longer to melt and clear during the breakup. Another GRU is located approximately 100 km upstream from the Slave River Delta with the downstream end near Long Island. This stretch is relatively wide and less steep with big islands and splitting flows through multiple channels. Several small stretches of Typology 3 are also dispersed along the river, most of which coincided with locations of persistent ice (Figure 4.10). The higher effective width and relatively less steep channel reduced the flow velocity and shear forces on the ice cover. The wider sections of the river are also marked by numerous islands which make them more susceptible to border ice cover formation along the river. The ice cover in the wider channel

sections may not be as affected by the main channel flow. Besides this, wider sections and sections whose flow is split around islands may not have as rapid a change in water levels as do narrower sections when the discharge increases during the breakup event. As a result, the ice cover in wider sections may persist until the end of breakup.

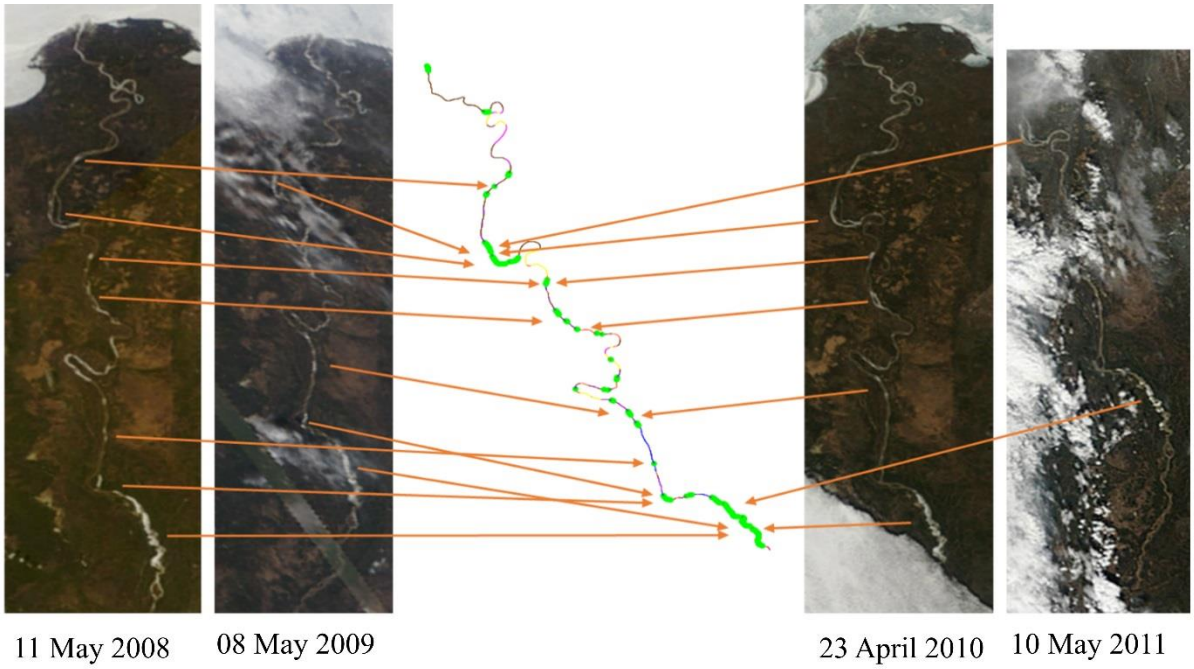

Fig. 4.10 Geomorphic Response Unit (GRU) of persistent ice cover throughout the breakup period along the Slave River.

Longitudinal profiles of the normalised values of the geomorphological parameters are shown in Figure 4.11. Unity-based normalization or feature scaling is applied to bring all the geomorphological parameters into the range between the two arbitrary points -2 and 2. Typology 0 indicates where initial breakup occurs whereas Typology 3 indicates the locations of persistent ice cover along the river. The normalized profiles indicate that channel width and bank slope have the largest influence on Typology 0. These two geomorphological variables are important for the areas of initial breakup whereas sinuosity may have the negligible influences on initial breakup. Narrower, steeper and relatively straight channels are more susceptible to initial breakup along the river. The Figure 4.11 also shows channel width having a significant impact on Typology 3, wider sections of the river more prone to persistent ice cover during the breakup event. However, bank

slope may also have some influence on Typology 3, downstream of the river where slope is comparatively lower having more potential for persistent ice cover until the end of breakup.

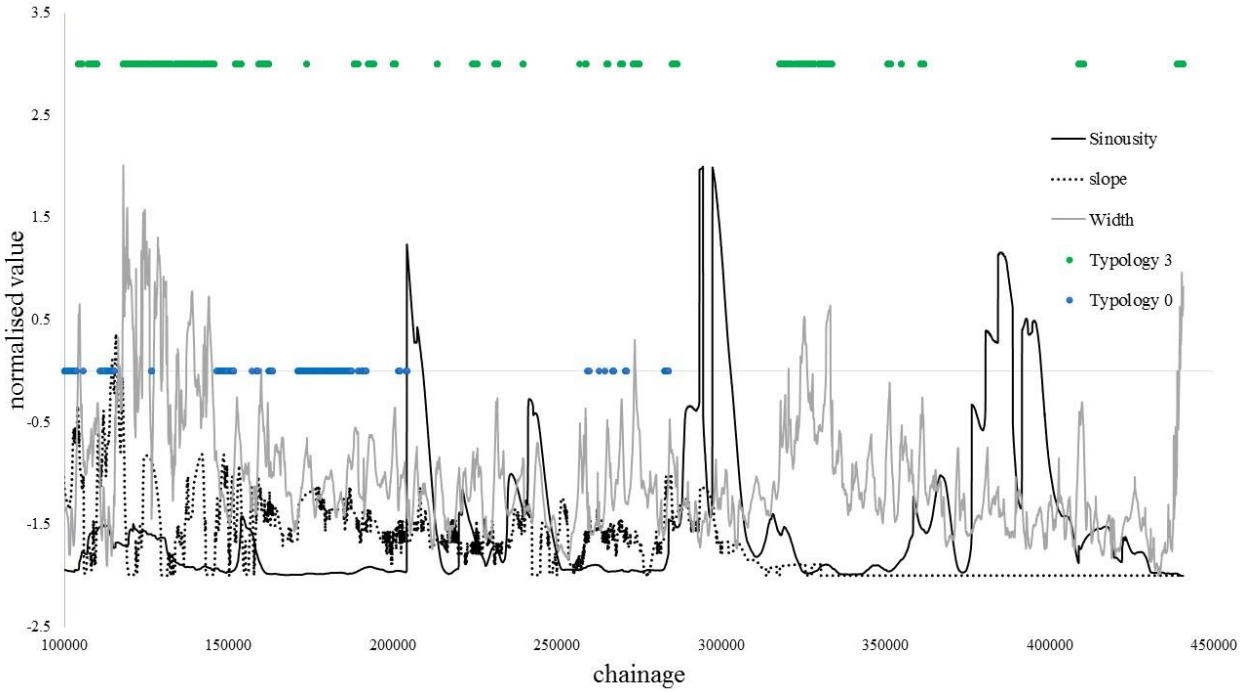

Fig. 4.11 Longitudinal profiles of the normalized values of the geomorphological variables (sinuosity, longitudinal bank slope, and channel width) of the Slave River from Fort Fitzgerald to Great Slave Lake.

Two-dimensional delineation of PCA scores of Typology 0 and 3 are shown in Figure 4.12 where variable vectors are plotted in terms of Principal Component 1 (PC1) on the x axis and Principal Component 2 (PC2) on the y axis. The data shows that the vectors representing effective width and sinuosity are pointing in opposite directions, therefore these two parameters are negatively correlated with each other. Based on Figure 4.12, Typology 0 is negatively correlated with effective width and positively correlated with bank slope and sinuosity, while Typology 3 is positively correlated with effective width and bank slope. Typology 0 also tends to have higher slope values, Typology 3 tends to have lower slope values. Geomorphologically, this corresponds to narrower and steeper sections for the groups of Typology 0 and relatively wider and less steep sections for the groups of Typology 3.

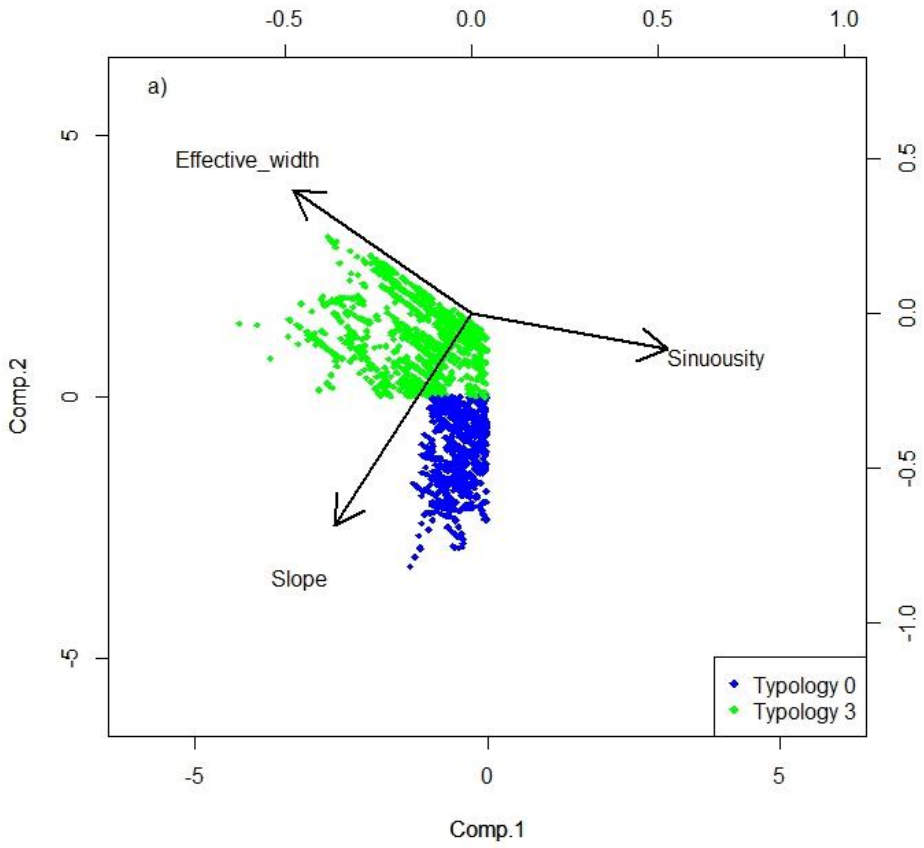

Fig. 4.12 Typology 0 and Typology 3 plotted in terms of PC1 vs PC2.

Geomorphological variables of the river may play a significant role in determineing the spatial patterns of the breakup event. The geospatial model shows that the effective width of the Slave River directly influences ice cover behaviour during spring breakup. Relatively narrower sections of the river initiate the spring breakup while wider sections of the river have a persistent ice cover until the end of breakup.

4.3.3 Meterological and hydraulic Conditions

Air temperature can also have an effect on the temporal patterns of spring ice breakup along the Slave River. Colder winters can increase the ice cover thickness whichresults in the periods ofthe thaw and decay of the ice along the river. In 2010, relatively warm air temperatures were recorded during the winter. By the end of April 2010, the maximum AFDD was calculated to be 2140 °C which was significantly lower than for the years 2008, 2009, and 2011, by the April the maximum AFDD of these years were calculated to be 2932 °C, 2863 °C and 2793.9 °C, respectively (Figure

4.6). Initiation of the ice cover breakup can also be triggered by increasing temperatures during the pre-breakup period. Higher air temperatures during the early breakup period may accelerate the ice decay process, resulting in earlier dislodgment of the ice from the shores. In 2010 air temperatures rose to above 0 °C from mid-February to mid-March, then dropped below -10 °C until the end of March, after which the temperature again rose and stayed above 0 °C into the spring (Figure 4.5). In the years 2008, 2009 and 2011 the air temperature trends were similar, with air temperature starting to increase mid-March and rising to above 0 °C during the first week of April. The mean daily air temperatures then dropped to below 0 °C and by the end of April temperatures were consistently above 0 °C into spring. In these years breakup began during the first week of May.

Fluctuations in the river flows during spring may also influence the patterns of breakup. Higher river discharge during the breakup period can lead to increased water level staging and subsequent flooding. A certain flood level along the Slave River during spring breakup is necessary for flooding to occur in the Slave River Delta (Brock et al. 2008). However, in the years of 2008, 2009 and 2011 relatively moderate flows were observed along the Slave River during breakup. In those years the river discharge peaked when the river was mostly free of solid ice. In 2010, low flow conditions may have contributed to the slow decay of the ice cover, prolonging the breakup period with little flooding in the Slave River Delta. Based on previous research on flooding in the delta (Brock et al. 2008), we can draw a baseline for the occurences of flooding in the delta in terms of the level of discharge during the breakup period. Figure 4.13 provides insight into the spring discharge required for different types of flooding. There may not have been major flooding during the years between 2008 and 2011, however, moderate flooding have occurred in 2008, 2009, and 2011, with no flooding in 2010.

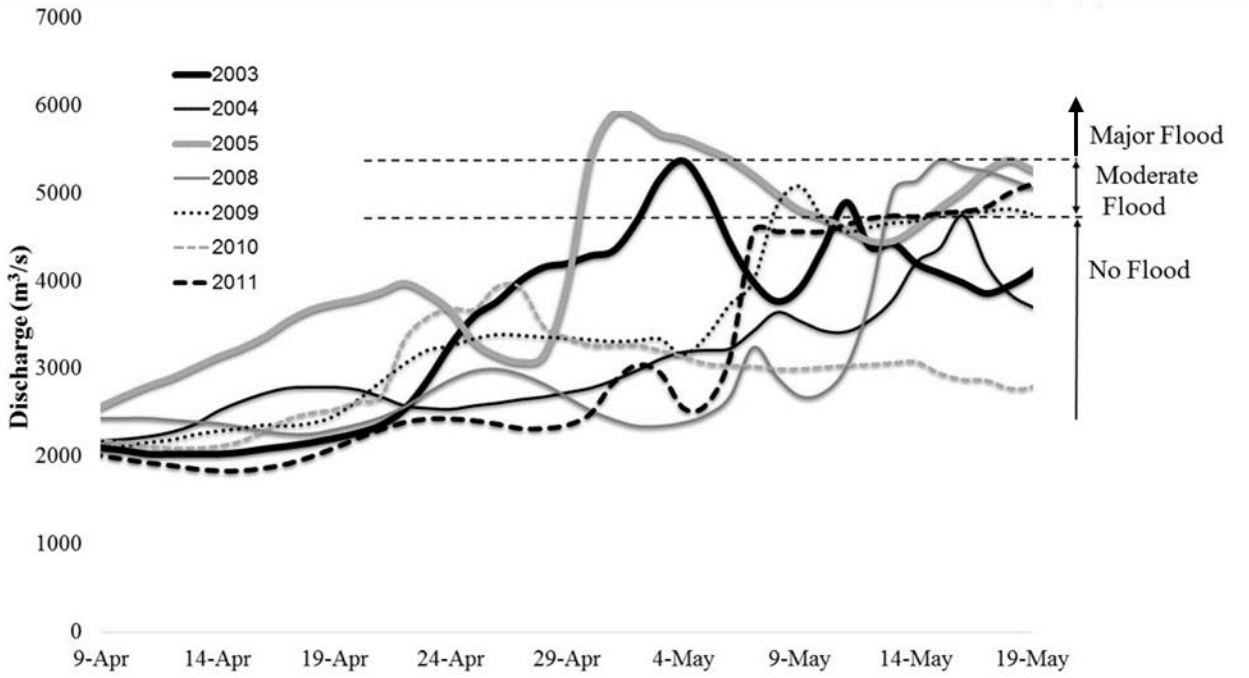

Fig. 4.13 Ranges of discharge for spring runoff occurring along the Slave River.

4.5 Conclusion

Variability in river ice cover breakup along the Slave River suggests that temperature and flow conditions along the river have a strong impact on spatial and temporal patterns of the spring ice cover breakup and flooding in the Slave River Delta. Increasing air temperatures during the pre-breakup period can lead to earlier spring breakup along the river.

Geomorphological typologies of the Slave River helped to identify the different geomorphological parameters impacting the spatial patterns of the spring ice cover breakup along the river. The geospatial modelling approach in this study was able to determine the locations of initiation of breakup (Typology 0, blue) and persistence of ice cover at the end of the breakup period (Typology 3, green). The model determined that relatively narrower and steeper river sections are conducive to initiation of breakup and wider sections of the river are predisposed to ice remaining intact longer throughout breakup. Several common locations with persistent ice cover and initiation of breakup have been identified with the help of MODIS imagery, coinciding with two GRU of common typologies extended over a reach in the geospatial model of the Slave River. Also, some

sections in the series of four rapids at Fort Smith was the last stretch to have the remaining ice dislodge between the years 2008 and 2011.

MODIS images offer continuous monitoring of ice cover behavior along the entire length of a large river, rather than just at specific locations. Historical data sets of MODIS images can also be beneficial in discerning year to year variations in both ice cover behavior and timing of ice cover breakup along the river. MODIS imagery is a useful tool to observe and to record the climatic and hydrologic patterns of a particular area. This tool is also essential to validate models, such as geospatial models, as well as to predict ice cover breakup patterns along the river.

Analysis of spring breakup patterns and identification of the most likely locations of persistent ice will provide guidance for future examination of ice jam flooding in the Slave River Delta. Also, the results from this research could aid in understanding the current hydrologic problems along the Slave River and in the Slave River Delta and specifically, the causes of its recent reduced flood frequency.

Chapter 5 : Discussion

5.1 Introduction

This research documents freeze-up processes, ice cover progression and spring ice cover breakup patterns along the Slave River. Field studies of the ice cover, RADARSAT-2 satellite imagery and time lapse imagery were used to identify different types of ice and examine freeze-up processes and ice cover progression along the river. This study also identifies the impact of flow regulation on the ice cover and some plausible reasons for air pocket and air layer formation along the river's ice cover. A geospatial modelling approach was applied to determine the influence of the river's geomorphology on the spring ice cover breakup. To support this work, data from a series of MODIS satellite images were used to track the cover breakup patterns along the river between 2008 and 2011. This chapter includes some additional information not provided in the previous chapters by providing a brief comparison of the ice cover characteristics between the winters 2013-2014 and 2014-2015 and an extended discussion on the spring ice-cover breakup along the river.

5.2 Ice cover formation along the Slave River

The ice regime along the Slave River is a result of interactions between the hydraulic, meteorological, and physical characteristics of the river. At the beginning of freeze-up, the high turbulence of the water in the main channel produces frazil crystals in the super-cooled water. Low turbulence areas of the water, especially near river banks, produce border ice. Border ice progresses towards the middle of the channel, constricting the channel and impeding the flow of ice pieces, then ultimately forming an ice bridge. Ice bridges in multiple locations along the river impede the passage of ice floes, which then accumulate and lead to the formation of juxtaposed ice covers. Thermal ice covers are formed due to the backup of water upstream ice bridging sections. High flows may deposit frazil ice underneath the ice cover and force the ice cover to compress into a consolidated ice cover. Steeper sections of the river keep the river open due to stronger turbulence of the water and also produce frazil ice during the entire course of winter. Once the solid ice cover is formed, the ice cover continues to thicken thermally in a downward direction.

The daily average flows along the Slave, Peace and Athabasca rivers from 2003 to 2012 are shown in Figure 5.1.The figure shows that the flow regime of the Peace River has a more significant effect on the flow regime of the Slave River than the flow regime of the Athabasca River or other

tributaries. The flows along the Athabasca River typically remain fairly smooth in the winter, steadily declining from October to December, reducing to a minimum of around 150 m^3/s by January, and then remaining stable until the end of April. By May the flow along the Athabasca River increases naturally due to snow and ice cover melt, rising to a maximum of approximately 1500 m^3/s in June. In contrast, the regulated flows along the Peace River at Hudson Hope increase in the winter and decrease in the spring. With daily fluctuation of the flows, average winter flows along the Peace River usually increase, ranging from 1300 m^3/s to 1700 m^3/s, while the spring flow steadily decreases to approximately 500 m^3/s. Similar winter flows occur further downstream of the Peace River at Peace Point between May and June. This suggests that the tributaries (e.g. Smoky River) of the Peace River have minimal effects on the winter flows along the Peace River. However, the tributaries may contribute to high flows along the Peace and Slave rivers in the summer. During this time, the maximum average flows along the Peace and Slave rivers are approximately 3500 m^3/s and 5000 m^3/s, respectively. It is also clear that summer retention of the Peace River flows, due to dam operation, may also reduce the magnitude of the summer flows downstream of the Peace River and also along the Slave River. Unlike the Athabasca River, winter flows along the Slave River fluctuate between 2000 m^3/s and 3000 m^3/s, which may be the result of daily flow fluctuations of the Peace River at Hudson Hope.

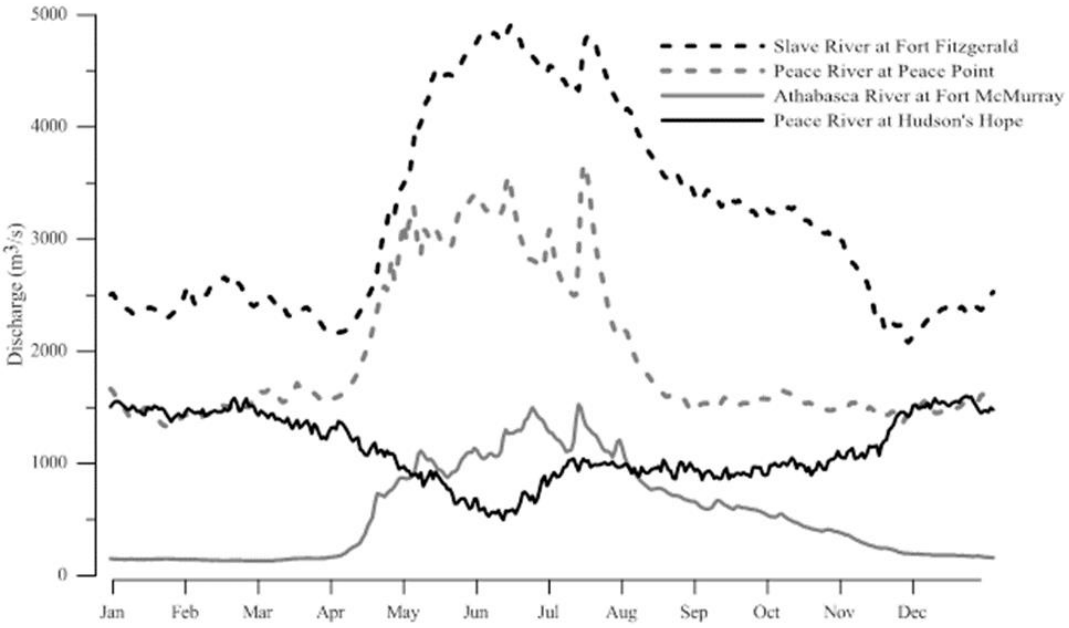

Fig. 5.1 The average discharge of the past 10 years (2003-2012) along the Peace, Athabasca and Slave rivers (Data source: Water Survey of Canada).

Although an increasing trend was observed in the discharge of the Peace River at Hudson Hope during the winters of both 2013-2014 and 2014-2015, the discharge was relatively higher during the first winter (Figure 5.2). In the 2013-2014 winter, the average discharge of the river fluctuated from approximately 800 m^3/s to 1680 m^3/s between November and December. By the end of December the flow was relatively stable at around 1270 m^3/s, before increasing sharply to a peak of approximately 1720 m^3/s in February. In the 2014-2015 winter, the flow ranged from 350 to 1400 m^3/s between November and December, and stabilized at around 1280 m^3/s by the end of December, before decreasing to approximately 400 m^3/s in February. Different trends were observed in the flows along the Slave River at Fort Fitzgerald during both winters. At the beginning of the freeze-up in 2014 the average river flow was approximately 2500 m^3/s, which was about 25% lower than during freeze-up of the previous year. In the 2013-2014 winter, the discharge along the river decreased to approximately 1680 m^3/s by mid-January and then sharply increased to approximately 3000 m^3/s in mid-February. In the 2014-2015 winter, the discharge reached a maximum of around 2590 m^3/s by the second week of January and then maintained a decreasing trend during the course of winter. Overall, the flows along both rivers were highly variable, with flows spiking up and down during both winters.

Relatively high flows, coupled with abrupt changes in flow conditions along the Slave River, forced the stationary ice covers to form consolidated ice covers during first winter. During the freeze-up, incoming ice floes were arrested at ice bridging sections or on existing ice cover to form an initial juxtaposed ice cover. At some point, the flow fluctuation was able to create sufficient shear forces to collapse the sheet-ice cover, which then submerged and traveled downstream to another existing ice cover. High flow velocities also transported and deposited frazil ice along the downstream ice cover to form a much thicker ice cover or consolidated cover along the river. Significant increases in mid-winter discharges in the first winter resulted in ice cover flooding. High winter discharges increased water pressure at the bottom of the ice cover, resulting in cracking or dislodging the ice cover from the shoreline, allowing water to seep to the surface of the ice cover. Relatively low flow conditions during the second winter's freeze-up resulted in the formation of very little consolidated ice. Therefore, the initial sheet ice cover thermally thickened, which led to the formation of more thermal ice along the river.

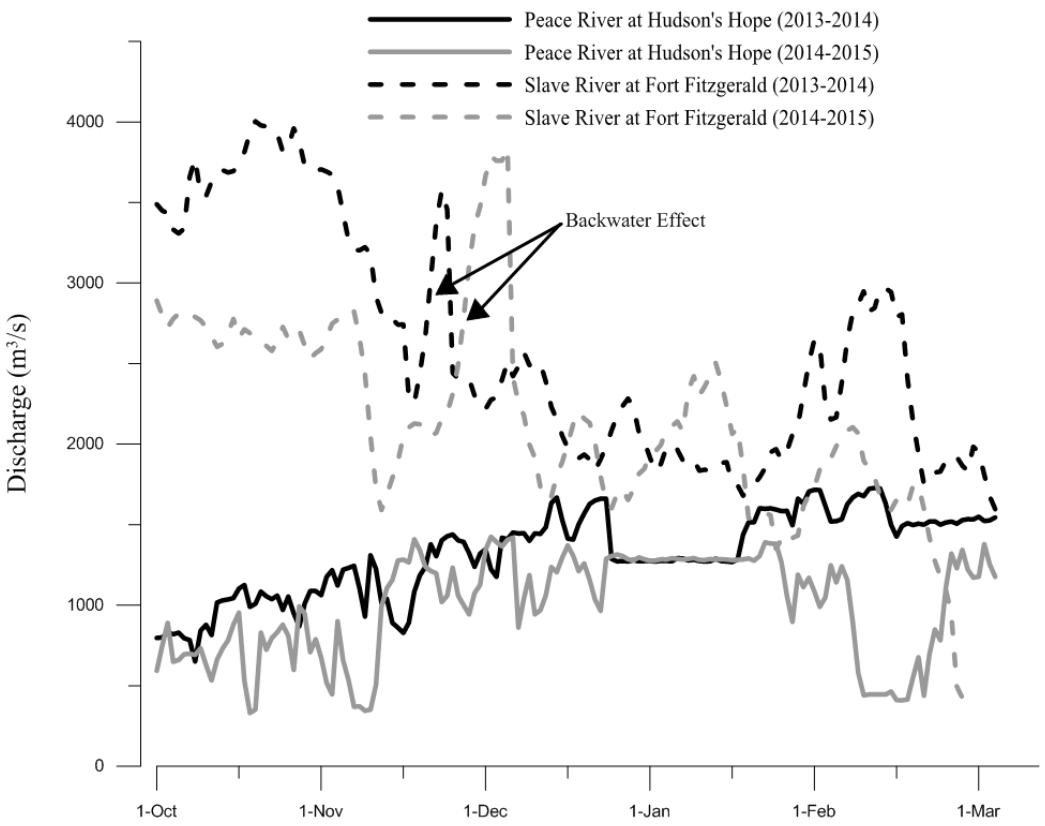

Fig. 5.2 Discharge along the Peace River at Hudson Hope and the Slave River at Fort Fitzgerald for winters 2013-2014 and 2014-2015 (Data source: Water Survey of Canada).

RADARSAT-2 satellite imagery was used to classify different types of ice based on backscatter values (dB) (Figure 5.3). The figure shows an overview of the ice cover formation and year to year differences in types of ice cover formation along the lower 45 km reach of the river between the winters 2013-2014 and 2014-2015. There are primarily three types of river ice cover forms during the winter- thermal, juxtaposed and consolidated ice covers. At the beginning of freeze-up, a long stretch of thermal ice cover typically forms from the mouth of Great Slave Lake to Big Eddy. The extent of the juxtaposed ice cover can be observed from Big Eddy to further upstream in the river. As winter progresses, the juxtaposed ice cover turns into a consolidated ice cover, which remains stable during the entire course of winter. In the 2013-2014 winter, a large extent of thermal ice cover in the lower reach of the river was observed until December 2013. However the section changed and brightened in the satellite image due to the build up of slush ice under the ice cover and an increase in air pocket densities by January 2014. In the 2014-2015 winter, although the river was ocasionally covered by the juxtaposed and consolidated ice cover, a thermal ice cover

dominated in many sections along the river until January 2015. Relatively high flow conditions during the first winter maintained the water velocity, which was sufficient to submerge the frazil ice or fragmented ice pieces under the ice cover, thus producing a consolidated ice cover upstream of the SRD. Submerged ice floes were randomly transported under the ice cover, resulting in a thickened and rough ice cover that also increased the backscattering values in the texture of the satellite image. However, relatively low flow conditions at freezeup in the second winter were unable to produce sufficient water velocity to transport ice floes under the ice cover, which reduced the chances of the formation of a consolidate ice cover along the river. Therefore, most of the sections of the river in the second winter were covered with thermal ice cover.

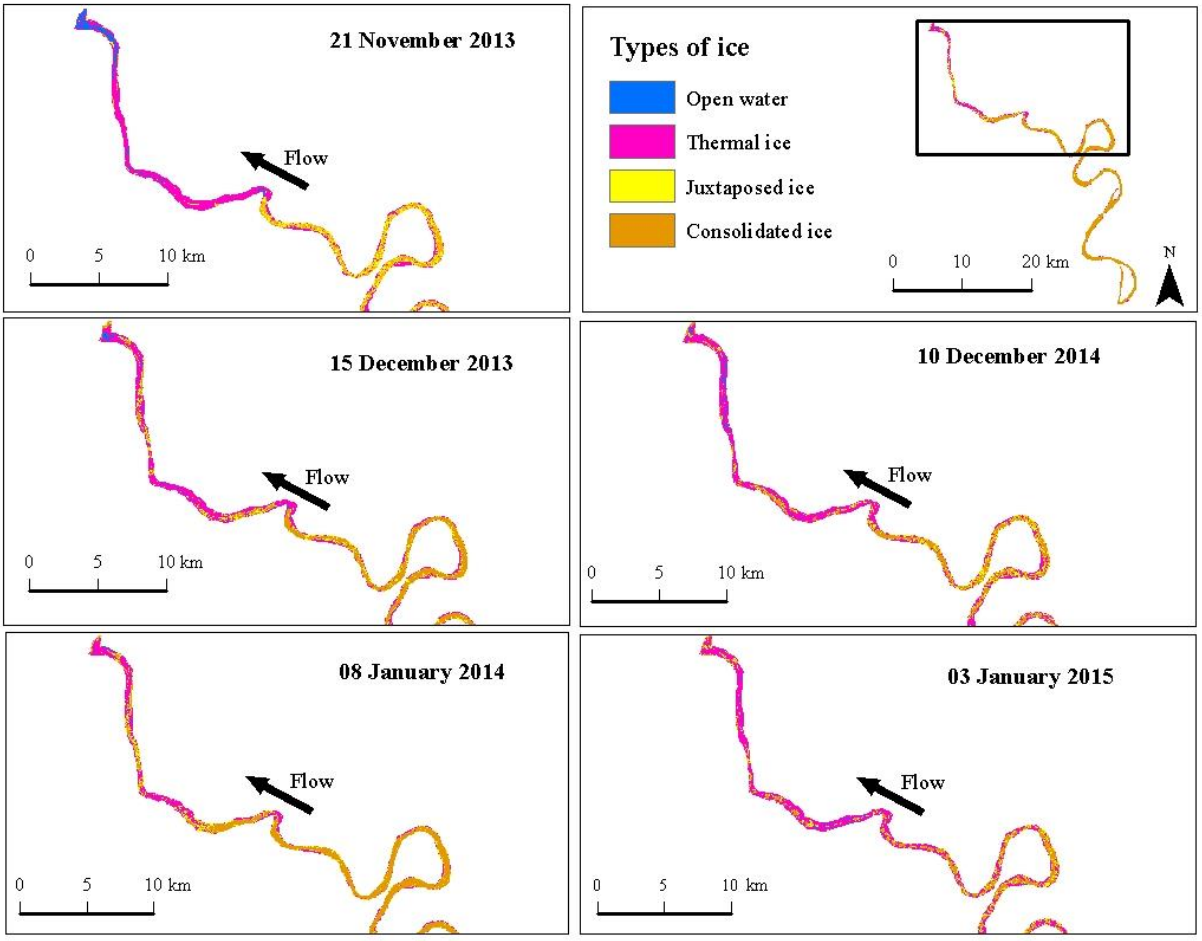

Fig. 5.3 Different types of ice cover along the Slave River Delta, during the winters of 2013-2014 (left panel) and 2014-2015 (right panel) (RADARSAT-2 Data and Products © MacDonald, Dettwiler and Associates Ltd. (2013) –All Rights Reserved. RADARSAT is an official trademark of the Canadian Space Agency).

Figure 5.4 shows the longitudinal profiles of the backscatter values of satellite imagery acquired during the 2013-2014 and 2014-2015 winters. Significantly higher backscatter values in the first winter revealed the high concentration of consolidated ice cover along the river. Only some portions of the river, approximately 15 km upstream of Great Slave Lake, had backscatter values less than -20 dB. However, significantly lower backscatter values in the second winter indicate that the river was mostly dominated by a thermal ice cover or very thin layers of ice cover. On 10 December 2014, the river was covered by very thin layers of ice cover with open sections, which caused very low backscatter values ranging from -20 dB to -39 dB. Although the backscatter values were increased by 03 January 2015, they were far lower than the backscatter values on 08 January 2014. The changes in backscatter values of the consolidated ice cover from 15 December 2013 to 08 January 2014 are low; however, the changes in backscatter values of the thermal ice cover from 10 December 2014 to 03 January 2015 are high. After consolidation, the ice cover becomes relatively stable and the texture of the images remain unchanged, with only small differences in the backscatter values. However, in the 2014-2015 winter, the ice cover changed from an incomplete thermal ice cover to a complete thermal ice cover, which resulted in a high difference in backscattering values between December 2014 and January 2015. Additionally, the reason for the differences in backscatter values can be related to the rate of ice cover thickening along the river, since backscatter values increase with an increase in ice cover thicknesses.

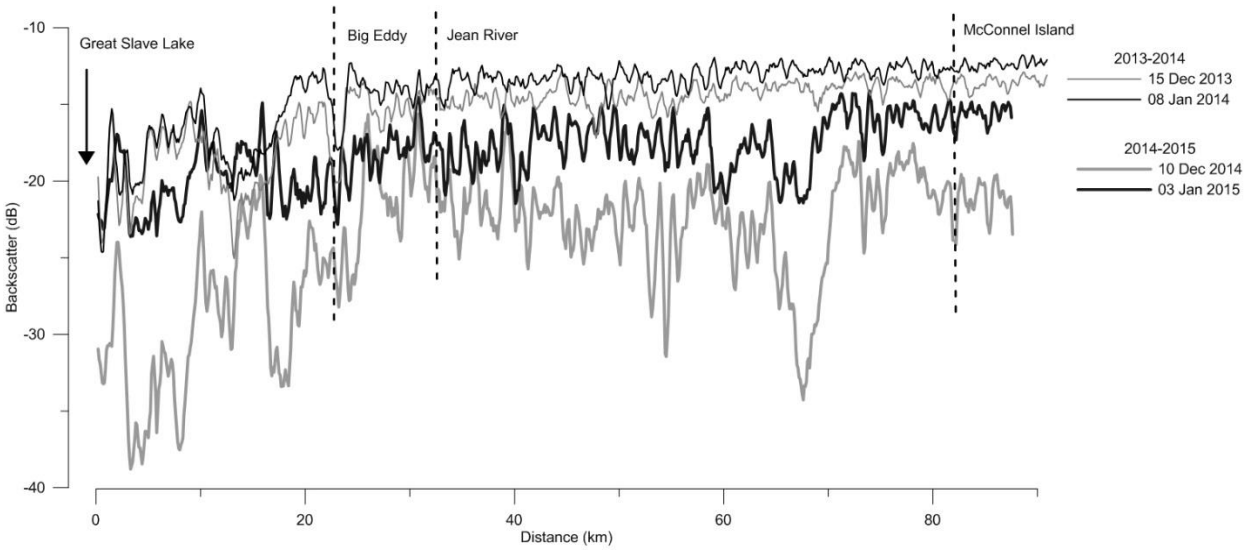

Fig. 5.4 Longitudinal profiles of the RADARSAT-2 satellite images along the Slave River.

According to the field surveys, the ice cover was thinner in the winter 2014-2015 than the ice cover of the preceding winter. The maximum ice thickness along the Slave River Delta was 0.66 m on 24 March 2015 (Figure 5.5) while the maximum ice thickness was 0.87 m on 01 March 2014 (Figure 2.13). An increase in the ice cover thickness increased the possibility of greater impurities, cracks and the presence of air inclusions (air pockets and bubbles) between the ice cover. These factors resulted in the volume scattering in the ice cover and increased total backscattering in the satellite image.

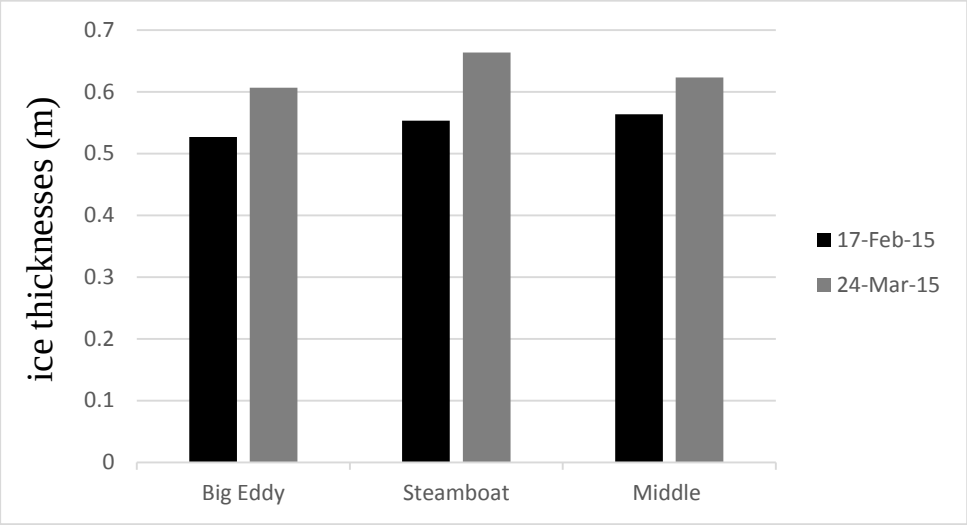

Fig. 5.5 Ice thickness at the Slave River Delta between February and March 2015.

The accumulated freezing degree days (AFDD) in the 2013-2014 winter was higher than during the following winter. At the beginning of the freeze-up of the second winter, the AFDD progressed at relatively the same rate as the previous winter. On 08 December 2013 the total AFDD was calculated to be 647.1 °C while on 08 December 2014 the total AFDD was calculated to be 648.5 °C. However, by the end of the second week of December 2014, the temperature was relatively warm, which kept the AFDD consistently lower than the previous winter (Figure 3.10). By 25 March 2014 the total AFDD along the river was calculated to be 3034.4 °C while by 25 March 2015, the total AFDD was 2655 °C. This lower value indicates less thickening of the ice cover and a decrease in backscattering picked up by the satellite receiver.

A linear relationship between ice cover thickness and square root of AFDD is shown in Figure 5.6. Ice thicknesses usually increase with a higher freezing degree days along the river. In the 2014-2015 winter, the rate of ice thickening was less than the rate of ice thickening in 2013-2014. Also, the variability in ice thicknesses during the first winter was much higher than during the second winter. Consolidation of the river ice produced highly varied ice thicknesses in the first winter, while thermal ice was more uniform ice in thickness in the second winter. When a consolidated ice cover forms, the frazil pans, slush and ice pieces deposit under the ice cover and produce a rough bottom surface, therefore ice cover thicknesses will vary more along the river. Thermal ice covers are smoother, leading to more uniform ice thicknesses.

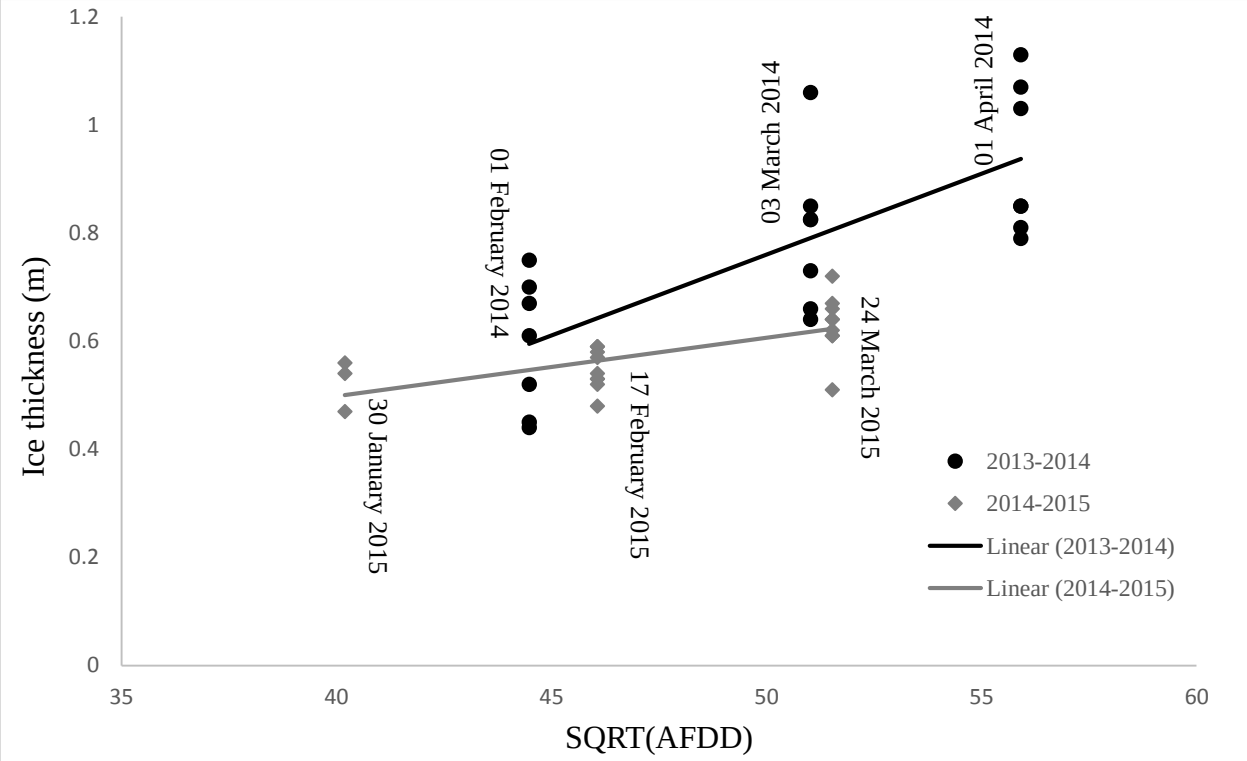

Fig. 5.6 Relationship between ice cover thicknesses and AFDD along the Slave River. Data collected in various locations from the Jean River to Middle channel, NWT.

Air pocket formation along the Slave River ice cover is attributed to the flow regime of the river. The characteristics of the flow change with the progression of the ice cover and lead to changes in ice cover characteristics. As the ice cover thickens downward, the cross sectional area constricts and funnels the water to the main channel, where flow resistance, water velocity and turbulence increase, to create more air bubbles, which become trapped in the ice cover. Steeper sections of

the river, along the series of four rapids at Fort Smith and some open water sections during the winter, are a major source of air entrainment into the water. Dissolved oxygen is then transported under the ice cover and at some point detrains and degasses to form air pockets along the ice cover. Air pocket formation may continue until the end of the winter season.

5.3 Ice cover breakup along the Slave River

By the end April, the mean daily air temperature along the river begins to increase (Figure 4.5), which decreases the ice cover thickness and initiates the pre-breakup process. At the same time, the discharge of the river is also increased due to snow melt. The combined effects of higher river flows and warmer temperatures then trigger the breakup of the ice cover. Breakup along the Slave River usually starts during the first week of May and continues for about one to two weeks.

MODIS satellite images tracked the ice cover breakup from 2008 to 2011. The geospatial modelling approach determined the geomorphological influences on the patterns of the spring ice cover breakup. Narrower and steeper sections of the river are conducive to the initiation of ice cover breakup and wider sections of the river are areas where the ice cover persists throughout the breakup event. When discharge of the river increases, changes in water level in the wider sections are less than in the narrower sections. The high water level in the narrower sections applies the high shear forces on the ice cover to initiate the ice cover breakup.

The magnitude of discharge along the river during spring break up is one of the major factors influencing flooding in the Slave River Delta. Certain thresholds of flow are required to flood the Delta during the ice cover breakup, 4800 m^3/s for a moderate flood and more than 5500 m^3/s for a major flood event (Figure 4.13).

As the runoff begins, the discharge of the river starts to increase by mid-April 2014 (Figure 5.7) and spring freshet occurs at the beginning of May 2014 when dislodgement and breakup of the intact ice cover occurs along the river. At the same time, the mean air temperature began to increase and remain above 0 °C after the first week of May 2014 (Figure 5.8). Warmer temperatures triggered the snow melt and reduced the thicknesses and strengths of the ice cover, thus initiating breakup. High river flows then facilitated the total breakup along the river. The magnitude of the discharge also exceeded the limit for a major flood (5500 m^3/s) during the breakup.

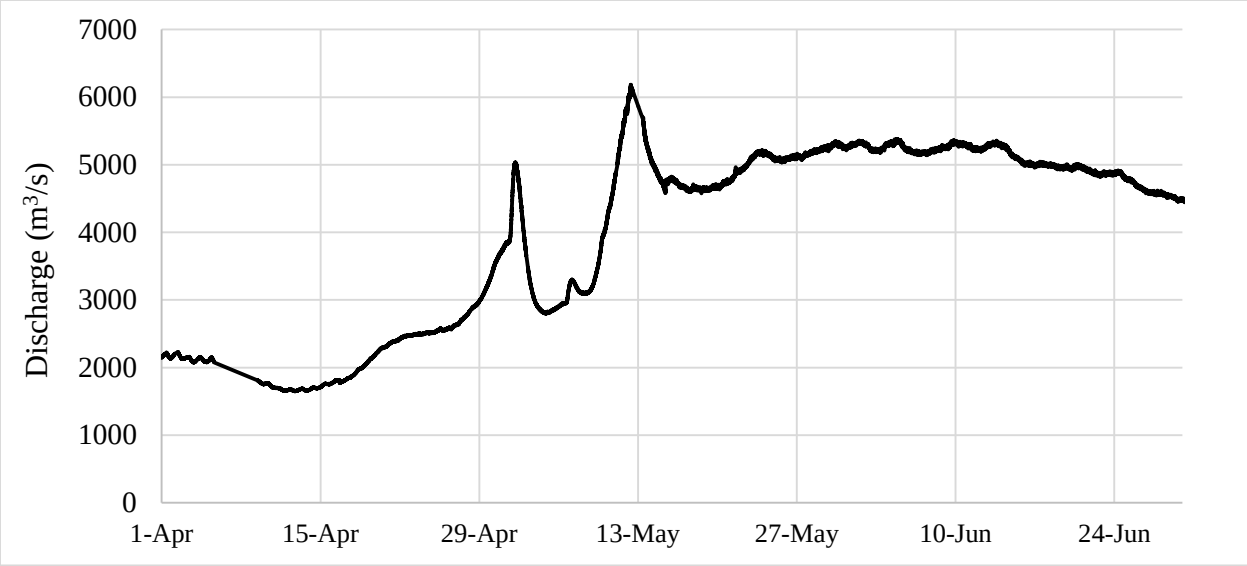

Fig. 5.7 Discharge along the Slave River at Fort Fitzgerald gauge station during the spring break up in 2014 (Data source: Water Survey Canada, Station: 07NB001).

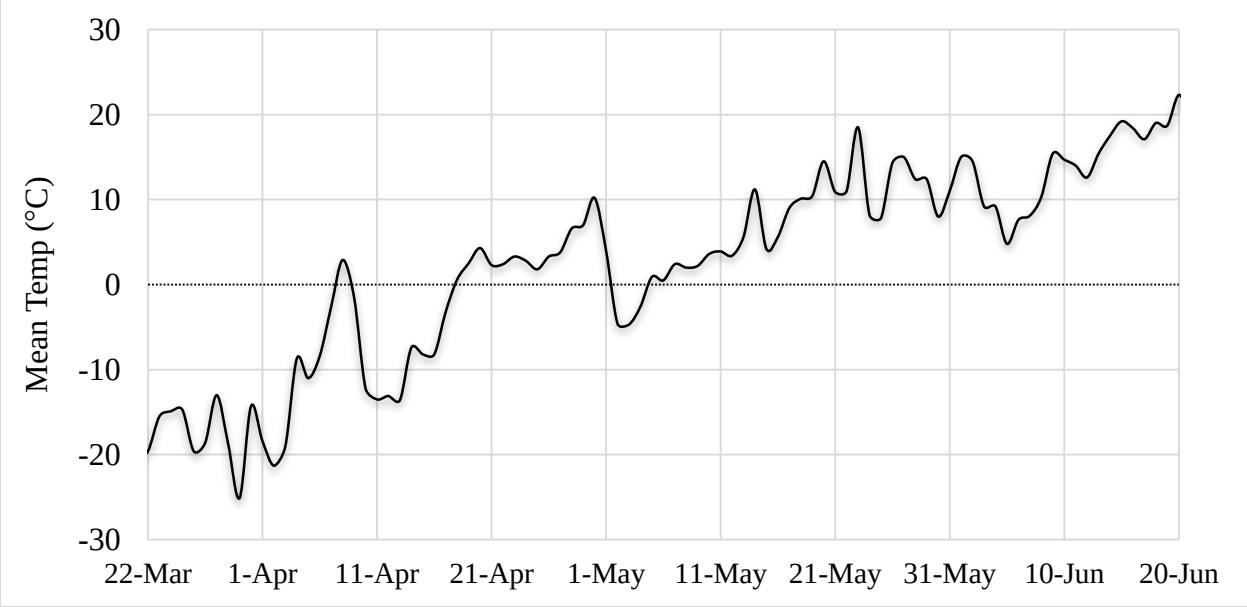

Fig. 5.8 Mean air temperature during the spring breakup 2014 along the Slave River at Fort Smith (Data source: Environment Canada).

The temporal and spatial patterns of the ice cover breakup along the Slave River were usually similar between the years 2008 and 2011. The MODIS images (Figure 5.9) acquired during the 2014 breakup also show similar patterns to those recorded between the years 2008 and 2011. The breakup along the river initiated on 07 May 2014 and continued until the third week of May. In

the images from 08 May 2014 to 12 May 2014, the river is obstructed by cloud cover. However, the persistent ice cover locations throughout the breakup can still be seen in the images acquired on 13 May 2014, which coincide with the geospatial model.

Fig. 5.9 MODIS images showing breakup patterns along the Slave River during the spring breakup event in 2014.

Overall, the research results suggest that the hydraulic and thermal regime of the river significantly influences the ice regime along the Slave River. The flow characteristics and degree days of freezing affect the types of ice cover formation and progression along the river, while the high spring discharge and warmer temperature, influence the temporal and spatial patterns of the ice cover breakup.

Chapter 6 Conclusion

6.1 Highlights

1 The ice regime of the Slave River is dominated by the three types of ice covers – thermal, juxtaposed and consolidated ice. Low flow conditions at freezeup of the river produces more thermal ice covers. Juxtaposed ice covers form upstream of ice bridging sections, which occur where the river channels are relatively narrow. Higher river flows compress the juxtaposed ice covers into consolidated ice cover. Open water areas are maintained in turbulence flow areas below of the rapids and also just downstream of ice bridging sections.

2 Meteorological (air temperature) of the river control the ice cover progression during the winter. Higher accumulated freezing degree days produce thicker ice cover while lower accumulated freezing degree days produce thinner ice covers.

3 The flow regime of the river is strongly influenced by the flows along the Peace River as well as the W.A.C Bennet Dam operations. High winter flows and daily peaks of the Peace River at Hudson Hope increase the variability in the Slave River flows and change the ice cover characteristics. High mid-winter flows cause of the formation of fractures in the ice cover or detachment of the ice cover from the river banks, allowing water below the ice cover to seep through and flood the surface. Subsequent freezing of the flood water further increases ice cover thickness along the river.

4 Flow characteristics control air pocket formation along the river's ice cover. Strong flow turbulence produces more air bubbles in the river which become entrapped in the ice cover to form air pockets. Consolidated ice covers produce rough bottom ice surfaces are potentially increase air pocket formation while thermal ice covers produce relatively smooth ice surfaces which usually reduce the chances of air pockets forming along the river ice cover.

5 Several open water sections during the winter are a source of air entrainment into the water surface along the river.

6 Flow regimes and thermal conditions drive the spring ice cover breakup and control the spatial and temporal patterns of the breakup along the river. Rising water levels and air temperatures typically initiate the breakup. A certain degree of discharge is required during the spring breakup for flooding along the Slave River Delta.

7 The narrower sections of the river initiate the breakup while wider sections of the river are potential areas for persistent ice cover throughout the breakup.

8 RADARSAT-2 satellite image is useful to track the winter ice cover regime while MODIS satellite image is effective to track spring ice cover breakup along the river. RADARSAT-2 imagery are able to determine open water sections, different types of ice, and changes of ice cover characteristics (e.g. ice cover flooding). Therefore this satellite is typically suitable for understanding winter ice regime along the river. MODIS imagery are frequent (~ 1/day) enough to track the successive changes of the ice cover during spring break up including open water sections and ice dislodgement, however it is unable to track the land surface while the areas are covered by cloud and also in the night.

6.2 Significance and Contributions

The results of this research provide valuable information on the Slave River ice regime for the communities of Fort Smith and Fort Resolution, NWT. The information about the mechanisms of different types of ice cover formation and the most plausible reasons of the air pocket formation along the river's ice cover can help local residents to identify safe travel routes along the river in the winter. They can use the different types of ice information to identify the potential locations of air pocket formation and avoid these locations to make their ice road or ice crossings along the river. The results of the changes in ice cover characteristics due to winter flow variations can be a good indicator for the impact of flow regulation on the hydrological regime of the river. Additionally, this information also increases predictability of local ice conditions and help identify safe ice cover areas during the winter.

The geospatial model provide guidance in monitoring river ice behavior and understanding the patterns of the spring ice cover breakup along the river. Also, the results from this research increases our knowledge of patterns in the spring ice cover breakup as well as flooding in the Slave River Delta.

6.3 Limitations

Extremely remote areas along the Slave River make it difficult to acquire adequate field measurements and data collection, so heavy reliance on remote sensing data and satellite images is necessary to understand the characteristics of the ice. Air pocket formations with very thin ice

covers may hamper the interpretation of remote sensing imagery, since the interaction of the microwaves with the river ice cover is dependent on the dielectric properties (ice-air and ice-water interfaces) of the ice cover. Field sampling and observation of the ice conditions along the river are difficult and sometimes unsafe due to numerous air pockets and thin layers of ice. Additionally, extreme cold air temperatures (-40 °C) and shorter day lengths (approximately 5 to 6 hours) limit field data collection and ice behavior observations along the river.

6.4 Future Research

The findings of this research provide good insight in the understanding of the overall ice regime along the Slave River. However, further investigations are required to understand more complex ice cover phenomena along the river in greater detail. Particularly, detailed observations of the air pocket and layer formation and flow regulation impact on the ice cover are needed. Hydraulic modeling is suggested to identify the processes of air pocket formation and the impact of flow variability on the ice cover, which can be the subject of future research. Correlation between upstream regulation and tributaries inflows along the Peace River with Slave River discharge and water level are difficult because of limitation in hydrological data. A large scale hydrological model is required to determine the cause of flow fluctuation along the Slave River. A river ice model can be used to simulate air pocket and layer formation along the ice cover to help with understanding the nature of dissolved air transportation and accumulation along the underside of ice covers.

More detailed spring ice cover breakup monitoring is also required to fully understand the role of the river ice on flooding in the Slave River Delta. Water level monitoring during breakup and identifying the potential locations for ice jams can help provide insight on the frequency and magnitude of flood events in the delta. A geospatial and hydraulic model with field observations can also be applied to identify the factors involving in ice jam flooding along the river as well as the delta.

References

AANDC and ENR 2012. Our Water, Our Life: Building Partnerships to Assess the Health of the Slave River and Slave River Delta. Summary Report for the Community Workshop Convened in the Fort Smith, NWT on March 1 and 2, 2011. Aboriginal Affairs and Northern Development Canada (AANDC) & Department of Environment and Natural Resources (ENR) of the Northwest Terriroties, Yellowknife, NT.

Andres, D., Van Der Vinne, G., Johnson, B., & Fonstad, G. 2003. Ice consolidation on the Peace River: release patterns and downstream surge characteristics. In Proc. 12th Workshop on the Hydraulics of Ice Covered Rivers, CGU HS CRIPE, Edmonton, AB, June (pp. 19-20).

Beltaos, S, ed. 2013. *River ice Formation*, Committee on River Ice Processes and the Environment, CGU-HS.

Beltaos, S., & Carter, T. 2009. Field studies of ice breakup and jamming in lower Peace River, Canada. Cold Regions Science and Technology, 56(2), 102-114.

Beltaos, S, ed. 2008. River ice breakup, Water Resources Publication.

Beltaos, S. 2008. Progress in the study and management of river ice jams. Cold Regions Science and Technology, 51(1), 2-19.

Brock, B. E., Martin, M. E., Mongeon, C. L., Sokal, M. A., Wesche, S. D., Armitage, D., and Edwards, T. W. 2010. Flood frequency variability during the past 80 years in the Slave River Delta, NWT, as determined from multi-proxy paleolimnological analysis. Canadian Water Resources Journal, 35(3), 281-300.

Brock, B. E., Wolfe, B. B. and Edwards, T. W. D. 2008. Spatial and temporal perspective on spring break-up flooding in the Slave River Delta, NWT. Hydrological Processes, 22**,** 4058-4072.

Brock BE, Wolfe BB, Edwards TWD. 2007. Characterizing the hydrology of shallow floodplain lakes in the Slave River Delta, NWT, using water isotope tracers. Arctic, Antarctic and Alpine Research 39: 388–401.

Carte, A. E. 1961. Air Bubbles in Ice. *Proceedings of the Physical Society,* 77**,** 757-768.

CCRS. 2009. Fundamentals of Remote Sensing, Canada Centre for Remote Sensing. Fundamentals of Remote Sensing, Canada Centre for Remote Sensing.

Chao L., Changyou L., Hongfang L., Honglan J. and Xiaohong S. 2014. Ice Process in Channel Bends of the Inner Mongolia Reach of Yellow River. 22nd IAHR International Symposium on Ice, Singapore, August 11 to 15, 2014.

Chaouch, N., Temimi, M., Romanov, P., Cabrera, R., Mckillop, G. & Khanbilvardi, R. 2014. An automated algorithm for river ice monitoring over the Susquehanna River using the MODIS data. Hydrological Processes, 28**,** 62-73.

Das, A., Sagin, J., Van der Sanden, J., Evans, E., McKay, H., and Lindenschmidt, K. E. 2015. Monitoring the freeze-up and ice cover progression of the Slave River. Canadian Journal of Civil Engineering.

De munck, S., Gauthier, Y., Bernier, M., Paulin, J. and Chokmani 2011.Preliminary development of a geospatial model to estimate a river channel's predisposition to ice jams. CGU HS Committee on River Ice Processes and the Environment (CRIPE). 16th workshop on river ice, Winnipeg, Manitoba, 18-22 September, 2011.

Dubé, M. G., and Wilson, J. E. 2013. Accumulated state assessment of the Peace-Athabasca-Slave River system. Integrated environmental assessment and management, 9(3), 405-425.

English M, Hill R, Stone M, Ormson R. 1997. Geomorphological and botanical change on the outer Slave River Delta, NWT, before and after impoundment of the Peace River. Hydrological Processes 11: 1707–1724.

Fjeldstad, H.-P., Bruland, O. and Alfredsen, K. 2002. Use of digital time lapse video to monitor river ice-preliminary report.

FEI 2014 "Dissolved Oxygen." Fundamentals of Environmental Measurements. Fondriest Environmental Inc. 5 June 2014. http://www.fondriest.com/environmental-measurements/parameters/water-quality/dissolved-oxygen/

Gauthier, Y., Weber, F., Savary, S., Jasek, M., Paquet, L. M., and Bernier, M. 2006. A combined classification scheme to characterise river ice from SAR data. EARSeL eProceedings, 5(1), 77-88.

Gherboudj, I., Bernier, M., Hicks, F. and Leconte, R. 2007. Physical characterization of air inclusions in river ice. *Cold regions science and technology,* 49**,** 179-194.

Ghobrial, T. R., Loewen, M. R. and Hicks, F. E. 2013. Continuous monitoring of river surface ice during freeze-up using upward looking sonar. *Cold Regions Science and Technology,* 86**,** 69-85.

F. Hicks, R. Andrishak and Y. She. 2009. Modeling Ice Cover Consolidation during Freeze-up on the Peace River, AB. 15th CRIPE Workshop on the Hydraulics of Ice Covered Rivers. St. John's, Newfoundland and Labrador.2009. http://www.cripe.ca/Downloads/15th_Workshop/Hicks-et-al-2009.pdf

Jasek, M., Marko, J., Fissel, D., Clarke, M., Buermans, J., and Paslawski, K. 2005. Instrument for detecting freeze-up, mid-winter and break-up ice processes in rivers. In Proc. 13th Workshop on River Ice. CGU-HS CRIPE, Hanover (pp. 151-183).

Jasek, M., Frank, W., and Jeff, H. 2003. "Ice thickness and roughness analysis on the Peace River using RADARSAT-1 SAR imagery." Proceedings of the 12th Workshop on River Ice, Canadian Geophysical Union—Hydrology Section, Communication on River Ice Processes and the Environment.

Jasek, M., Gauthier, Y., Poulin, J. and Bernier, M. 2013. Monitoring of Freeze-up on the Peace River at the Vermilion Rapids using RADARSAT-2 SAR data. CGU HS Committee on River Ice Processes and the Environment. 17th Workshop on River Ice, Edmonton, Alberta, July 21 – 24. http://www.cripe.ca/Downloads/17th_Workshop/Jasek-et-al-2013.pdf

Jasek M., Ghobrial T.,Loewen M., and Hicks F. 2011. Comparison of CRISSP modeled and SWIPS measured ice concentrations on the Peace River 16th Workshop on River Ice 2011, Winnipeg, 249-273.

Kalinin, V. G. 2008. Study of spatial distribution and occurrence frequency of ice jams in rivers of the Votkinsk reservoir catchment. Russian Meteorology and Hydrology, 33**,** 819-822.

Li, L., Qin, C., Peng, Q., Yan, Z. & Gao, Q. 2010. Numerical simulation of dissolved oxygen supersaturation flow over the Three Gorges Dam spillway. Tsinghua Science & Technology, 15, 574-579.

Lindenschmidt, K.-E., Syrenne, G. and Harrison, R. 2010. Measuring Ice Thicknesses along the Red River in Canada Using RADARSAT-2 Satellite Imagery. *Communications & Network,* 2.

Lindenschmidt, K.-E., Van der sanden, J.J., Demski, A., Drouin, H., and Geldsetzer. T. 2011. Characterising river ice along the Lower Red River using RADARSAT-2 imagery. 16th CRIPE Workshop on the Hydraulics of Ice Covered Rivers, Winnipeg, September 2011, pp. 198 -213. http://cripe.civil.ualberta.ca/Downloads/16th_Workshop/Lindenschmidt-et-al-2011a.pdf.

Lindenschmidt, K.-E. and Chun, K. P. 2013. Geospatial modelling to determine the behaviour of ice cover formation during freeze-up of the Dauphin River in Manitoba. Hydrology Research.Lindenschmidt, K.-E. and Davies J.-M. 2014. Winter Flow Testing of the Upper Qu'Appelle River. Lambert Academic Publishing. Saarbrucken, Germany ISBN 978-3-659-53427-0

Lindenschmidt, K.-E. & Long, J. 2013. A GIS approach to define the hydro geomorphological regime for instream flow requirements using geomorphic response units (GRU). River Systems, 20**,** 261-275.

Marko J. and Jasek M. 2009. Estimation of Frazil Particle Size and Concentration from SWIPS Measurements in the Peace River: an Assessment of Options and Prospects. 15th CRIPE Workshop on the Hydraulics of Ice Covered Rivers. St. John's, Newfoundland and Labrador.

Mäkynen, M. 2007. Investigation of the Microwave Signatures of the Baltic Sea Ice.Dissertation at Helsinki University of Technology (Espoo, Finland).

Pavelsky, T. M. & Smith, L. C. 2004. Spatial and temporal patterns in Arctic river ice breakup observed with MODIS and AVHRR time series. Remote Sensing of Environment, 93, 328-338.

Prowse, T. D., Beltaos, S., Gardner, J. T., Gibson, J. J., Granger, R. J., Leconte, R., ... & Toth, B. 2006. Climate change, flow regulation and land-use effects on the hydrology of the Peace-Athabasca-Slave system; Findings from the Northern Rivers Ecosystem Initiative. Environmental Monitoring and Assessment, 113(1-3), 167-197.

Prowse, T. D., Conly, F. M., Church, M. & English, M. C. 2002. A review of hydroecological results of the Northern River Basins Study, Canada. Part 1. Peace and Slave rivers. River Research and Applications, 18, 429-446.

Reed, B., Budde, M., Spencer, P. & miller, A. E. 2009. Integration of MODIS-derived metrics to assess inter annual variability in snowpack, lake ice, and NDVI in southwestAlaska. Remote Sensing of Environment, 113, 1443-1452.

Sandven, S. and Johannesen, O.M. 2006. Sea Ice Monitoring by Remote Sensing. In: J.F.R. Gower (Ed.) Manual of Remote Sensing: Remote Sensing of the Marine Environment (3rd edition, volume 6), Bethesda: American Society for Photogrammetry Remote Sensing, pp. 241-283.http://gs.mdacorporation.com/products/sensor/radarsat2/RS2_Product_Description.pdf.

Scheiber, E. and Gutmann, V. 1993. The oxygen content in supercooled water. Monatshefte für Chemie/Chemical Monthly, 124, 277-281.

Spencer, P., Miller, A. E., Reed, B. & Budde, M. 2008. Monitoring lake ice seasons in Southwest Alaska with MODIS images. Pecora 17 – The Future of Land Imaging…Going Operational, Denver, Colorado.

Unterschultz, K. D., Van der sanden, J.J. and Hicks, F. E. 2009. Potential of RADARSAT-1 for the monitoring of river ice: Results of a case study on the Athabasca River at Fort McMurray, Canada. *Cold Regions Science and Technology*, 55**,** 238-248.

Van der sanden, J.J. and Drouin, H. 2011. Satellite SAR observations of river ice cover: A RADARSAT-2 (C-band) and ALOS PALSAR (L-band) comparison. Proc. 16th Workshop Hydraulics Ice Covered Rivers. CGU HS/CRIPE, 2011. 179-197.

Van der sanden, J.J., Drouin, H., Hicks, F.E. and Beltaos, S. 2009. Potential of RADARSAT-2 for the Monitoring of River Freeze-up Processes. Proc. 15th Workshop on River Ice, St.John's, NF, 15-17 June 2009, Vol. pp. 364-377.

Vuyovich, C. M., Daly, S. F., Gagnon, J. J., Weyrick, P. and Zaitsoff, M. 2009. Monitoring river ice conditions using web-based cameras. *Journal of Cold Regions Engineering,* 23**,** 1-17.

Woo, M.-K., Modeste, P., Martz, L., Blondin, J., Kochtubajda, B., Tutcho, D., Gyakum, J., Takazo, A., Spence, C. and Tutcho, J. 2007. Science Meets Traditional Knowledge: Water and Climate in the Sahtu (Great Bear Lake) Region, Northwest Territories, Canada. *Arctic,* 60.4.

Woo, M.-K. ed. 2008. Cold Region Atmospheric and Hydrologic Studies. The Mackenzie GEWEX Experience. Springer Berlin Heidelberg.

Yoshimura, K., Inada, T., Koyama, S., 2008. Growth of Spherical and Cylindrical Oxygen Bubbles at an Ice-Water Interface. Crystal Growth & Design, vol. 8, no. 7, 2108-2115.

Appendix A: Supplemental information for Chapter 5

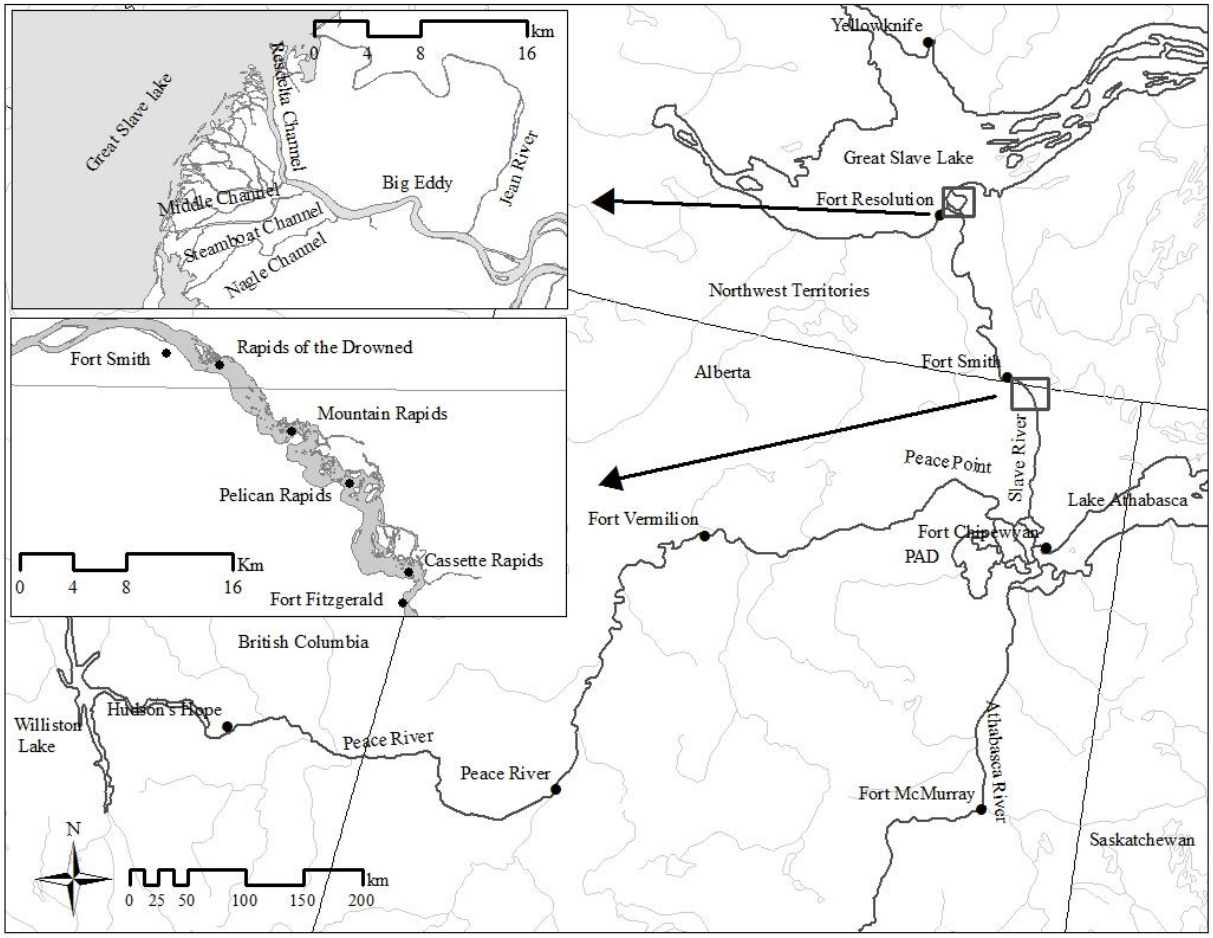

Fig. A1 Peace, Slave and Athabasca River Network.

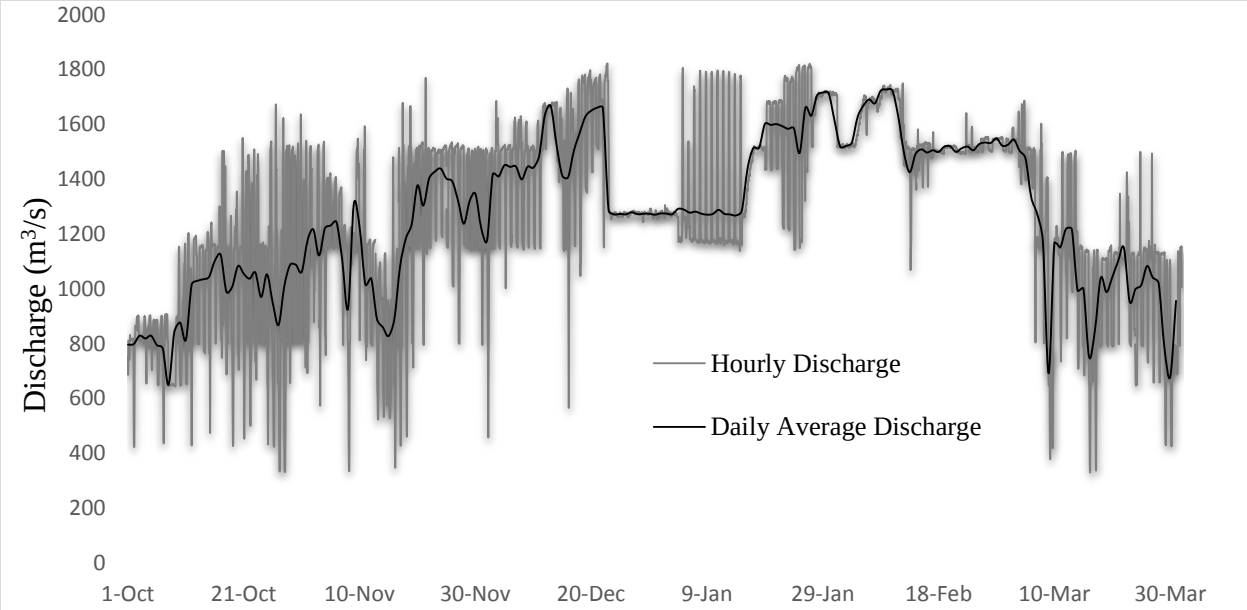

Fig. A2 Discharge along the Peace River at Hudson Hope in the 2013-2014 winter (Data source: Water Survey Canada, Gauge Station: 07EF001).

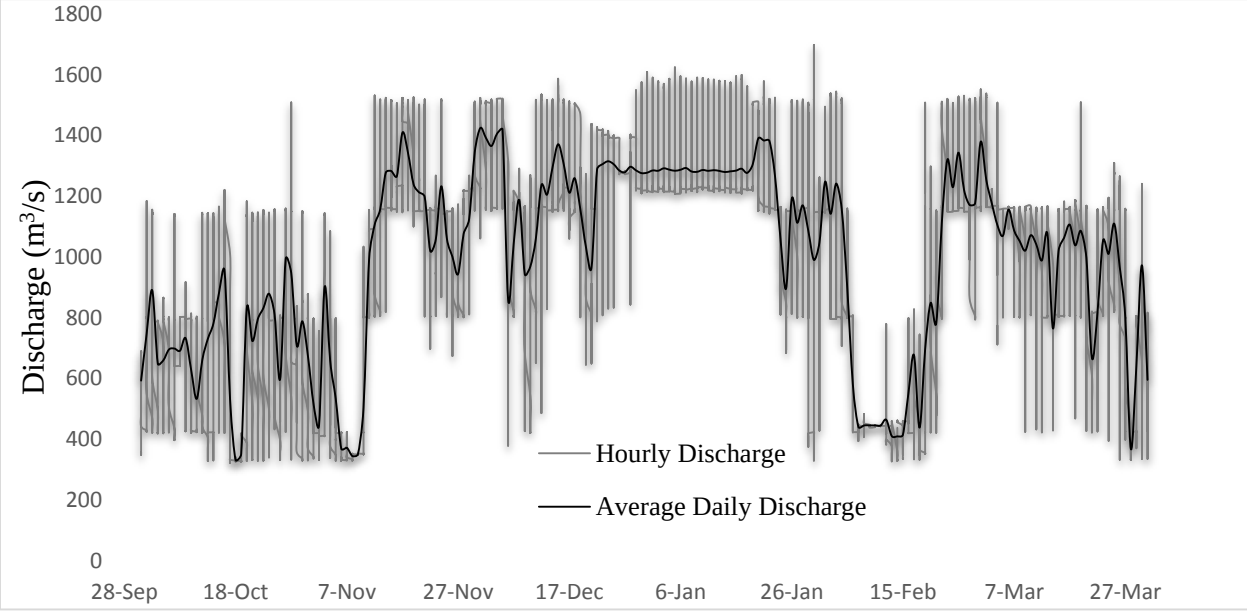

Fig. A3 Discharge along the Peace River at Hudson Hope in the 2014-2015 winter (Data source: Water Survey Canada, Gauge Station: 07EF001).

Appendix B: Permissions for use of published manuscripts

Canadian Science Publishing LICENSE
TERMS AND CONDITIONS

Jul 15, 2015

This is a License Agreement between University of Saskatchewan -- Apurba Das ("You") and Canadian Science Publishing ("Canadian Science Publishing") provided by Copyright Clearance Center ("CCC"). The license consists of your order details, the terms and conditions provided by Canadian Science Publishing, and the payment terms and conditions.

All payments must be made in full to CCC. For payment instructions, please see information listed at the bottom of this form.

License Number	3667290386773
License date	Jul 13, 2015
Licensed Content Publisher	Canadian Science Publishing
Licensed Content Publication	Publication1
Licensed Content Title	Canadian journal of civil engineering : Revue canadienne de génie civil
Licensed Content Author	None
Licensed Content Date	Jan 1, 1996
Type of Use	Thesis/Dissertation
Requestor type	Author of requested content
Format	Print, Electronic
Portion	chapter/article
Title or numeric reference of the portion(s)	Full Article
Title of the article or chapter the portion is from	Monitoring the freeze-up and ice cover progression of the Slave River
Editor of portion(s)	N/A
Author of portion(s)	N/A
Volume of serial or monograph.	N/A
Page range of the portion	None
Publication date of portion	6 January 2015
Rights for	Main product
Duration of use	Current edition and up to 5 years
Creation of copies for the disabled	no
With minor editing privileges	no

For distribution to	Canada
In the following language(s)	Original language of publication
With incidental promotional use	no
The lifetime unit quantity of new product	Up to 499
Made available in the following markets	education
The requesting person/organization is:	Apurba Das, University of Saskatchewan
Order reference number	None
Author/Editor	Apurba Das
The standard identifier	10.1139/cjce-2014-0286
Title	Monitoring the freeze-up and ice cover progression of the Slave River
Publisher	NRC Research Press
Expected publication date	Aug 2015
Estimated size (pages)	13
Terms and Conditions	

Canadian Science Publishing LICENSE TERMS AND CONDITIONS

Jul 15, 2015

This is a License Agreement between University of Saskatchewan -- Apurba Das ("You") and Canadian Science Publishing ("Canadian Science Publishing") provided by Copyright Clearance Center ("CCC"). The license consists of your order details, the terms and conditions provided by Canadian Science Publishing, and the payment terms and conditions.

All payments must be made in full to CCC. For payment instructions, please see information listed at the bottom of this form.

License Number	3667290389574
License date	Jul 13, 2015
Licensed Content Publisher	Canadian Science Publishing
Licensed Content Publication	Publication1
Licensed Content Title	Canadian journal of civil engineering : Revue canadienne de génie civil
Licensed Content Author	None

Licensed Content Date	Jan 1, 1996
Type of Use	Thesis/Dissertation
Requestor type	Author of requested content
Format	Print
Portion	chapter/article
Title or numeric reference of the portion(s)	Full Article
Title of the article or chapter portion is from	A geospatial model to determine patterns of ice cover breakup along the Slave River
Editor of portion(s)	N/A
Author of portion(s)	N/A
Volume of serial or monograph.	N/A
Page range of the portion	None
Publication date of portion	10 February 2015
Rights for	Main product
Duration of use	Current edition and up to 5 years
Creation of copies for the disabled	no
With minor editing privileges	no
For distribution to	Canada
In the following language(s)	Original language of publication
With incidental promotional use	no
The lifetime unit quantity of new product	Up to 499
Made available in the following markets	education
The requesting person/organization is:	Apurba Das, University of Saskatchewan
Order reference number	None
Author/Editor	Karl-Erich Lindenschmidt, Apurba Das
The standard identifier	10.1139/cjce-2014-0377
Title	A geospatial model to determine patterns of ice cover breakup along the Slave River
Publisher	NRC Research Press
Expected publication date	Aug 2015
Estimated size (pages)	11
Terms and Conditions	

TERMS AND CONDITIONS

The following terms are individual to this publisher:

TERMS AND CONDITIONS

The following terms are individual to this publisher:

Other Terms and Conditions:

<%=specialTerms%>

STANDARD TERMS AND CONDITIONS

1. Description of Service; Defined Terms. This Republication License enables the User toobtain licenses for republication of one or more copyrighted works as described in detail on the relevant Order Confirmation (the "Work(s)"). Copyright Clearance Center, Inc. ("CCC") grants licenses through the Service on behalf of the rightsholder identified on the Order Confirmation (the "Rightsholder"). "Republication", as used herein, generally means the inclusion of a Work, in whole or in part, in a new work or works, also as described on the Order Confirmation. "User", as used herein, means the person or entity making such republication.

2. The terms set forth in the relevant Order Confirmation, and any terms set by theRightsholder with respect to a particular Work, govern the terms of use of Works in connection with the Service. By using the Service, the person transacting for a republication license on behalf of the User represents and warrants that he/she/it (a) has been duly authorized by the User to accept, and hereby does accept, all such terms and conditions on behalf of User, and (b) shall inform User of all such terms and conditions. In the event such person is a "freelancer" or other third party independent of User and CCC, such party shall be deemed jointly a "User" for purposes of these terms and conditions. In any event, User shall be deemed to have accepted and agreed to all such terms and conditions if User republishes the Work in any fashion.

3. **Scope of License; Limitations and Obligations.**

    3.1 All Works and all rights therein, including copyright rights, remain the sole andexclusive property of the Rightsholder. The license created by the exchange of an Order Confirmation (and/or any invoice) and payment by User of the full amount set forth on that document includes only those rights expressly set forth in the Order Confirmation and in these terms and conditions, and conveys no other rights in the Work(s) to User. All rights not expressly granted are hereby reserved.

    3.2 General Payment Terms: You may pay by credit card or through an account with uspayable at the end of the month. If you and we agree that you may establish a

standing account with CCC, then the following terms apply: Remit Payment to: Copyright Clearance Center, Dept 001, P.O. Box 843006, Boston, MA 02284-3006. Payments Due: Invoices are payable upon their delivery to you (or upon our notice to you that they are available to you for downloading). After 30 days, outstanding amounts will be subject to a service charge of 1-1/2% per month or, if less, the maximum rate allowed by applicable law. Unless otherwise specifically set forth in the Order Confirmation or in a separate written agreement signed by CCC, invoices are due and payable on "net 30" terms. While User may exercise the rights licensed immediately upon issuance of the Order Confirmation, the license is automatically revoked and is null and void, as if it had never been issued, if complete payment for the license is not received on a timely basis either from User directly or through a payment agent, such as a credit card company.

3.3 Unless otherwise provided in the Order Confirmation, any grant of rights to User (i) is"one-time" (including the editions and product family specified in the license), (ii) is non-exclusive and non-transferable and (iii) is subject to any and all limitations and restrictions (such as, but not limited to, limitations on duration of use or circulation) included in the Order Confirmation or invoice and/or in these terms and conditions. Upon completion of the licensed use, User shall either secure a new permission for further use of the Work(s) or immediately cease any new use of the Work(s) and shall render inaccessible (such as by deleting or by removing or severing links or other locators) any further copies of the Work (except for copies printed on paper in accordance with this license and still in User's stock at the end of such period).

3.4 In the event that the material for which a republication license is sought includes thirdparty materials (such as photographs, illustrations, graphs, inserts and similar materials) which are identified in such material as having been used by permission, User is responsible for identifying, and seeking separate licenses (under this Service or otherwise) for, any of such third party materials; without a separate license, such third party materials may not be used.

3.5 Use of proper copyright notice for a Work is required as a condition of any licensegranted under the Service. Unless otherwise provided in the Order Confirmation, a proper copyright notice will read substantially as follows: "Republished with permission of [Rightsholder's name], from [Work's title, author, volume, edition number and year of copyright]; permission conveyed through Copyright Clearance Center, Inc. " Such notice must be provided in a reasonably legible font size and must be placed either immediately adjacent to the Work as used (for example, as part of a by-line or footnote but not as a separate electronic link) or in the place where substantially all other credits or notices for the new work containing the republished Work are located. Failure to include the required notice results in loss to the Rightsholder and CCC, and the User shall be liable to pay

liquidated damages for each such failure equal to twice the use fee specified in the Order Confirmation, in addition to the use fee itself and any other fees and charges specified.

3.6 User may only make alterations to the Work if and as expressly set forth in the OrderConfirmation. No Work may be used in any way that is defamatory, violates the rights of third parties (including such third parties' rights of copyright, privacy, publicity, or other tangible or intangible property), or is otherwise illegal, sexually explicit or obscene. In addition, User may not conjoin a Work with any other material that may result in damage to the reputation of the Rightsholder. User agrees to inform CCC if it becomes aware of any infringement of any rights in a Work and to cooperate with any reasonable request of CCC or the Rightsholder in connection therewith.

4. Indemnity. User hereby indemnifies and agrees to defend the Rightsholder and CCC, andtheir respective employees and directors, against all claims, liability, damages, costs and expenses, including legal fees and expenses, arising out of any use of a Work beyond the scope of the rights granted herein, or any use of a Work which has been altered in any unauthorized way by User, including claims of defamation or infringement of rights of copyright, publicity, privacy or other tangible or intangible property.

5. Limitation of Liability. UNDER NO CIRCUMSTANCES WILL CCC OR THE RIGHTSHOLDER BE LIABLE FOR ANY DIRECT, INDIRECT, CONSEQUENTIAL OR INCIDENTAL DAMAGES (INCLUDING WITHOUT LIMITATION DAMAGES FOR LOSS OF BUSINESS PROFITS OR INFORMATION, OR FOR BUSINESS INTERRUPTION) ARISING OUT OF THE USE OR INABILITY TO USE A WORK, EVEN IF ONE OF THEM HAS BEEN ADVISED OF THE POSSIBILITY OF SUCH DAMAGES. In any event, the total liability of the Rightsholder and CCC (including their respective employees and directors) shall not exceed the total amount actually paid by User for this license. User assumes full liability for the actions and omissions of its principals, employees, agents, affiliates, successors and assigns.

6. Limited Warranties. THE WORK(S) AND RIGHT(S) ARE PROVIDED “AS IS”. CCC HAS THE RIGHT TO GRANT TO USER THE RIGHTS GRANTED IN THE ORDER CONFIRMATION DOCUMENT. CCC AND THE RIGHTSHOLDER DISCLAIM ALL OTHER WARRANTIES RELATING TO THE WORK(S) AND RIGHT(S), EITHER EXPRESS OR IMPLIED, INCLUDING WITHOUT LIMITATION IMPLIED WARRANTIES OF MERCHANTABILITY OR FITNESS FOR A PARTICULAR PURPOSE. ADDITIONAL RIGHTS MAY BE REQUIRED TO USE ILLUSTRATIONS, GRAPHS, PHOTOGRAPHS, ABSTRACTS, INSERTS OR OTHER PORTIONS OF THE WORK (AS OPPOSED TO THE ENTIRE WORK) IN A MANNER CONTEMPLATED BY USER; USER UNDERSTANDS AND AGREES THAT NEITHER CCC NOR THE RIGHTSHOLDER MAY HAVE SUCH ADDITIONAL RIGHTS TO GRANT.

7. Effect of Breach. Any failure by User to pay any amount when due, or any use by User ofa Work beyond the scope of the license set forth in the Order Confirmation and/or these terms and conditions, shall be a material breach of the license created by the Order Confirmation and these terms and conditions. Any breach not cured within 30 days of written notice thereof shall result in immediate termination of such license without further notice. Any unauthorized (but licensable) use of a Work that is terminated immediately upon notice thereof may be liquidated by payment of the Rightsholder's ordinary license price therefor; any unauthorized (and unlicensable) use that is not terminated immediately for any reason (including, for example, because materials containing the Work cannot reasonably be recalled) will be subject to all remedies available at law or in equity, but in no event to a payment of less than three times the Rightsholder's ordinary license price for the most closely analogous licensable use plus Rightsholder's and/or CCC's costs and expenses incurred in collecting such payment.

8. **Miscellaneous.**

8.1 User acknowledges that CCC may, from time to time, make changes or additions to the

Service or to these terms and conditions, and CCC reserves the right to send notice to the User by electronic mail or otherwise for the purposes of notifying User of such changes or additions; provided that any such changes or additions shall not apply to permissions already secured and paid for.

8.2 Use of User-related information collected through the Service is governed by CCC'sprivacy policy, available online here: http://www.copyright.com/content/cc3/en/tools/footer /privacypolicy.html.

8.3 The licensing transaction described in the Order Confirmation is personal to User.Therefore, User may not assign or transfer to any other person (whether a natural person or an organization of any kind) the license created by the Order Confirmation and these terms and conditions or any rights granted hereunder; provided, however, that User may assign such license in its entirety on written notice to CCC in the event of a transfer of all or substantially all of User's rights in the new material which includes the Work(s) licensed under this Service.

8.4 No amendment or waiver of any terms is binding unless set forth in writing and signedby the parties. The Rightsholder and CCC hereby object to any terms contained in any writing prepared by the User or its principals, employees, agents or affiliates and purporting to govern or otherwise relate to the licensing transaction described in the Order

Confirmation, which terms are in any way inconsistent with any terms set forth in the Order Confirmation and/or in these terms and conditions or CCC's standard operating procedures, whether such writing is prepared prior to, simultaneously with or subsequent to the Order

Confirmation, and whether such writing appears on a copy of the Order Confirmation or in a separate instrument.

8.5 The licensing transaction described in the Order Confirmation document shall begoverned by and construed under the law of the State of New York, USA, without regard to the principles thereof of conflicts of law. Any case, controversy, suit, action, or proceeding arising out of, in connection with, or related to such licensing transaction shall be brought, at CCC's sole discretion, in any federal or state court located in the County of New York, State of New York, USA, or in any federal or state court whose geographical jurisdiction covers the location of the Rightsholder set forth in the Order Confirmation. The parties expressly submit to the personal jurisdiction and venue of each such federal or state court.If you have any comments or questions about the Service or Copyright Clearance Center, please contact us at 978-750-8400 or send an e-mail to info@copyright.com.

v 1.1

Other Terms and Conditions:

None

STANDARD TERMS AND CONDITIONS

1. Description of Service; Defined Terms. This Republication License enables the User toobtain licenses for republication of one or more copyrighted works as described in detail on the relevant Order Confirmation (the "Work(s)"). Copyright Clearance Center, Inc. ("CCC") grants licenses through the Service on behalf of the rightsholder identified on the Order Confirmation (the "Rightsholder"). "Republication", as used herein, generally means the inclusion of a Work, in whole or in part, in a new work or works, also as described on the Order Confirmation. "User", as used herein, means the person or entity making such republication.

2. The terms set forth in the relevant Order Confirmation, and any terms set by theRightsholder with respect to a particular Work, govern the terms of use of Works in connection with the Service. By using the Service, the person transacting for a republication license on behalf of the User represents and warrants that he/she/it (a) has been duly authorized by the User to accept, and hereby does accept, all such terms and conditions on behalf of User, and (b) shall inform User of all such terms and conditions. In the event such person is a "freelancer" or other third party independent of User and CCC, such party shall be deemed jointly a "User" for purposes of these terms and conditions. In any event, User shall be deemed to have accepted and agreed to all such terms and conditions if User republishes the Work in any fashion.

3. **Scope of License; Limitations and Obligations.**

3.1 All Works and all rights therein, including copyright rights, remain the sole andexclusive property of the Rightsholder. The license created by the exchange of an Order Confirmation (and/or any invoice) and payment by User of the full amount set forth on that document includes only those rights expressly set forth in the Order Confirmation and in these terms and conditions, and conveys no other rights in the Work(s) to User. All rights not expressly granted are hereby reserved.

3.2 General Payment Terms: You may pay by credit card or through an account with uspayable at the end of the month. If you and we agree that you may establish a standing account with CCC, then the following terms apply: Remit Payment to: Copyright Clearance Center, Dept 001, P.O. Box 843006, Boston, MA 02284-3006. Payments Due: Invoices are payable upon their delivery to you (or upon our notice to you that they are available to you for downloading). After 30 days, outstanding amounts will be subject to a service charge of 1-1/2% per month or, if less, the maximum rate allowed by applicable law. Unless otherwise specifically set forth in the Order Confirmation or in a separate written agreement signed by CCC, invoices are due and payable on "net 30" terms. While User may exercise the rights licensed immediately upon issuance of the Order Confirmation, the license is automatically revoked and is null and void, as if it had never been issued, if complete payment for the license is not received on a timely basis either from User directly or through a payment agent, such as a credit card company.

3.3 Unless otherwise provided in the Order Confirmation, any grant of rights to User (i) is"one-time" (including the editions and product family specified in the license), (ii) is non-exclusive and non-transferable and (iii) is subject to any and all limitations and restrictions (such as, but not limited to, limitations on duration of use or circulation) included in the Order Confirmation or invoice and/or in these terms and conditions. Upon completion of the licensed use, User shall either secure a new permission for further use of the Work(s) or immediately cease any new use of the Work(s) and shall render inaccessible (such as by deleting or by removing or severing links or other locators) any further copies of the Work (except for copies printed on paper in accordance with this license and still in User's stock at the end of such period).

3.4 In the event that the material for which a republication license is sought includes thirdparty materials (such as photographs, illustrations, graphs, inserts and similar materials) which are identified in such material as having been used by permission, User is responsible for identifying, and seeking separate licenses (under this Service or otherwise) for, any of such third party materials; without a separate license, such third party materials may not be used.

3.5 Use of proper copyright notice for a Work is required as a condition of any licensegranted under the Service. Unless otherwise provided in the Order Confirmation, a proper copyright notice will read substantially as follows:

"Republished with permission of [Rightsholder's name], from [Work's title, author, volume, edition number and year of copyright]; permission conveyed through Copyright Clearance Center, Inc. " Such notice must be provided in a reasonably legible font size and must be placed either immediately adjacent to the Work as used (for example, as part of a by-line or footnote but not as a separate electronic link) or in the place where substantially all other credits or notices for the new work containing the republished Work are located. Failure to include the required notice results in loss to the Rightsholder and CCC, and the User shall be liable to pay liquidated damages for each such failure equal to twice the use fee specified in the Order Confirmation, in addition to the use fee itself and any other fees and charges specified.

3.6 User may only make alterations to the Work if and as expressly set forth in the OrderConfirmation. No Work may be used in any way that is defamatory, violates the rights of third parties (including such third parties' rights of copyright, privacy, publicity, or other tangible or intangible property), or is otherwise illegal, sexually explicit or obscene. In addition, User may not conjoin a Work with any other material that may result in damage to the reputation of the Rightsholder. User agrees to inform CCC if it becomes aware of any infringement of any rights in a Work and to cooperate with any reasonable request of CCC or the Rightsholder in connection therewith.

4. Indemnity. User hereby indemnifies and agrees to defend the Rightsholder and CCC, andtheir respective employees and directors, against all claims, liability, damages, costs and expenses, including legal fees and expenses, arising out of any use of a Work beyond the scope of the rights granted herein, or any use of a Work which has been altered in any unauthorized way by User, including claims of defamation or infringement of rights of copyright, publicity, privacy or other tangible or intangible property.

5. Limitation of Liability. UNDER NO CIRCUMSTANCES WILL CCC OR THE RIGHTSHOLDER BE LIABLE FOR ANY DIRECT, INDIRECT, CONSEQUENTIAL OR INCIDENTAL DAMAGES (INCLUDING WITHOUT LIMITATION DAMAGES FOR LOSS OF BUSINESS PROFITS OR INFORMATION, OR FOR BUSINESS INTERRUPTION) ARISING OUT OF THE USE OR INABILITY TO USE A WORK, EVEN IF ONE OF THEM HAS BEEN ADVISED OF THE POSSIBILITY OF SUCH DAMAGES. In any event, the total liability of the Rightsholder and CCC (including their respective employees and directors) shall not exceed the total amount actually paid by User for this license. User assumes full liability for the actions and omissions of its principals, employees, agents, affiliates, successors and assigns.

6. Limited Warranties. THE WORK(S) AND RIGHT(S) ARE PROVIDED "AS IS". CCC HAS THE RIGHT TO GRANT TO USER THE RIGHTS GRANTED IN THE ORDER CONFIRMATION DOCUMENT. CCC AND THE RIGHTSHOLDER DISCLAIM ALL

OTHER WARRANTIES RELATING TO THE WORK(S) AND RIGHT(S), EITHER EXPRESS OR IMPLIED, INCLUDING WITHOUT LIMITATION IMPLIED WARRANTIES OF MERCHANTABILITY OR FITNESS FOR A PARTICULAR PURPOSE. ADDITIONAL RIGHTS MAY BE REQUIRED TO USE ILLUSTRATIONS, GRAPHS, PHOTOGRAPHS, ABSTRACTS, INSERTS OR OTHER PORTIONS OF THE WORK (AS OPPOSED TO THE ENTIRE WORK) IN A MANNER CONTEMPLATED BY USER; USER UNDERSTANDS AND AGREES THAT NEITHER CCC NOR THE RIGHTSHOLDER MAY HAVE SUCH ADDITIONAL RIGHTS TO GRANT.

7. Effect of Breach. Any failure by User to pay any amount when due, or any use by User ofa Work beyond the scope of the license set forth in the Order Confirmation and/or these terms and conditions, shall be a material breach of the license created by the Order Confirmation and these terms and conditions. Any breach not cured within 30 days of written notice thereof shall result in immediate termination of such license without further notice. Any unauthorized (but licensable) use of a Work that is terminated immediately upon notice thereof may be liquidated by payment of the Rightsholder's ordinary license price therefor; any unauthorized (and unlicensable) use that is not terminated immediately for any reason (including, for example, because materials containing the Work cannot reasonably be recalled) will be subject to all remedies available at law or in equity, but in no event to a payment of less than three times the Rightsholder's ordinary license price for the most closely analogous licensable use plus Rightsholder's and/or CCC's costs and expenses incurred in collecting such payment.

8. **Miscellaneous.**

8.1 User acknowledges that CCC may, from time to time, make changes or additions to the

Service or to these terms and conditions, and CCC reserves the right to send notice to the User by electronic mail or otherwise for the purposes of notifying User of such changes or additions; provided that any such changes or additions shall not apply to permissions already secured and paid for.

8.2 Use of User-related information collected through the Service is governed by CCC'sprivacy policy, available online here: http://www.copyright.com/content/cc3/en/tools/footer /privacypolicy.html.

8.3 The licensing transaction described in the Order Confirmation is personal to User.Therefore, User may not assign or transfer to any other person (whether a natural person or an organization of any kind) the license created by the Order Confirmation and these terms and conditions or any rights granted hereunder; provided, however, that User may assign such license in its entirety on written notice to CCC in the event of a transfer of all or substantially all of User's rights in the new material which includes the Work(s) licensed under this Service.

8.4 No amendment or waiver of any terms is binding unless set forth in writing and signedby the parties. The Rightsholder and CCC hereby object to any terms contained in any writing prepared by the User or its principals, employees, agents or affiliates and purporting to govern or otherwise relate to the licensing transaction described in the Order

Confirmation, which terms are in any way inconsistent with any terms set forth in the Order Confirmation and/or in these terms and conditions or CCC's standard operating procedures, whether such writing is prepared prior to, simultaneously with or subsequent to the Order Confirmation, and whether such writing appears on a copy of the Order Confirmation or in a separate instrument.

8.5 The licensing transaction described in the Order Confirmation document shall begoverned by and construed under the law of the State of New York, USA, without regard to the principles thereof of conflicts of law. Any case, controversy, suit, action, or proceeding arising out of, in connection with, or related to such licensing transaction shall be brought, at CCC's sole discretion, in any federal or state court located in the County of New York, State of New York, USA, or in any federal or state court whose geographical jurisdiction covers the location of the Rightsholder set forth in the Order Confirmation. The parties expressly submit to the personal jurisdiction and venue of each such federal or state court.If you have any comments or questions about the Service or Copyright Clearance Center, please contact us at 978-750-8400 or send an e-mail to info@copyright.com. v 1.1

Questions? customercare@copyright.com or +1-855-239-3415 (toll free in the US) or +1-978-646-2777.